# REPORT 1163

## A VISUALIZATION STUDY OF SECONDARY FLOWS IN CASCADES[1]

By Howard Z. Herzig, Arthur G. Hansen, and George R. Costello


### SUMMARY

*Flow-visualization techniques are employed to ascertain the streamline patterns of the nonpotential secondary flows in the boundary layers of cascades, and thereby to provide a basis for more extended analyses in turbomachines. The three-dimensional deflection of the end-wall boundary layer results in the formation of a vortex within each cascade passage. The size and tightness of the vortex generated depend upon the main-flow turning in the cascade passage. Once formed, a vortex resists turning in subsequent blade rows, with consequent unfavorable angles of attack and possible flow disturbances on the pressure surfaces of subsequent blade rows when the vortices impinge on these surfaces.*

*Two major tip-clearance effects are observed, the formation of a tip-clearance vortex and the scraping effect of a blade with relative motion past the wall boundary layer. The flow patterns indicate methods for improving the blade tip-loading characteristics of compressors and of low- and high-speed turbines.*


### INTRODUCTION

An important problem arising in the design of turbomachines and in the analysis of their performance is an understanding of the nature and influence of so-called secondary flows, which are here defined as any motions of boundary-layer fluid having components of motion normal to the through-flow directions. These secondary flows, which are directly responsible for boundary-layer accumulations and boundary-layer flows within the passages of the turbomachine, often lead to significant aerodynamic losses. The ideal answer to this problem would be a practical design procedure based on the complete solution of the three-dimensional viscous-flow equations in the actual turbomachine configuration. At the present time, such solutions have not been obtained because of the mathematical complexity of the problem involved. In practice, therefore, the fluid flow in turbomachines is studied by considering separately the main flow (taken to be a perfect, inviscid fluid) and the boundary-layer flow (in which all the viscosity phenomena are considered to be concentrated). This, of course, qualifies somewhat the results of the analysis. Furthermore, practical three-dimensional solutions have not been obtained even for the thus differentiated flow regions, and additional simplifying assumptions are required, which, in turn, further qualify the results.

On this account, current blade design methods for turbomachines are based mainly on modified two-dimensional or, more recently, on quasi-three-dimensional flow theories of perfect, inviscid fluids. The design is then refined by allowing for such factors as boundary-layer thickness and growth by use of formulas developed from classical studies of simple flow configurations. Inherent in this procedure is the assumption that such corrections for the effects of viscosity can yield good approximations of the real-fluid behavior in actual turbomachines. This combination of simplified flow theories with adjustments for boundary-layer effects has made possible the achievement of fairly satisfactory design procedures for turbomachines that operate at low- and moderate-flow speeds. However, with the trend toward high-speed, high-mass-flow turbomachines, these boundary-layer effects become increasingly significant. As transonic velocities are approached within the flow passages, the boundary-layer accumulations and three-dimensional boundary-layer flows, together with their effects upon the mainstream flow, give rise to such large deviations from the design flow conditions that these ordinary rough, qualitative adjustments are no longer adequate. With useful solutions of the complete flow equations still remote, the designer has no recourse but to refine his qualitative adjustment procedures in an effort to compensate more successfully for the increased boundary-layer deviations. The designer is then confronted squarely with the need for obtaining more accurate, fundamental information concerning the nature of the secondary flows in turbomachines.

[1] Supersedes NACA TN 2947, "A Visualization Study of Secondary Flows in Cascades," by Arthur G. Hansen, Howard Z. Herzig, and George R. Costello.

With the direct approach to the problem (i. e., solving the complete flow equations) barred, various theoretical and experimental investigations have been made, each of which by means of certain simplifying assumptions describes partially the manner in which secondary flows affect the performance of turbomachines. In these analyses, usually one of two methods has been used to estimate the deviations in the exit flow angles and velocities due to boundary-layer behavior. The first method (ref. 1) is based principally on airfoil theory, and the flow deviations are considered as arising from (or at least measured by) trailing-edge vortices associated with spanwise variations in circulation. The second method (refs. 2 and 3, e. g.) is based on the flow of an ideal fluid in a channel with varying inlet total pressure, and deviations arise from the appearance of a vorticity component in the direction of the main flow.

In the investigations considered, attempts were made to give a qualitative picture of secondary-flow behavior and to provide some foundations for approximate loss calculations. Because of the simplifying assumptions involved, however, the question remains as to how accurately these methods and various extensions of these methods describe actual flow phenomena, for example, in a cascade. And while the knowledge concerning the detailed streamline patterns of the actual flow in a blade row is essential to an accurate understanding of the nature and influence of secondary flows, such information has not been obtained to date from the aforementioned techniques.

These considerations motivated a series of experimental investigations at the NACA Lewis laboratory to determine the streamline patterns in a cascade. This report presents the results of these investigations, in which flow visualization by means of smoke and chemical traces, as well as total-pressure and flow-angle measurements, was used in order to obtain an insight into the three-dimensional boundary-layer flow patterns in typical axial-flow turbomachines. Photographs of the various flow patterns obtained by the visualization procedures are presented. By obtaining direct evidence of the flow paths by the careful application of these visualization techniques, the fundamental assumptions that might qualify the results of theoretical analyses were avoided.

The particular boundary-layer phenomena considered are (1) secondary flows in the shroud region, (2) radial transport of boundary-layer material, and (3) blade tip-clearance-region secondary flows with and without relative motion between the blades and end walls or shrouds.

Unfortunately, because of the complicated three-dimensional flow patterns, it is difficult to arrive at an understanding of the secondary flows in a turbomachine by instituting the study of such flows directly in the machine. Accordingly, for the first step, the visualization techniques were used to obtain the streamline patterns in a stationary two-dimensional cascade for a range of Reynolds numbers. The secondary-flow behavior in the end-wall (shroud) boundary layers was thus observable without such disturbing influences as over-all radial pressure gradients or rotative effects.

In order to extend this study to more general configurations, the influence of blade geometry was then investigated qualitatively by independently varying stagger angle, aspect ratio, solidity, and angle of attack, and by using blade fillets in the two-dimensional cascade. As part of a more detailed study of the effects of high-turning on secondary flows, the secondary flows in rectangular bends (which have been the subject of many recent investigations (cf., ref. 4)) were also studied by means of flow visualization. Furthermore, a comparison was made between the boundary-layer flows in such bends and in blade rows with similar turning sections.

The flow-visualization technique was applied to an annular-turbine-nozzle cascade at high subsonic and at supersonic Mach numbers in order to extend the scope of this investigation to typical turbomachine flow conditions where radial pressure gradients and shock phenomena do exist. The results of these visualization procedures were instrumental in successful interpretations of total-pressure and flow-angle measurements made in reference 5.

In order to simulate more closely the mechanical conditions in a turbomachine, the two-dimensional cascade was modified to enable the study of the influence of blade tip clearance and relative motion between the wall and blades. Also, the interactions of the secondary flows in successive blade rows were investigated briefly in tandem cascades.

The investigation presented in this report is intended mainly as an exploratory inquiry into some fundamental aspects of the boundary-layer flows in turbomachines. The results of the exploratory secondary-flow studies outlined constitute an informational unit intended to be basic to general investigations of the actual secondary flows in turbomachines and are preliminary to a more complete analysis of the flow in turbomachines. Nevertheless, the insight obtained into the secondary-flow patterns and behavior is fundamental in nature. Thus, it may provide a basis for correlation and interpretation of other experimental data. When flow conditions are sufficiently similar to those existing in these studies, the conclusions drawn herein may likewise serve to extend the understanding and correlation of other experimental data.

It is further anticipated that the flow behavior observed experimentally in the various configurations may prove useful as a means for evaluating the reasonableness of various simplifying assumptions used in theoretical analyses. In particular, it might serve as a criterion both in the initial selection of the assumptions and in estimations of the physical validity of analytically obtained results.

## APPARATUS AND PROCEDURES

### EXPERIMENTAL SETUPS

All configurations discussed in this section will be shown in the figures throughout the report. Where necessary, an insert appears on the photographs depicting schematically an overhead view of the configuration and the smoke trace appearing in the photograph.

**Basic two-dimensional cascade.**—The initial experimental investigation was intended as a study of the secondary-flow phenomena in a cascade end-wall boundary layer uncomplicated by radial pressure gradients or rotative forces. Therefore, these basic tests were carried out in a two-dimensional steady-flow cascade (see fig. 1). The air to the cascade was supplied by the laboratory combustion-air system and was discharged directly into the room. Because of the construction of the cascade, the inlet-air velocities were limited to Mach numbers below approximately 0.4.

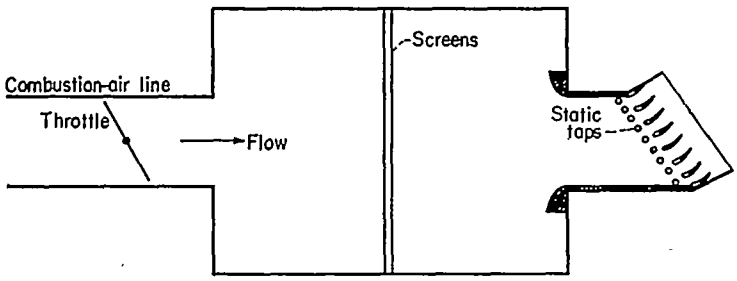


FIGURE 1.—Two-dimensional steady-flow cascade.

The blade row consisted of six NACA 65(12)–10 blades mounted between two channel walls at a stagger angle of 45°, an angle attack of 11°, and a turning angle of 20°. The solidity of the cascade was 1.5, and the aspect ratio for the blades was 2.34. A row of static taps was located on one wall one-half chord upstream of the blades. At this same axial location, a $\frac{1}{16}$-inch-outside-diameter probe was mounted in a slot in the other wall for the introduction of smoke into the air stream at any desired point. All tests were conducted in the half of the passage adjacent to the smooth wall containing the static taps in order to avoid any disturbances that might arise because of the probe slot.

**Modified two-dimensional cascade.**—The construction of the basic two-dimensional cascade was such that the blade-geometry parameters could readily be varied independently over a wide range. In this fashion the flows through more general configurations could be studied. The geometric parameters that were varied were stagger angle, aspect ratio, solidity, and angle of attack. Other tests involved the use of fillets between the blade tips and the wall.

The 65(12)–10 blade mountings were such that the blade could be moved to provide tip clearance between the blade tips and the wall. The wall could further be replaced by an endless moving belt, the direction and speed of which could be varied in order to study the influence of relative motion between the blades and the wall. The tension on the belt was adjusted to prevent flow disturbances due to belt flap. The tests were conducted at three belt speeds: low speed (belt speed well below airspeed), moderate speed (belt speed approximately equal to airspeed), and high speed (belt speed well above airspeed).

**Three-dimensional cascade.**—An annular-turbine-nozzle cascade was used to extend the investigation of secondary flows to high subsonic and to supersonic Mach numbers in a three-dimensional flow configuration (ref. 5). A schematic view of the apparatus is shown in figure 2. Air was supplied to this cascade from the laboratory combustion-air system and was discharged into the laboratory altitude exhaust system.

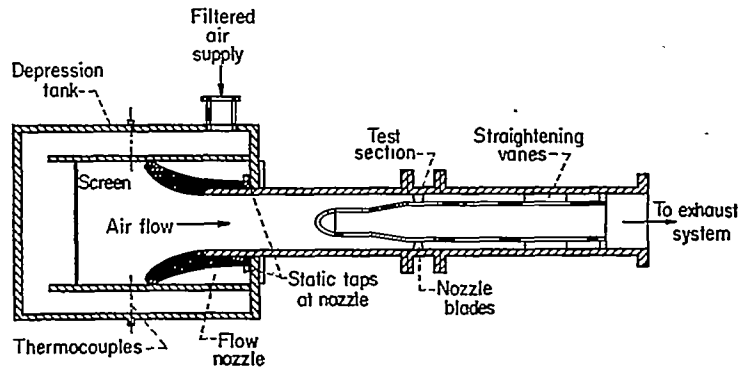


FIGURE 2.—Schematic view of annular-nozzle cascade test unit.

**Rectangular bends.**—The blade row of the two-dimensional cascade was replaced by a row of sheet-metal blades. The turning sections of these blades were concentric circular arcs having turning angles of 45°. When long straight inlet and exit guides were provided, the passages thus formed were, in effect, rectangular bends. The end wall in which the probe was mounted was replaced by a Lucite wall to make it possible to look directly into the entire bend. The overhead photographs of the bend flows were taken from this position.

Another investigation was made of the rectangular-bend configuration, in which the blade turning sections were 60° circular arcs, all having the same radius of curvature. The bends were made of sheet aluminum and were mounted in a two-dimensional cascade with a stagger angle of zero.

**High-turning cascades.**—The boundary-layer behavior in the 60° bends was compared with that in a set of 60°-circular-arc blades. These blades were sheet aluminum and were mounted in the 0°-stagger-angle configuration. The sole difference between this 60° cascade and the 60° bends was that the cascade did not have the straight guidance sections at the inlet. In order to investigate the effects of relative motion between end wall and blades at high flow-turning angles, sheet-aluminum blades with

approximately 125° turning were used in the 45°-stagger-angle configuration.

**Tandem cascade.**—The blades for the tandem cascade, which were also made of sheet aluminum, were used in the 0°-stagger-angle configuration. Each of the two blade rows of the tandem cascade was mounted on an individual aluminum strip, which enabled the positions of the two blade rows to be shifted relative to each other in both the blade-to-blade and axial directions.

The blades in the tandem cascades were bent in circular arcs to give a turning of approximately 60° each. The upstream cascade turned the flow 60° from axial (to the left as seen in the figures of this report). The second or downstream cascade turned the flow back to the axial direction.

### FLOW VISUALIZATION

Three methods were used to visualize the flow patterns: (1) smoke traces in the passage and on the blades and walls, (2) hydrogen sulfide gas reacting with a lead carbonate suspension in glycerin painted on the walls and blades, and (3) paint flow traces on the surfaces at the higher gas-flow speeds. The smoke flow-visualization method was used in the two-dimensional cascades for tests made at low speeds (30 ft/sec). At the higher speeds (Mach numbers of approximately 0.4 in the two-dimensional configuration and higher Mach numbers in the annular cascade), the hydrogen sulfide–lead carbonate visualization method was used. At the highest speeds studied in the annular cascade, the flow of the paint on the shrouds and blades provided additional information concerning the secondary-flow behavior.

Photographs were taken of the traces obtained by admitting smoke or hydrogen sulfide through the wall static taps and through the probe at either the wall itself or in the passage. As will be demonstrated, the agreement between the probe and static-tap traces showed that the probe did not disturb the flow in the passage sufficiently to affect these tests.

**Smoke traces.**—Smoke was produced by burning oil-soaked cigars with service air (fig. 3). This method of generating smoke was found to be superior, for this application, to other methods used elsewhere. In particular, the smoke was nontoxic, noncorrosive, easily generated, and of sufficient intensity to be photographed. The rates of smoke production and injection into the air stream were carefully controlled by means of settling bottles, pressure regulators, and bleeds in order to make possible close matching of the local direction, velocity, and density of the air stream. In order to maintain the smoke traces intense enough for photographing, the inlet-air velocity was held at approximately 30 feet per second when the smoke visualization method was used. The smoke-trace method was particularly advantageous, because it was possible thereby to visualize the streamlines any place in the passage as well as directly on the walls and blades. No difficulty was encountered with diffusion of smoke into air. However, it is difficult to present the results photographically, because the photographs cannot show the three-dimensional movement of the traces, which appear, instead, as projections against the passage walls or against the blades. In addition, suitable photographs are difficult to obtain for regions of low contrast.

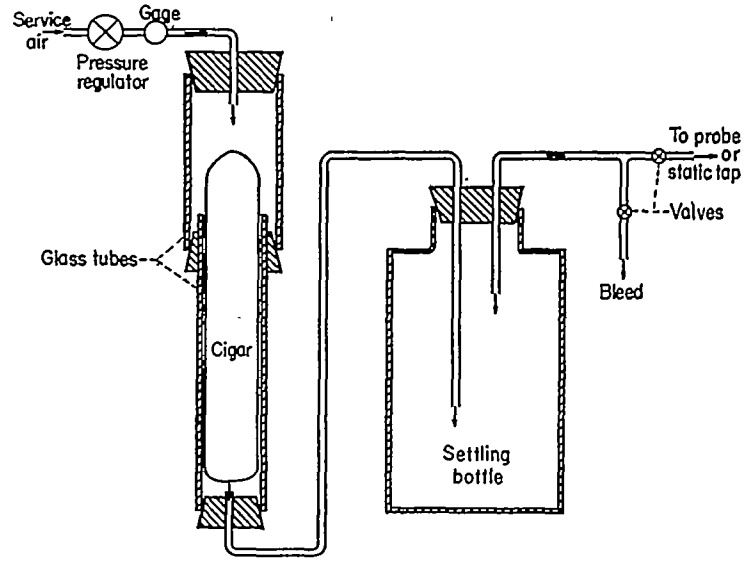


FIGURE 3.—Smoke generator.

**Hydrogen sulfide traces.**—In order to obtain flow traces at higher airspeeds, the following procedure was adopted. The wall and the blades were covered with a paint of lead carbonate in glycerin and alcohol. As the hydrogen sulfide was introduced through the static taps or through the probe, its path along the blades and on the wall was observable as a brown trace on a white background. This reaction is semipermanent and accumulative. The procedure, therefore, was to introduce the hydrogen sulfide at such rates that the local velocity and direction of the air stream could be matched closely and the disturbance of the local flow minimized. This was continued until a photographable trace was obtained. Furthermore, the molecular weight of hydrogen sulfide is close to that of air, which minimizes the diffusion due to density differences. Disadvantages of the method are that the gas is highly toxic and corrosive and the reaction must proceed for a long time in order to obtain sufficient color contrast for photographing.

**Paint flow traces.**—At the higher Mach numbers, the soft, nondrying paint used in these tests would flow along the painted surfaces and trace out flow patterns. It will be demonstrated by comparison with hydrogen sulfide traces that the paint flow traces can indicate the flow conditions directly at the surfaces involved.

### TEST PROCEDURES

In any experimental investigation it is necessary to establish the validity of the procedures involved in order to ensure the reliability of the results. In the following paragraphs, the test procedures are discussed, and the bases for confidence in the results obtained are briefly indicated. References are made to the various sections of the report where each of the considerations involved here is discussed in greater detail.

**Probe investigation.**—The experimental investigation of secondary flows was begun with the basic two-dimensional cascade at low airspeeds. Smoke visualization techniques were employed to trace out the flow patterns in the end-wall

boundary layer of this cascade, in which such complicating factors as radial pressure gradients or rotative forces were eliminated. It was considered desirable to use the probe for the introduction of the smoke for the low-speed tests, because with the probe a point-by-point traverse across the inlet section just upstream of the blades could be made. Thus, it was necessary to establish the reliability of the probe results; this was done by comparing the streamline patterns obtained by use of the probe and the static taps for introducing smoke. Figures 4 to 7, which show the deflection patterns in the wall boundary layer, are used for this purpose and will be discussed fully in the INITIAL LOW-SPEED INVESTIGATION section of RESULTS AND DISCUSSION. (Throughout this report, except when specified otherwise, the photographs presented were taken with a camera downstream looking upstream into the discharge section.) Examples of probe surveys of the secondary-flow patterns in the basic two-dimensional-cascade wall boundary layer are shown in figures 8 and 9.

**Hydrogen sulfide investigation.**—As noted earlier, the use of smoke traces proved unsuitable at the higher air velocities, and under these conditions one method of visualizing the flow was by means of hydrogen sulfide. The tendency of the hydrogen sulfide to spread out rendered impossible the maintenance of the trace as a well-defined line. Because of the increased turbulence at the higher air velocities, the hydrogen sulfide could not be confined to a layer at a specified distance from the wall but was distributed throughout the entire height of the boundary layer. Therefore, the hydrogen sulfide traces indicate the flow paths of a region of the entering boundary layer instead of an individual path. Hence, pictures of these traces, in general, resemble figures 4 (b) and 6 (b), where the smoke was introduced at some position away from the wall. Figures 10 to 12 illustrate the kind of "wide" trace typically obtained with hydrogen sulfide.

**Paint-trace investigation.**—Justification for considering the patterns obtained by the flow of the nondrying paint indicative of boundary-layer flow paths directly at the surface was obtained by a comparison of the hydrogen sulfide trace with the paint trace in figure 10 (c), where the similarity between the patterns obtained is noteworthy. The obvious precautions are that the paint must be nondrying and capable of flowing when subjected to the air-flow gradients, and also that the test duration must be sufficient to ensure that the paint attain a final pattern rather than merely some intermediate patterns. Nevertheless, the assumption that paint flow traces correspond to air-flow paths can be considered valid only when confirmed by additional experimental evidence.

**Inlet boundary-layer conditions.**—For convenience in the course of making the modifications to the cascade as required for the geometric configurations under study, various lengths of inlet section, constructed of different materials, were used, because preliminary checks showed (within wide limits) that the thickness of the inlet boundary layer did not affect the type of results obtained. This conclusion is affirmed by noting that the general character of the fundamental secondary-flow phenomena is unchanged over the wide range of conditions investigated.

## RESULTS AND DISCUSSION

### INITIAL LOW-SPEED INVESTIGATION

The first stage of the experimental investigation of secondary flows was the visualization of the streamline patterns in the wall boundary layer of the basic two-dimensional cascade. The mainstream air velocity was maintained at approximately 30 feet per second, which permitted the use of smoke for visualizing.

**Spanwise variation of deflection.**—The initial phase of the experimental program was concerned with determining the nature and magnitude of the deflection of the wall boundary layer from the pressure surface of one blade toward the suction surface of the adjacent blade. The progressive increase in flow deflection as the wall is approached is qualitatively discussed in the literature. The flow deflection of smoke traces for three spanwise positions is shown in figure 4. In figure 4 (a), the smoke is admitted from the static tap with a velocity sufficient to project the smoke stream approximately ¼ inch from the wall. In figure 4 (b), the smoke velocity is reduced to the point where the smoke is projected approximately ⅛ inch from the wall. In figure 4 (c), the smoke velocity is further reduced so that the smoke tube lies against the wall in the vicinity of the tap. By superimposition of these three photographs, the variations in deflections are evident (fig. 4 (d)).

The results of the spanwise survey, shown in figure 4, demonstrate visually the increase in flow deflection in the wall boundary layer as the wall is approached, as anticipated in the literature. In figure 4 (c), the streamline path in the boundary layer very near the wall is clearly seen to cross the passage and to arrive at the suction surface of the passage well upstream of the blade trailing edge.

**Reliability of probe and static-tap results.**—The deflection in the boundary layer along the wall when smoke is admitted through a static tap located upstream of the blades is shown in figure 5. The smoke trace in figure 5 (b) was made by the smoke that remained in the static tap from the time of the previous photograph (fig. 5 (a)). In figure 5 (b), the pressure drop from outside the tunnel to the static pressure at the wall inside was negligible, and so the residual smoke must be considered to have assumed the direction of the air flow at the wall; that is, it was not projected out into the air stream. Figure 5 (c), a superimposition of figures 5 (a) and (b), indicates that, as these tests are conducted, each of the smoke traces so represented must be considered as lying along the wall in the neighborhood of its respective tap. This procedure was useful in establishing that the flow patterns at the wall itself could be visualized properly by means of smoke traces.

The deflection patterns obtained by a spanwise survey through the boundary layer, using the probe to introduce the smoke, are shown in figure 6. Paralleling the tests for figure 4, the probe was positioned so that the smoke was admitted ¼ inch from the wall (fig. 6 (a)), ⅛ inch from the wall (fig. 6 (b)), and at the wall (fig. 6 (c)). The superimposition of figure 4 on figure 6 is shown in figure 7. The close agreement between the streamline patterns obtained demonstrates that the presence of the probe does not unduly disturb the flow and that, under the test conditions, the probe results are reliable.

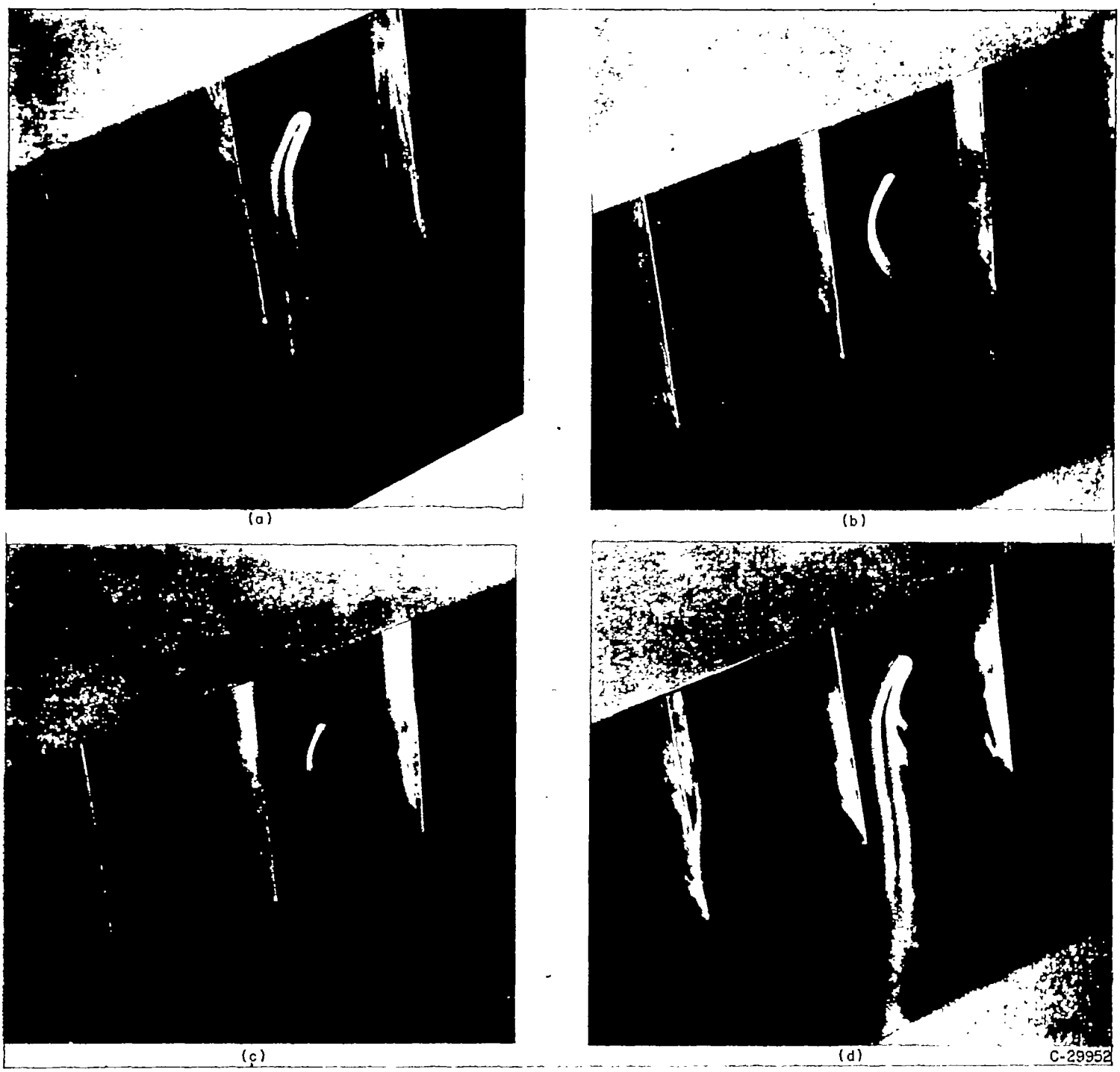


(a) Smoke trace ¼ inch from wall.
(b) Smoke trace ⅛ inch from wall.
(c) Smoke trace on wall.
(d) Superimposition of (a), (b), and (c).

FIGURE 4.—Variation of flow deflection in boundary layer. Smoke introduced through wall static tap.

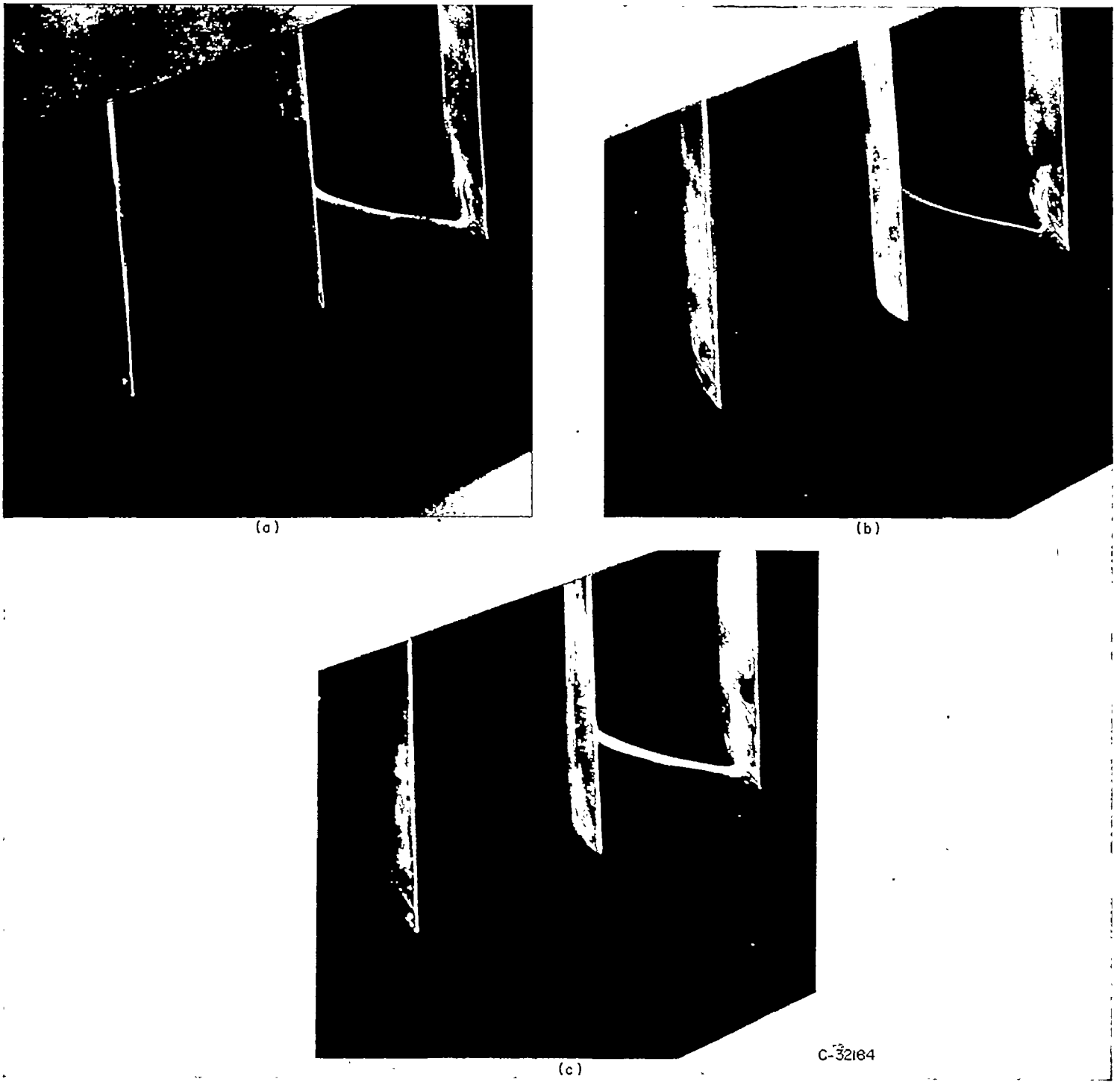


(a) Smoke through static tap. (b) Residual smoke through static tap.
(c) Superimposition of (a) and (b).

FIGURE 5.—Deflection of boundary layer along wall. Smoke introduced through static tap upstream of blades.

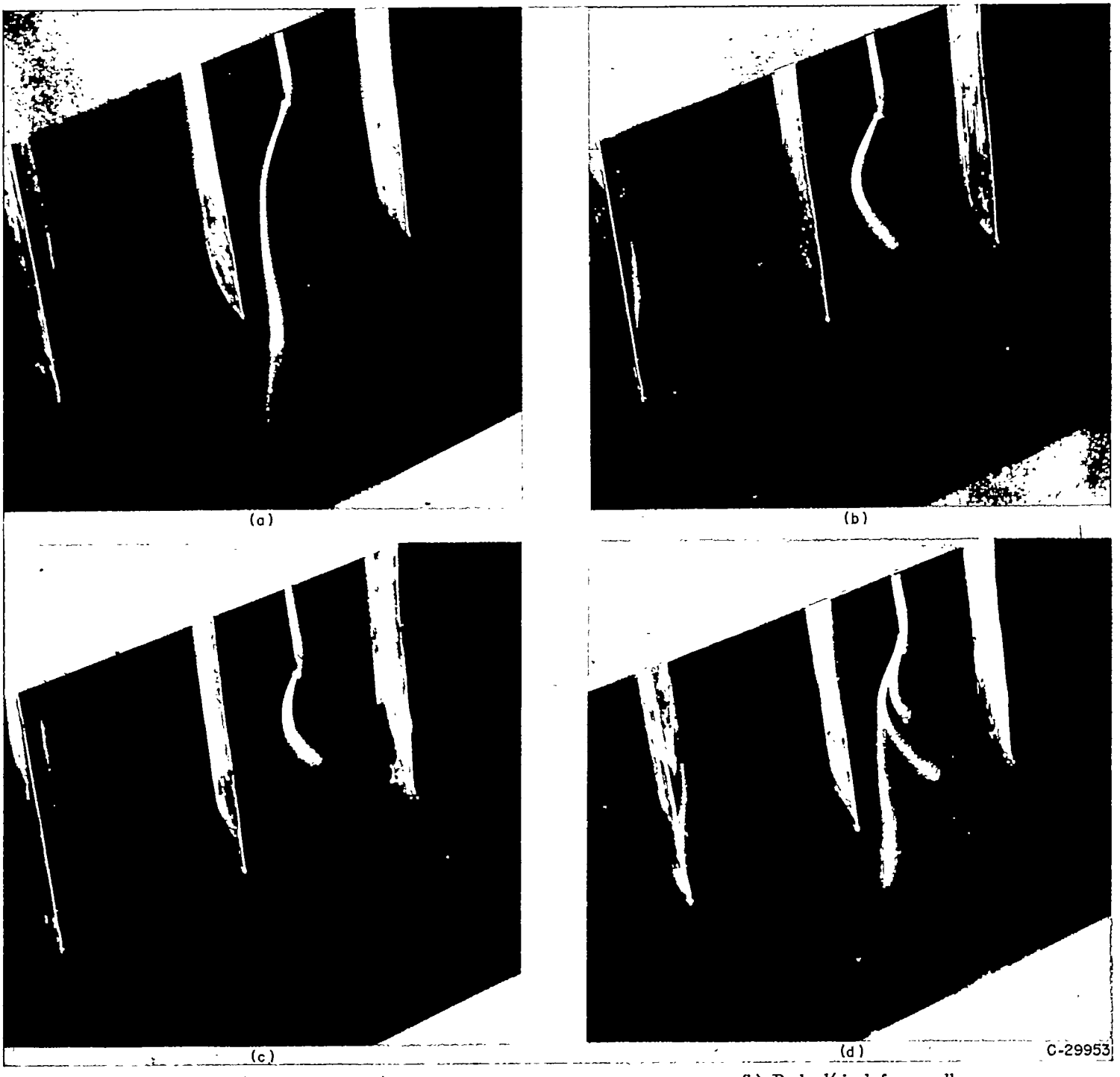


(a) Probe ¼ inch from wall. (b) Probe ⅛ inch from wall.
(c) Probe against wall. (d) Superimposition of (a), (b), and (c).

FIGURE 6. Variation of flow deflection in boundary layer. Smoke introduced through probe.

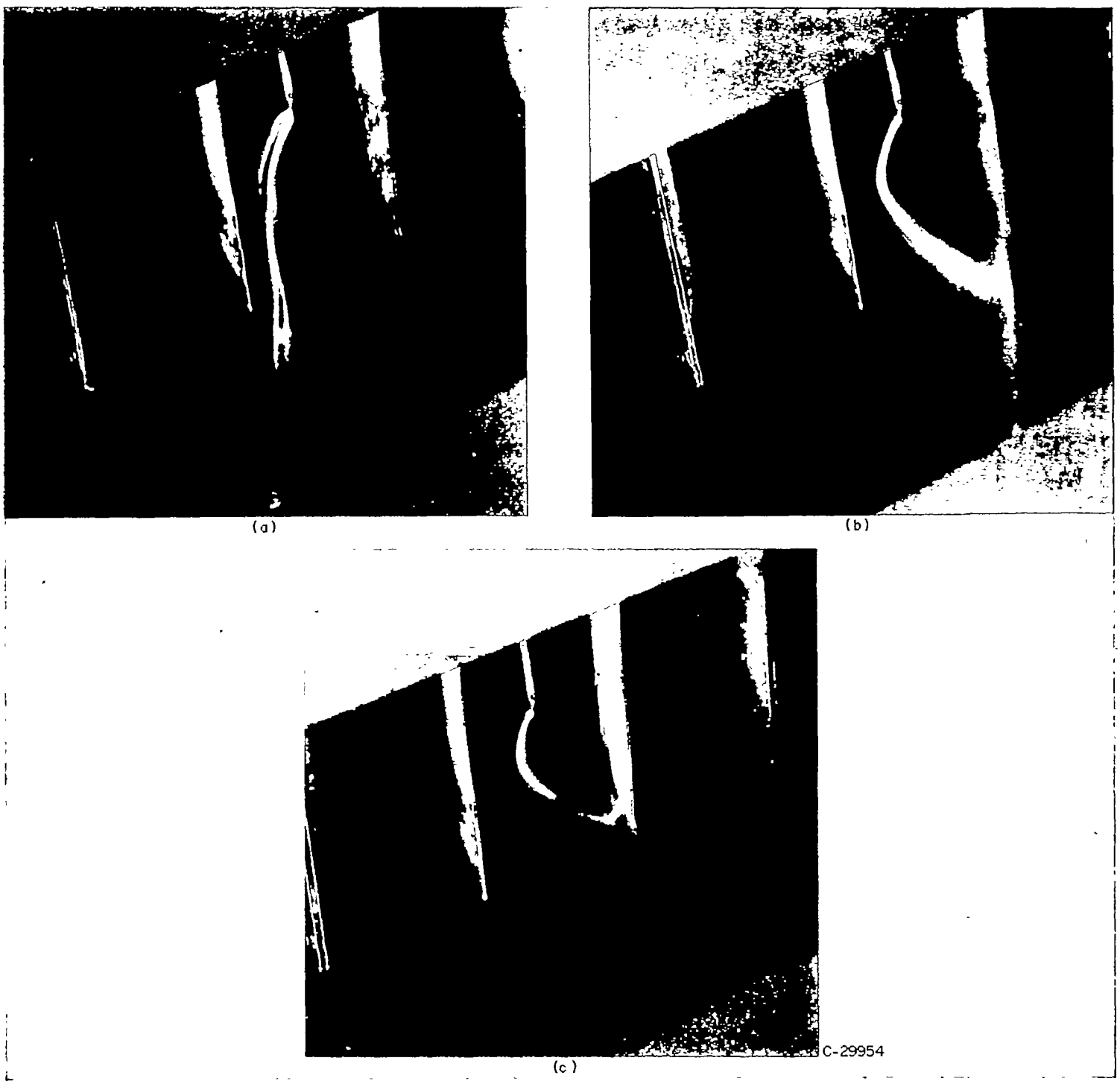


(a) Figures 6 (a) and 4 (a). (b) Figures 6 (b) and 4 (b).

(c) Figures 6 (c) and 4 (c).

FIGURE 7.—Superimposition of figures 6 and 4 demonstrating the reliability of probe results for flow visualization.

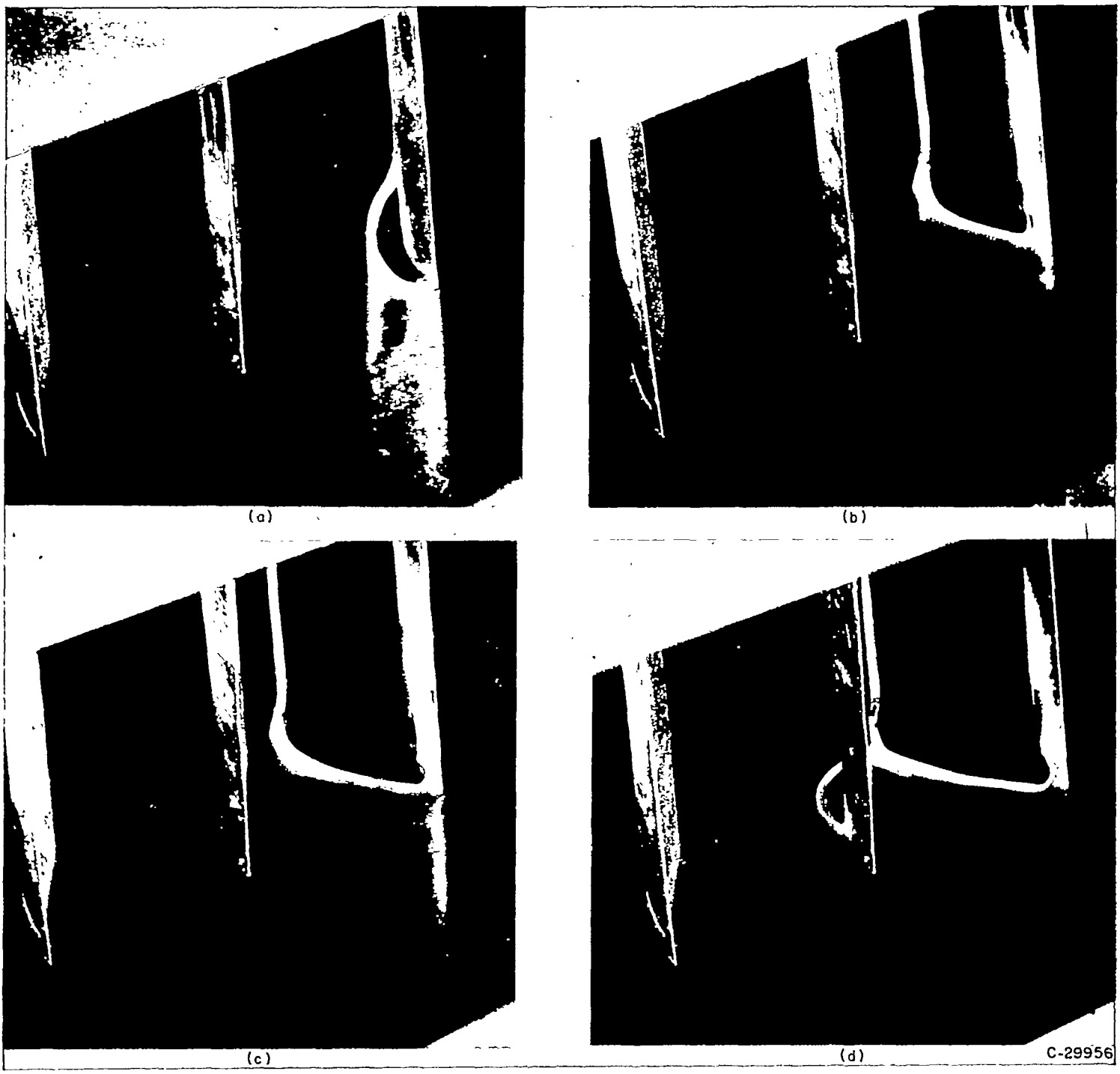


FIGURE 8.—Flow deflection in wall boundary layer of one passage. Smoke introduced by probe traverse along wall.

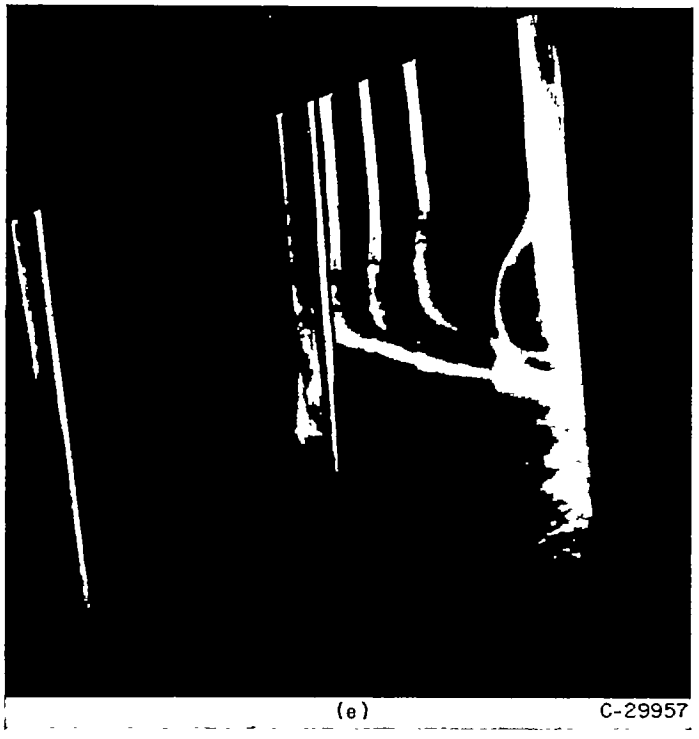


(e) Superimposition of (a), (b), (c), and (d).

FIGURE 8.—Concluded. Flow deflection in wall boundary layer of one passage. Smoke introduced by probe traverse along wall.

**Deflections along wall.**—Spanwise surveys through the boundary layer at other positions across the passage yielded patterns essentially similar to those in figures 4 and 6. In each case, the streamlines at the wall arrived at the suction surface of the blade at some point upstream of the trailing edge.

Figure 8 enables a direct comparison of representative paths of the streamlines obtained in one passage by a probe traverse along the wall. In each case shown in figure 8, the smoke was introduced with the probe directly against the wall, which, as was demonstrated by figure 7, serves to trace out the streamline of flow in the boundary layer on the wall itself at the probe location. These paths are seen in figure 8 (e), a superimposition of figures 8 (a) to (d), to be confluent in the corner at the suction surface of the passage near the trailing edge. This particular phenomenon of the convergence of these streamlines to a small region in the corner was neither anticipated nor implied elsewhere.

**Passage vortex formation.**—One of the chief drawbacks of the photographic presentation is that the smoke traces are seen in the photographs only as projections against the passage walls or against the blades. To an actual observer present at the time the tests were made, the streamlines pictured in figures 8 (a) to (d) appeared to be drawn, as if by a flow sink, to the corner made by the suction surface of the passage and the wall, as shown in figure 8 (e). As the streamlines approached this region, their paths took on a spiral twist (counterclockwise in the figures presented herein). Thus, the smoke streamline crossing the passage in figure 8 (d) remained on the wall until it reached the corner. Upon reaching the corner, the major portion of the smoke trace rolled up in a vortex and came off downstream; however, the smoke in this vortex (fig. 8 (d)) was diluted by the rest of the boundary-layer air comprising the vortex to the extent that it could not be perceived photographically at this camera angle.

As the smoke, during the probe traverse, was introduced progressively closer to the suction surface of the blade (figs. 8 (c), (b), and (a), respectively), the smoke streamlines were observed to deflect away from the wall as they proceeded downstream. The spanwise deflection of these smoke traces increased in this order, while the curvature of their paths of approach to the blade decreased in the same order. Therefore, in figure 8 (e), although the streamline of figure 8 (a) appears to cross the other streamlines, which is patently impossible, it actually deflected away from the wall farther than the other streamlines and passed over them. This process, whereby the boundary-layer streamlines at and near the wall cross the passage while some of them are displaced spanwise farther from the wall than others, results in the formation of the so-called passage vortex. The patterns shown in figure 8 illustrate how part of the inlet boundary layer rolls up to form part of the passage vortex.

The vortex formation, as described here, occurred well in the passage and not as a trailing-edge phenomenon. When a smoke stream was introduced near the blade leading edge in the corner formed by the suction surface and the wall, it was observed to assume the same type of counterclockwise spiral rotation in the passage axially at approximately the blade midchord position. Because of the tightness of the spiral and because the photographs show only path projections, it has not been possible to obtain a suitable photograph of this evidence of vortex formation within the passage of the basic two-dimensional cascade. Photographic evidence of passage vortex formation is presented with the section on

SECONDARY FLOWS IN BENDS AND HIGH-TURNING CASCADES

At the flow speeds used for these tests, laminar separation probably occurred on the suction surfaces of the blades near the trailing edges. When smoke was introduced into the wall boundary layer (fig. 8), a small portion of this smoke eddied out onto the blades into the separated-flow region. This slow accumulation of smoke in the stagnant region produced the dense traces seen on the blades.

**Deflections on blades.**—The streamline deflection on the blades caused by secondary flow is noted and pictured in reference 1. Figure 9 presents the smoke-trace patterns of this deflection. The smoke (fig. 9 (a)) was admitted through the probe approximately $\frac{3}{16}$ inch from the wall and in such a position that the smoke stream split and divided on the blade. In figure 9 (b), the probe was $\frac{1}{2}$ inch from the wall, positioned so that the smoke path lay on the pressure surface of the blade. In figure 9 (c), with the probe at the wall, the smoke followed the suction surface of the blade.

The manner in which the flow on the blade was deflected spanwise toward the wall on the blade pressure surface and spanwise away from the wall on the blade suction surface is clear in figure 9. A comparison of figures 9 (b) and (c) shows that the deflection on the suction surface was much greater than that on the pressure surface. Such large deflection differences were not to be anticipated from secondary-flow mechanisms similar to that described in reference 1. The large deflection difference evident in figure 9 is here principally attributed to the area-blockage effect of the passage vortex near the suction surface, which causes a large deflection of the flow on the blade suction surface. The region between the smoke trace in figure 9 (c) and the wall is, therefore, a rough measure of the size of the passage vortex.

As a result of the flow deflection off the blade pressure surface, air flowed onto the passage wall and was observed to become the wall boundary layer for the region downstream of the smoke trace of figure 8 (d). The presentation of this phenomenon photographically was prevented by the rapid thinning of the smoke as it left the blade and diffused on the wall. This deflection will be shown photographically later with the higher-turning configurations.

**Remarks on initial low-speed investigation.**—The secondary-flow pattern in the basic two-dimensional cascade at low airspeeds is a three-dimensional deflection of the flow in the end-wall boundary layer, both in the spanwise direction normal to the wall and across the passage along the wall. As a result, the boundary layer rolls up to form a passage vortex well up in the passage and not as a trailing-edge phenomenon. In the region near the low-pressure side of the passage where the vortex forms, large gradients of pressure and flow direction make it difficult to take accurate measurements. The complicated three-dimensional nature of this flow makes questionable, too, the applications to date of any two-dimensional, or quasi-three-dimensional, analyses of the flow patterns in the wall region and certainly influences the entire flow through the passage.

### INITIAL HIGH-SPEED INVESTIGATION

In order to visualize the flow patterns at higher air velocities (larger Reynolds numbers), it was necessary to use the hydrogen sulfide and the paint flow-trace methods. The construction of the two-dimensional cascade precluded its use for flows above a Mach number of approximately 0.4. Therefore, the annular-turbine-nozzle cascade rig was used for the higher subsonic and for the supersonic Mach numbers.

**Deflections on wall in two-dimensional cascade.**—The visualization of the flow along the passage wall and blade at Mach numbers of approximately 0.4 is shown in figure 10. The pattern in figure 10 (a) was made by hydrogen sulfide introduced through a static tap upstream of the blades. A portion of the hydrogen sulfide trace that actually reached and flowed onto the suction surface of the blade but was too faint to photograph is shown by the dotted line in figure 10 (a). The toxicity and obnoxious odor of the hydrogen sulfide prevented its use in this cascade (which discharges into the room) for the extended period of time required to darken the trace further.

In order to circumvent this difficulty, an effort was made to concentrate the hydrogen sulfide trace in the region of chief interest by use of a passage wall static tap. In figure 10 (b), the hydrogen sulfide was introduced through a static tap in the passage; the flow to the corner and onto the blade can be seen somewhat more clearly.

The dark trace on the first blade on the left shown in figure 10 (c) was due to hydrogen sulfide released from a wall static tap so located that the flow divided on the blade. A faint hydrogen sulfide trace is, of course, obtained immediately upon release of the gas, but it was necessary to run the test for a prolonged period of time in order to intensify the trace sufficiently for photographing. During this protracted run, the paint on the rest of the blades in figure 10 (c) was observed to flow slowly until it assumed the final pattern apparent in the picture. The similarity between the hydrogen sulfide trace and the paint patterns is noteworthy.

**Deflections on shrouds of three-dimensional cascade.**—The deflection patterns at Mach numbers higher than 0.4 were obtained by applying the hydrogen sulfide flow-visualization method to the annular-nozzle ring of a typical modern high-speed turbine. In the annular-turbine-nozzle cascade it was possible to use the hydrogen sulfide for a sufficient length of time to make the clear, dark traces presented in figures 11 and 12. Figure 11 shows the hydrogen sulfide traces obtained with the annular cascade at a hub discharge Mach number of approximately 0.9 and a tip discharge Mach number of approximately 0.7. A view of the cascade inner shroud at the blade-row inlet is shown in figure 11 (a). The hydrogen sulfide was admitted through one wall static tap in each of two adjacent passages, and the tap positions relative to the blades can be seen in figure 11 (a).

The results in figure 11 (b) show that again the pattern has been repeated: In each case the flow deflects across the passage, arrives at the suction surface of the blade, and flows out on the blade. The shape of the flow traces on the blades and shrouds indicates possibly the formation of a vortex within the passage in the annular cascade as well as in the two-dimensional cascade. In figure 11 (c), the pattern is repeated at the outer shroud with high subsonic Mach numbers.

The hydrogen sulfide traces for the same annular cascade when the approximate hub and tip discharge Mach numbers were 1.5 and 1.2, respectively, are presented in figure 12. The inner- and outer-shroud static taps used here were the same ones used for figure 11. Despite flow discontinuities caused by the supersonic flow velocities involved, the deflection pattern on the shrouds is repeated and the possible formation of passage vortices is indicated.

**Remarks on initial high-speed investigation.**—The pattern of deflection of the wall boundary-layer flow across the passage was repeated at Mach number 0.4 in the two-dimensional cascade and again at the high subsonic and supersonic Mach numbers in the annular cascade. Although, strictly speaking, the hydrogen sulfide and paint flow-visualization methods used in this section show what happens in the boundary layer only at the boundary itself, there are indications that passage vortex formation may also occur at the high speeds.

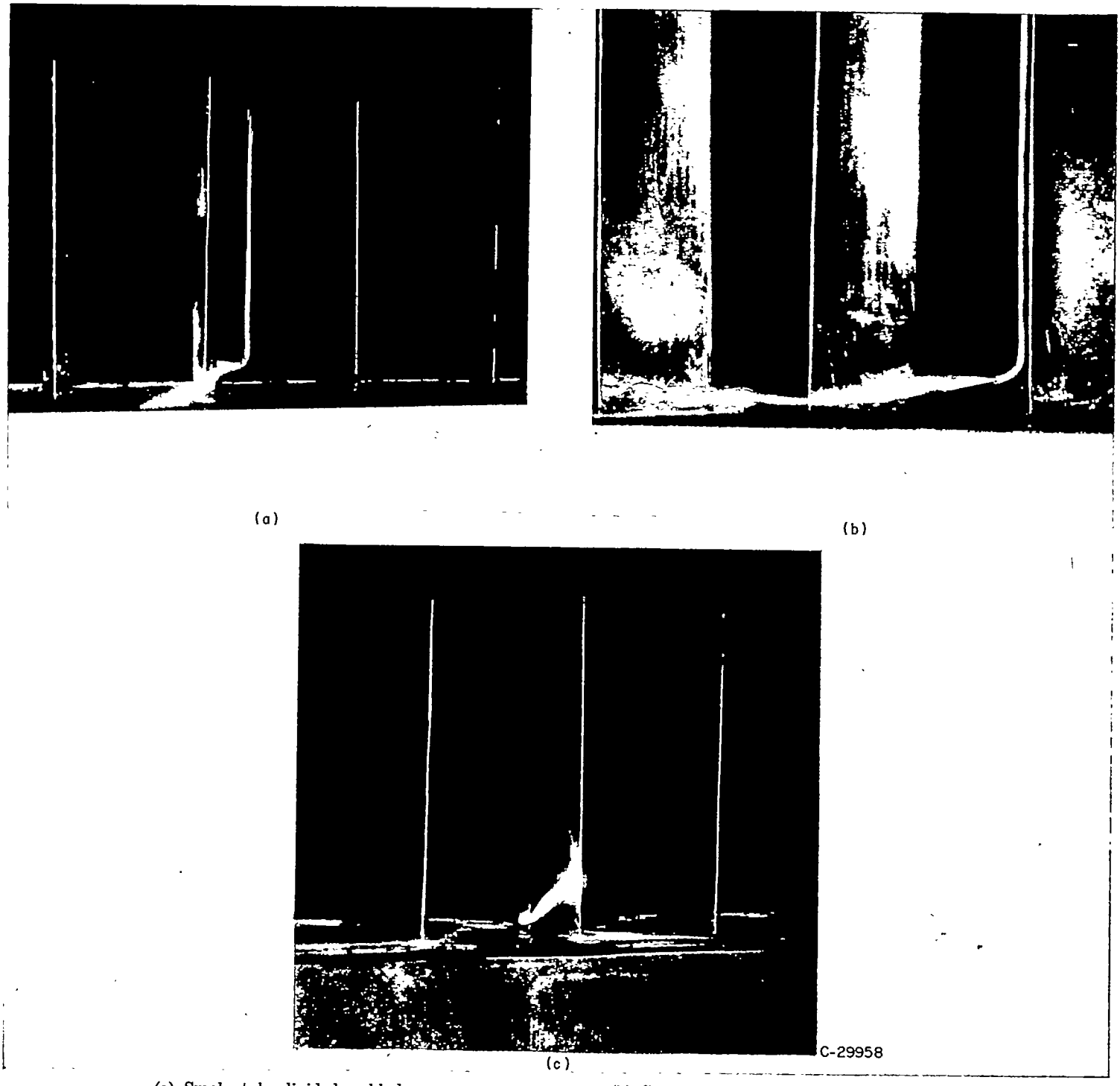


(a) Smoke tube divided on blade. (b) Smoke tube on pressure surface of blade.
(c) Smoke tube on suction surface of blade.

FIGURE 9.—Flow deflections on blade.

368555—56——12

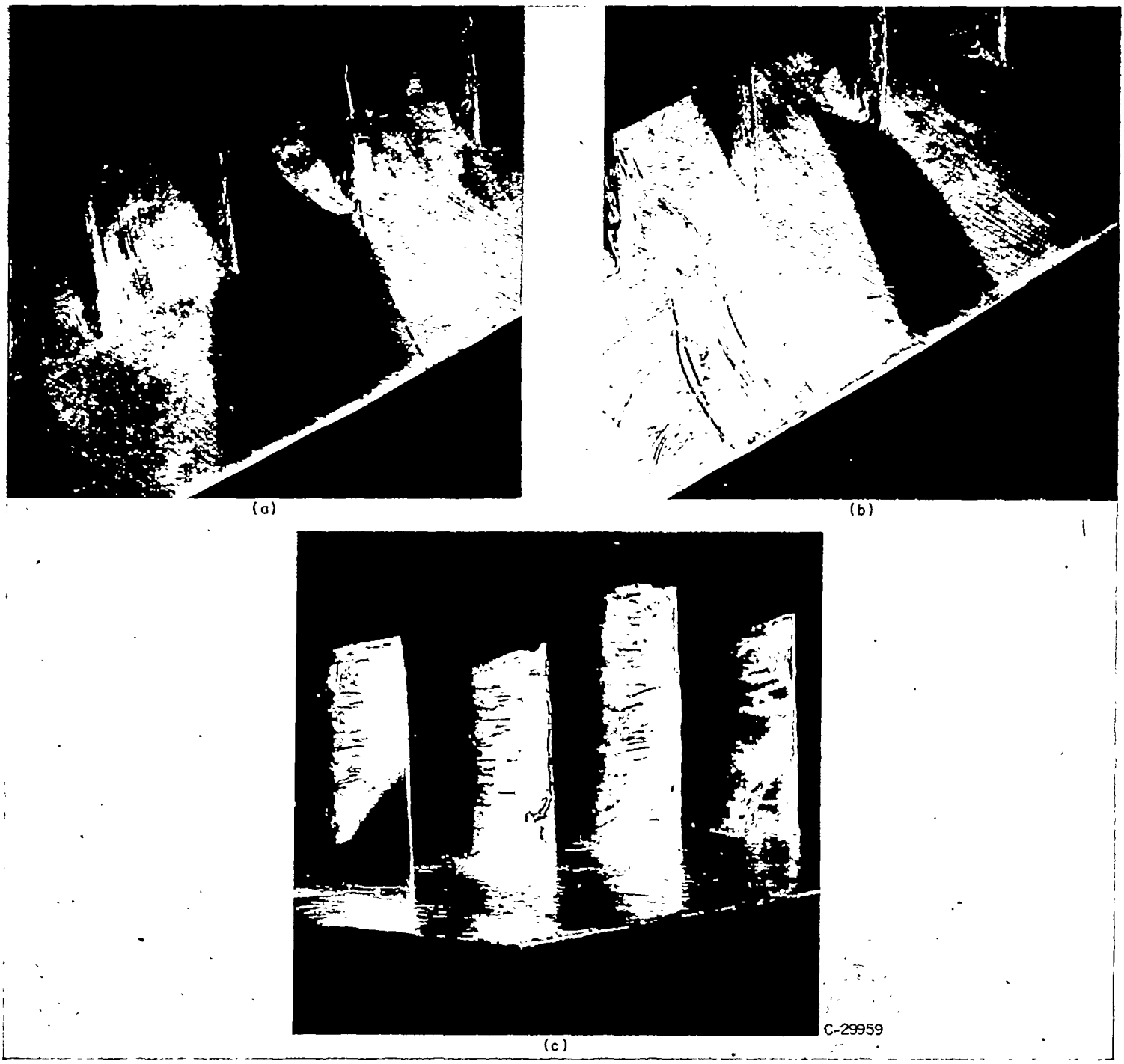


(a) Hydrogen sulfide introduced through upstream static tap. (b) Hydrogen sulfide introduced through tap in passage.
(c) Hydrogen sulfide and paint traces on blade suction surfaces.

FIGURE 10.—Flow traces in two-dimensional cascade at Mach numbers of approximately 0.4.

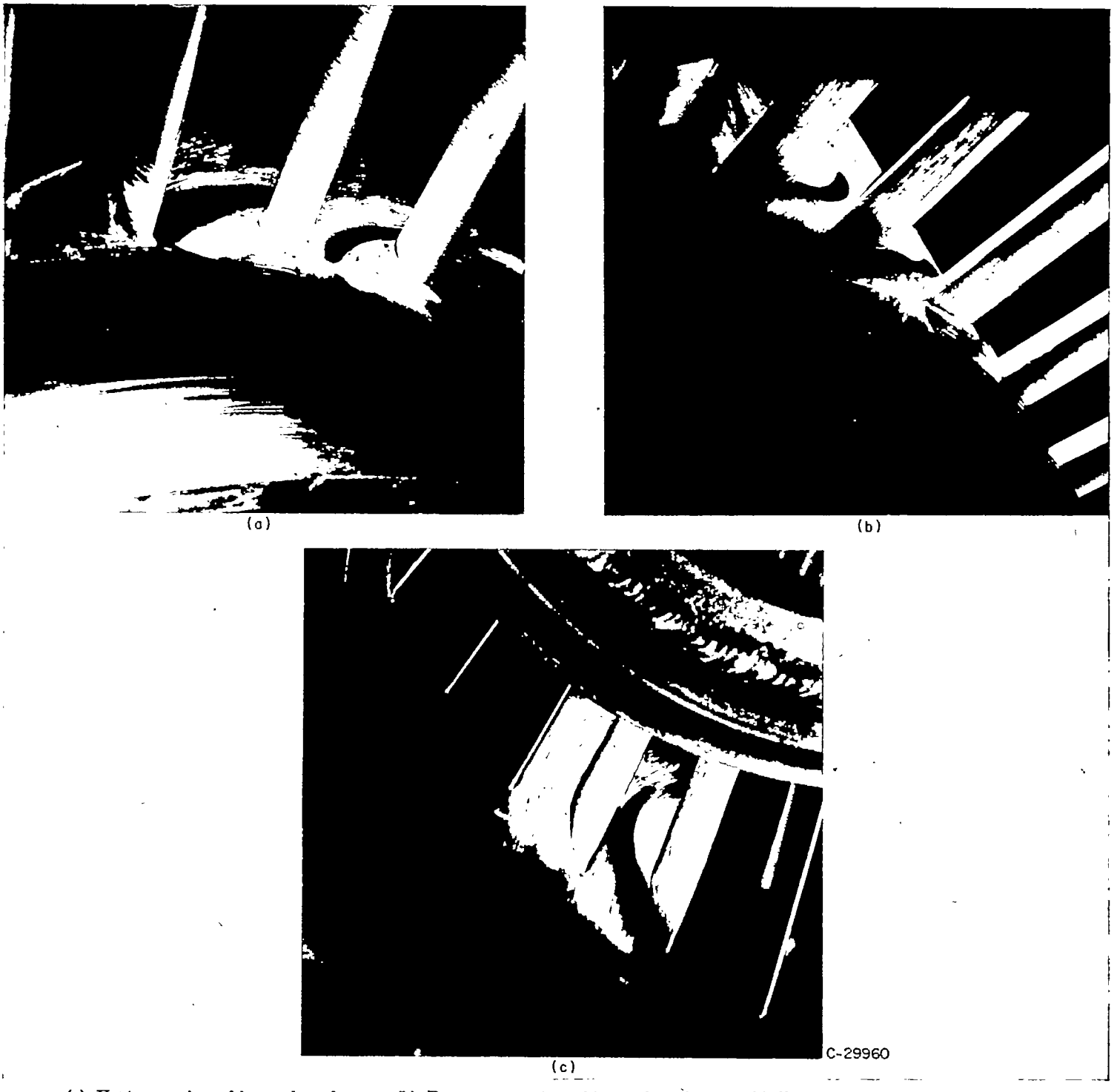


(a) Upstream view of inner shroud. (b) Downstream view of inner shroud. (c) Downstream view of outer shroud.

FIGURE 11.—Hydrogen sulfide traces in annular-turbine-nozzle cascade at high subsonic velocities. Hub discharge Mach number, approximately 0.9; tip discharge Mach number, approximately 0.7.

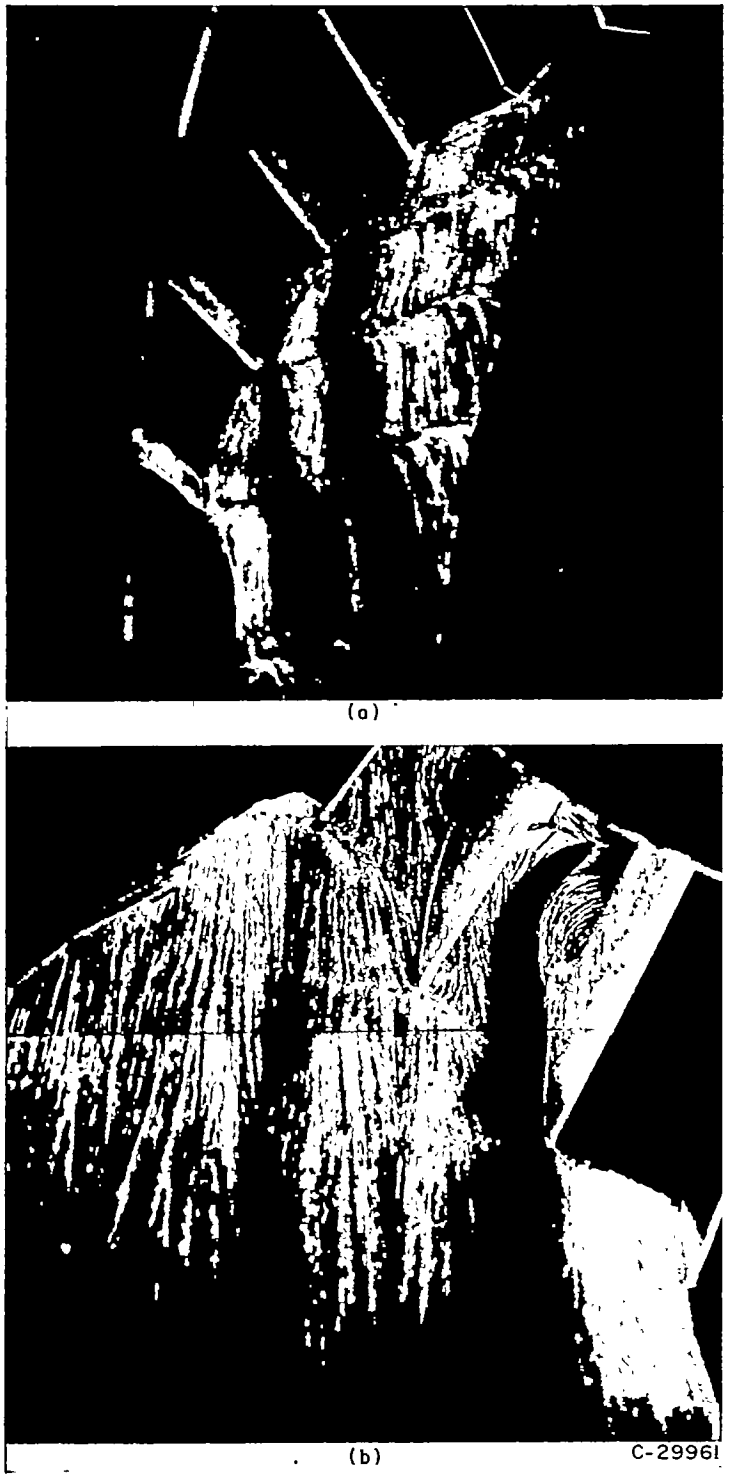


(a) Downstream view of inner shroud.
(b) Downstream view of outer shroud.

FIGURE 12.—Hydrogen sulfide traces in annular-turbine-nozzle cascade at supersonic velocities. Hub discharge Mach number, approximately 1.5; tip discharge Mach number, approximately 1.2.

### CASCADE PARAMETER INVESTIGATION

In this section, the effects of variations of the cascade parameters (blade geometry) on the secondary flows are investigated. In the region of extremely large velocity gradients and angle deflections, where the passage vortex is formed, the accuracy of total-pressure and flow-angle measurements is severely limited and the interpretation of such quantitative measurements must be made with care. For these reasons, the influence of blade geometry on secondary flows was investigated qualitatively by means of appropriate modifications to the basic two-dimensional cascade. The cascade was modified for the investigation of the following numerical values of parameters in addition to those already reported for the basic two-dimensional cascade (the parenthetical values are those of the basic cascade): stagger angle, 0° (45°); aspect ratio, 1.67 (2.34); solidity, 2.0 (1.5), and 0.75; angles of attack, 4°, 7° (11°), 15°, and 20°. Also, blade fillets were added on the suction surface, on the pressure surface, and on both surfaces, successively, to evaluate their effects on the secondary flows.

In each case with the mainstream velocity about 30 feet per second, the secondary-flow patterns were observed by the smoke flow-visualization techniques, and the results are presented photographically.

Stagger angle.—The deflections of the streamlines in the inlet boundary layer that join in a region near the suction surface are demonstrated in figures 13 (a) to (c) for a cascade with a stagger angle of zero (where stagger angle is the angle between the cascade axis and the incoming air). The values of the parameters are given in the legend for each photograph of this section. The streamline pattern can be seen, by comparison, to be essentially identical with the pattern in figure 8, where the stagger angle is 45°. Therefore, for convenience in photographing, the 0°-stagger-angle configuration was used for the remainder of the tests.

The path of a streamline in the main flow through the cascade with a stagger angle of zero is shown in figure 13 (d). It was observed during the tests that the total turning of the flow is essentially unchanged from that of the cascade with a stagger angle of 45°.

Aspect ratio.—The aspect ratio for the two-dimensional cascade was reduced from 2.34 to 1.67 by means of specially devised inserts along the end walls. The boundary-layer streamlines (fig. 14) remained unaffected. It was observed during the test that the spanwise deflection of corresponding streamlines in the boundary layer was also unaffected by the change in aspect ratio.

Solidity.—With the solidity (ratio of blade chord to blade spacing) reduced from 1.5 to 0.75, the main portion of the inlet boundary-layer streamline at a blade nose was not deflected completely across the channel (fig. 15 (a)). Most of the smoke was deflected part way across the channel and then proceeded downstream. The wisp of smoke seen at the trailing edge reached there by flowing upstream in the separated region behind the suction surface of the blade. For the case with the solidity reduced to 0.75, it was observed that the three-dimensional aspects of the boundary-layer flow, namely, the deflection of streamlines near the

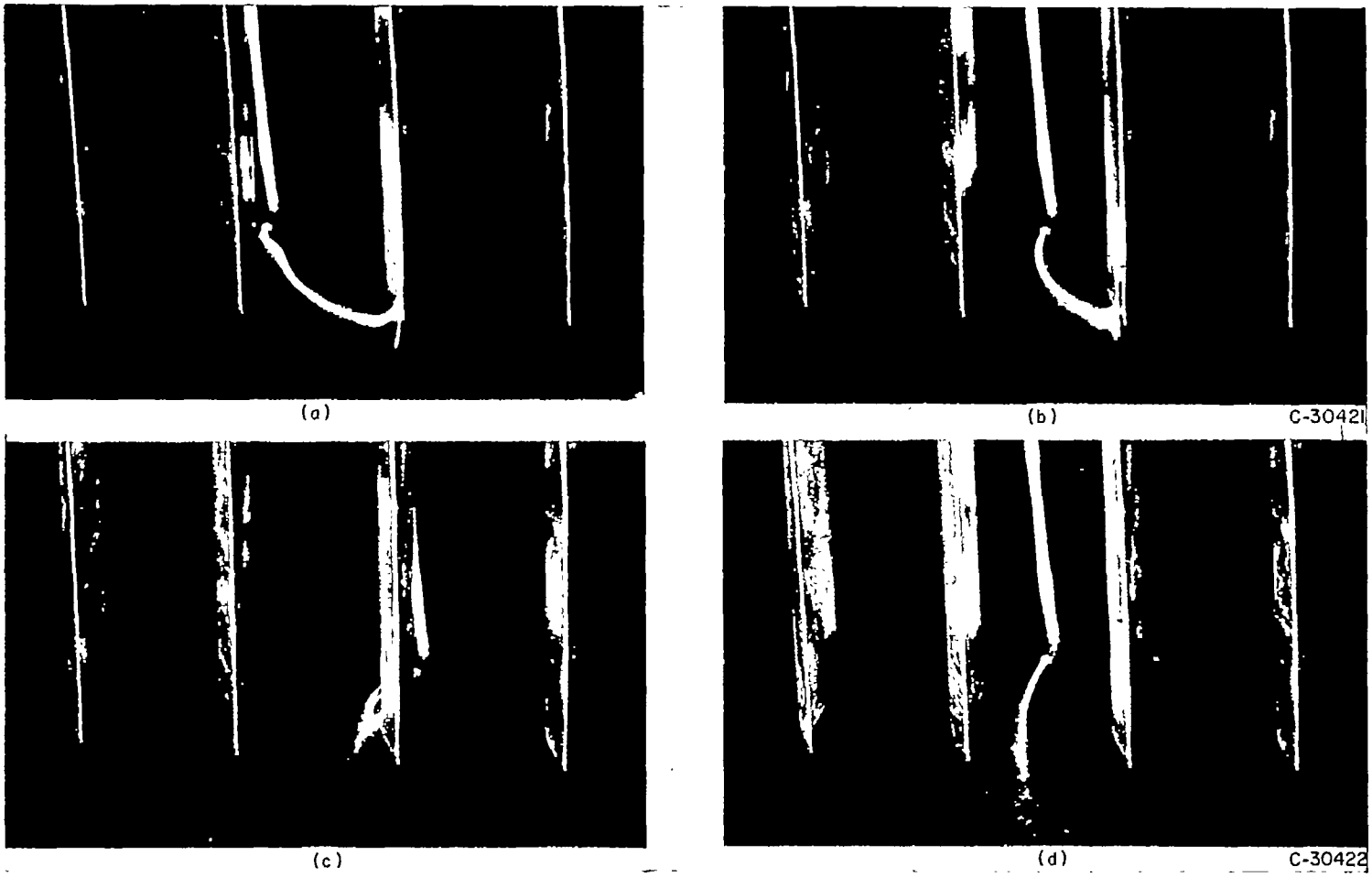


(a) Probe on wall near pressure surface.
(b) Probe on wall in midchannel.
(c) Probe on wall near suction surface.
(d) Probe away from wall in mainstream.

FIGURE 13.—Streamline pattern in cascade with stagger angle of zero. Solidity, 1.5; angle of attack, 11°; aspect ratio, 2.34.

suction surface in a direction away from the wall, had decreased considerably and the passage vortex was smaller. Because the camera shows only projections, the deflections away from the wall could not be photographed here. Consequently, the photographs show only cross-channel deflection; but the three-dimensional aspects of the flow cannot be ignored for proper interpretation of the phenomena reported.

The streamline for the first probe location at which the suction surface was reached by cross-channel flow is shown in figure 15 (b). The turning of the mainstream (fig. 15 (c)) is less at the low solidity of 0.75 than at the design solidity of 1.5 (fig. 13 (d)).

The results of tests at a solidity of 2.0 are shown in figure 16. Figure 16 (a) shows that the boundary-layer streamline at the nose of one blade is deflected all the way across the channel, as might be expected. The deflections of the secondary-flow streamlines in the spanwise direction are observed to have increased over those in the basic cascade. The mainstream flow illustrated in figure 16 (b) is turned somewhat more than in the basic cascade (solidity, 1.5).

**Angle of attack.**—The streamline patterns were investigated for the cascade at the original solidity of 1.5 and at angles of attack of 4°, 7°, 15°, and 20° (original angle of attack, 11°). Figures 17 and 18 show the results of the tests at 4° and 20°, respectively. At a 4° angle of attack (fig. 17), it was necessary to move the probe halfway across the channel at the inlet in order to find a streamline that would deflect to the suction surface. As the angle of attack increased, the deflections across the channel and spanwise away from the wall increased and the passage vortex became larger.

**Combined solidity and angle of attack.**—The streamline paths for the cascade with solidity of 0.75 and angle of attack of 4° are shown in figure 19. Again, it was necessary to move the probe almost halfway across the channel at the inlet in order to find a streamline that was deflected to the suction

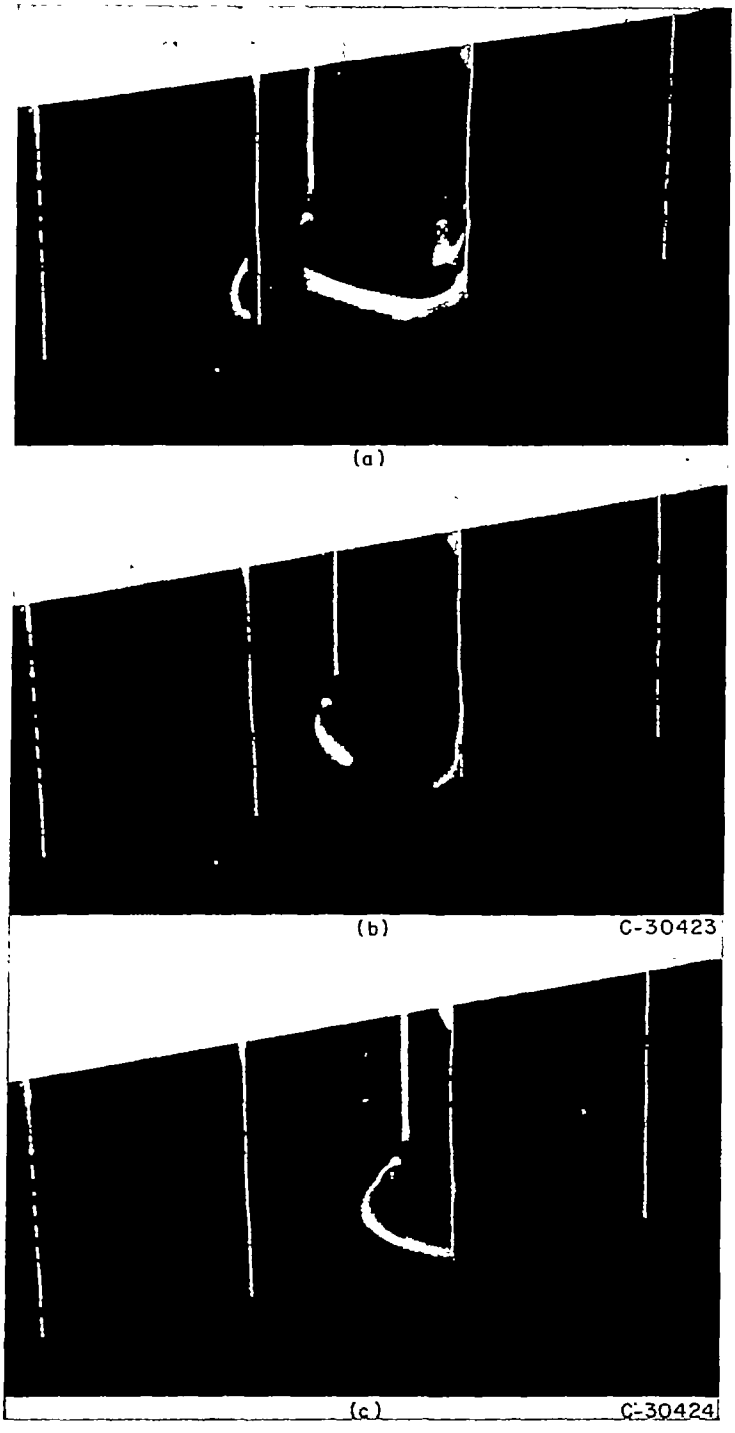


(a) Probe on wall at nose of blade.
(b) Probe on wall near pressure surface.
(c) Probe on wall near suction surface.

FIGURE 14.—Streamline pattern in cascade with aspect ratio of 1.67. Stagger angle, 45°; solidity, 1.5; angle of attack, 11°.

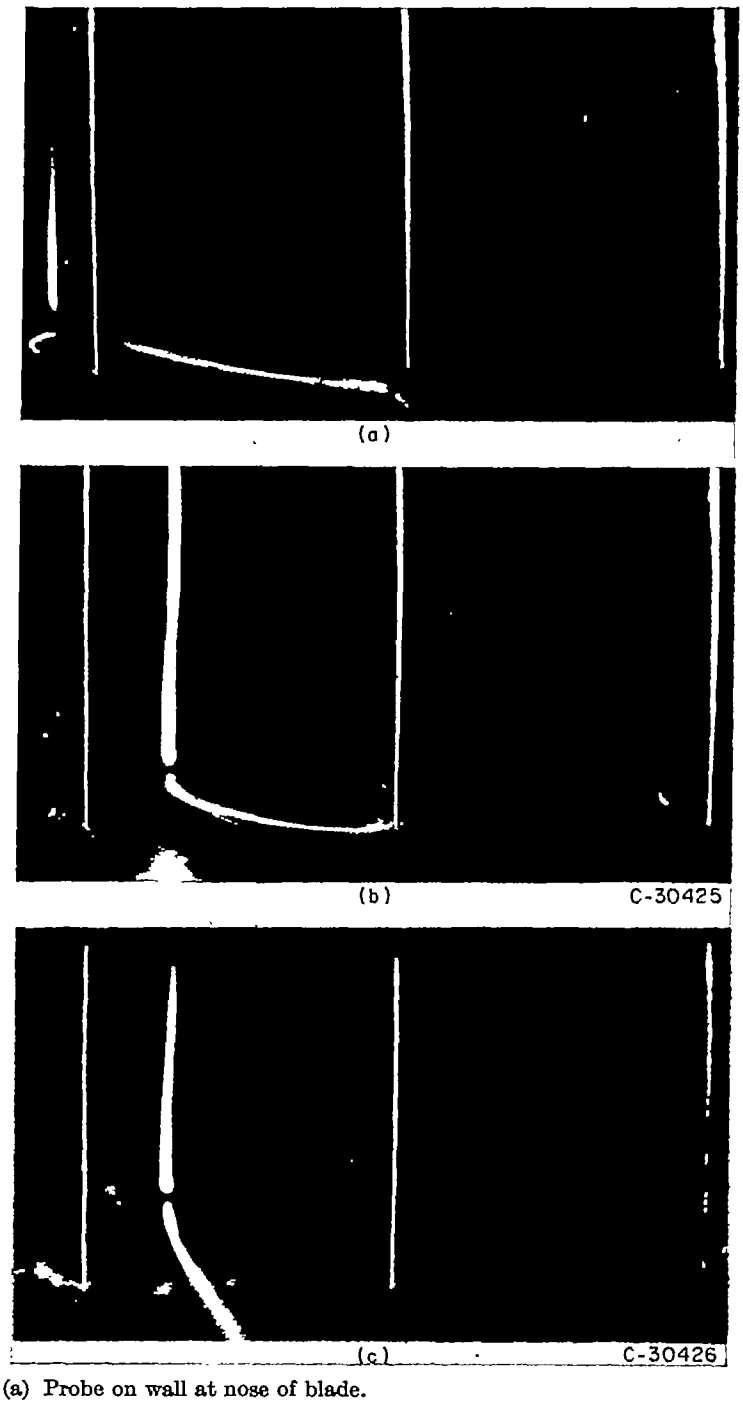


(a) Probe on wall at nose of blade.
(b) Probe on wall at point where smoke first reached suction surface.
(c) Probe away from wall in mainstream.

FIGURE 15.—Streamline pattern in cascade with solidity of 0.75. Stagger angle, 0°; angle of attack, 11°; aspect ratio, 2.34.

surface. It was observed that in this case the deflections away from the wall were smaller than for the basic configuration. At a solidity of 2.0, an angle of attack of 20°, and with the probe away from the wall (fig. 20 (a)), some streamlines in the blade boundary layer well up on the pressure surface of a blade deflect to the wall and cross the channel to the suction surface of the next blade, there to comprise part of the passage vortex. A comparison of the amounts of turning of the mainstreams for the two configurations, which represent the extremes of the ranges investigated, is possible with the use of figures 19 (c) and 20 (b).

This study of solidities and angles of attack indicates that the over-all turning of the mainstreams of the blade rows is a

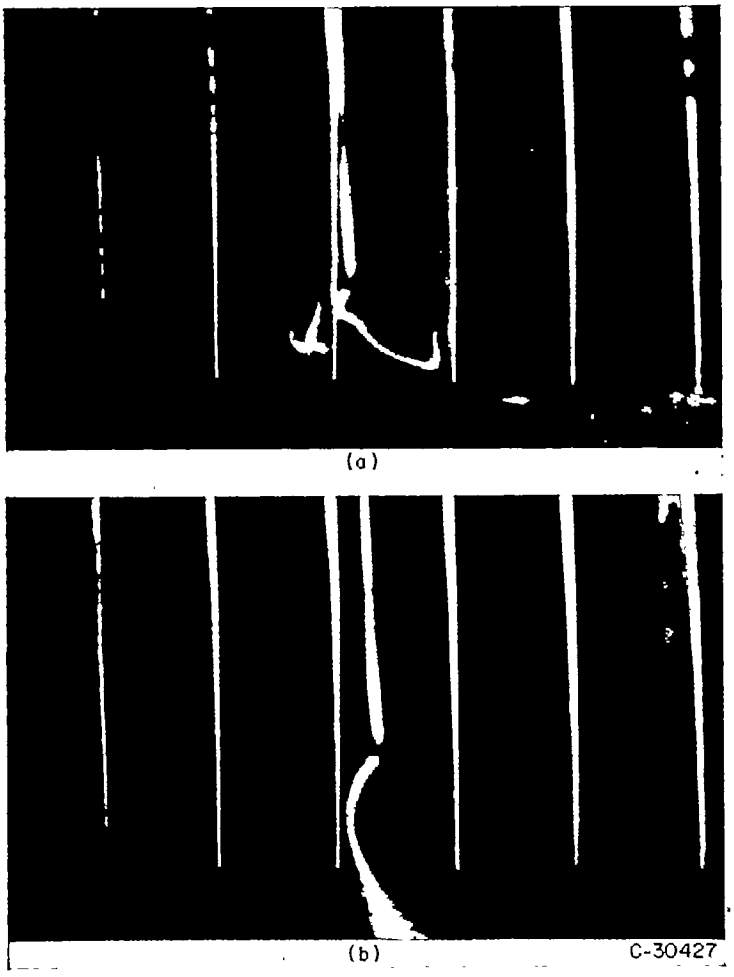


(a) Probe on wall at nose of blade.
(b) Probe away from wall in mainstream.

FIGURE 16.—Streamline pattern in cascade with solidity of 2.0. Stagger angle, 0°; angle of attack, 11°; aspect ratio, 2.34.

major factor in the cross-channel and spanwise deflections of the inlet wall boundary layer. Furthermore, it was observed during these tests that, for the configurations involving greater turning of the mainstream, the spanwise deflection of the corresponding streamlines in the boundary layers increased, the roll-up into the passage vortex was tighter, and the vortex was larger.

The study of flows through bends in the next section of this report presents more qualitative information on the effects of mainstream turning variation on secondary flows.

**Blade fillets.**—Streamlines for configurations having fillets of approximately $\frac{3}{16}$-inch radius of curvature on the blade pressure surface, blade suction surface, and on both blade surfaces are shown in figures 21 (a), (b), and (c), respectively. The fillets apparently had little effect on the formation of the passage vortices. Similar results were obtained with larger fillets.

**Remarks on cascade parameter investigation.**—Throughout the investigation of various geometric configurations of the two-dimensional cascade, the basic mechanism of the formation of a secondary-flow passage vortex was unchanged; however, the degree to which the wall boundary layer deflected away from the wall and across the channel, as well as the size and tightness of the passage vortices, was influenced by those parameters which involved the turning of the main flow. These parameters, as illustrated by the figures, were solidity and angle of attack. Parameters such as aspect ratio and stagger angle, which did not alter the turning, had no apparent influence on this secondary flow. Furthermore, the fillets on the blades had no appreciable effect on the passage vortex roll-up.

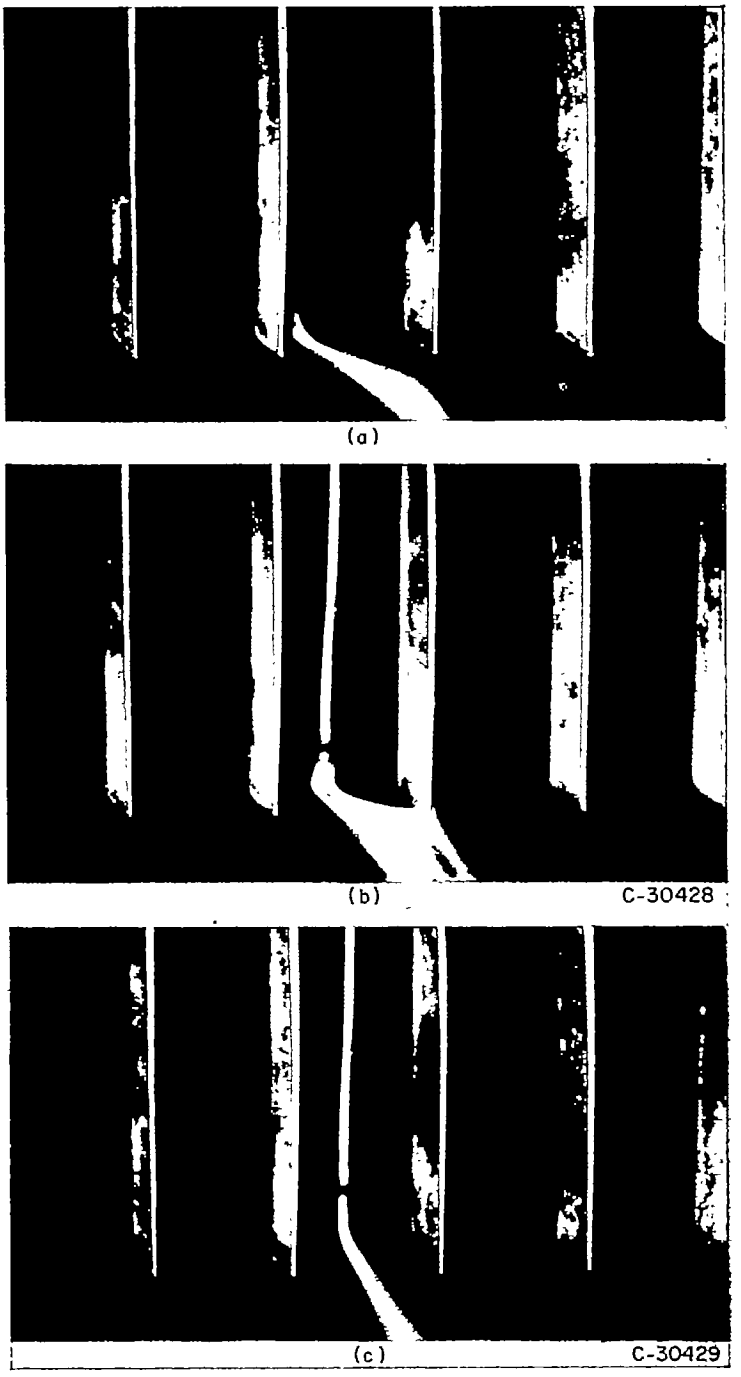


(a) Probe on wall at nose of blade.
(b) Probe on wall at point where smoke first reached suction surface.
(c) Probe away from wall in mainstream.

FIGURE 17.—Streamline pattern in cascade with angle of attack of 4°. Stagger angle, 0°; solidity, 1.5; aspect ratio, 2.34.

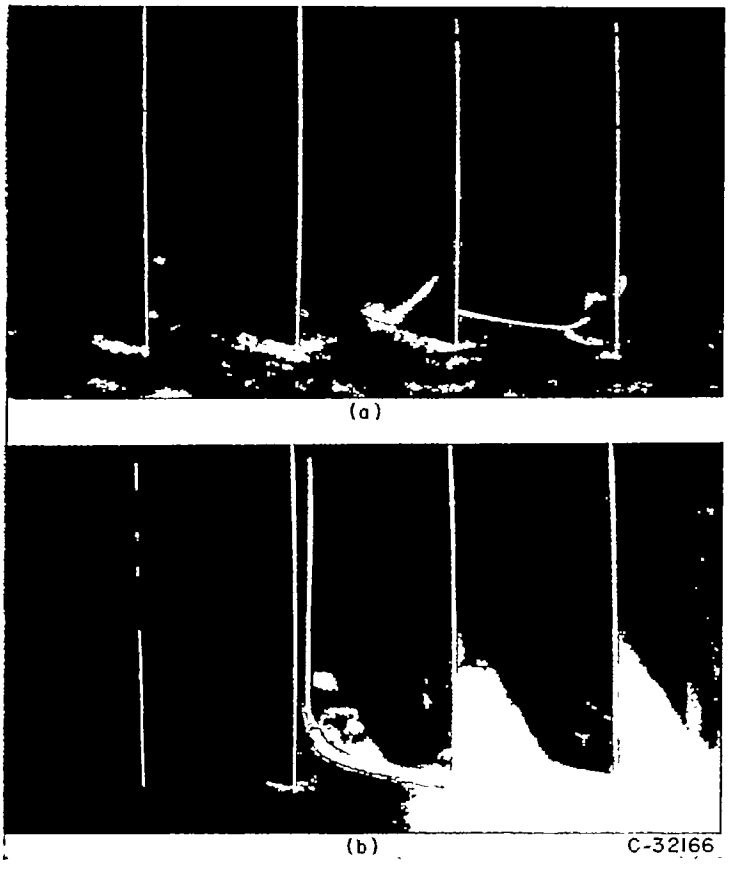


(a) Probe on wall at nose of blade.
(b) Probe away from wall in mainstream.

FIGURE 18.—Streamline pattern in cascade with angle of attack of 20°. Stagger angle, 0°; solidity, 1.5; aspect ratio, 2.34.

### SECONDARY FLOWS IN BENDS AND HIGH-TURNING CASCADES

**Secondary flow in bends.**—It has been noted in the literature (cf. ref. 4) that low-stagnation-pressure fluid in the end-wall boundary layers of rectangular bends moves across the passage from the pressure toward the suction side. It has been indicated further that, upon reaching the suction surface, the low-stagnation-pressure fluid is displaced away from the wall and out into the mainstream.

The smoke visualization technique was applied to the study of the boundary-layer flow in two sets of rectangular bends with the following results. As noted earlier, the curved walls of the 45° rectangular bends are concentric circular arcs, so that the main-flow streamlines may be as nearly circular as possible in the turning section of the elbow. Figure 22 shows the typical pattern of passage vortex formation described for cascades earlier in this report. The smoke, introduced at the wall and near the pressure surface of the bend, crossed the passage and rolled up near the suction surface. Because of the greater turning involved in this case than heretofore, the roll-up and vortex formation are much more distinct, and more satisfactory photographs of the passage vortex phenomenon are possible.

The smoke filament in any of these pictures actually traces out the path of only one of the streamlines comprising a passage vortex. Because of the symmetry of the flow in such a vortex, however, the behavior of any one streamline can be considered representative of the entire vortex flow. Accordingly, in this report, when the roll-up of a streamline into a vortex is shown, it is characterized as the entire vortex in the discussion of the figure.

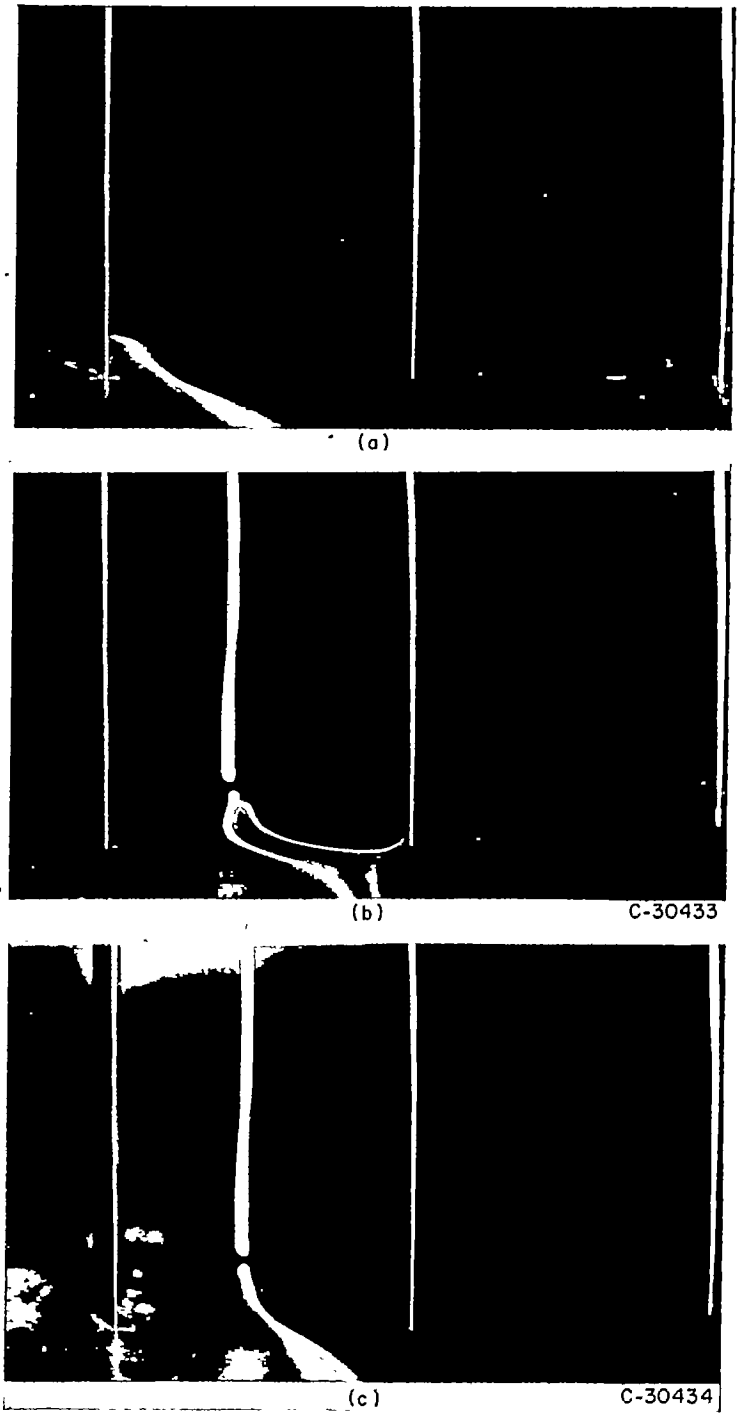


(a) Probe on wall at nose of blade.
(b) Probe on wall at point where smoke first reached suction surface.
(c) Probe away from wall in mainstream.

FIGURE 19.—Streamline pattern in cascade with solidity of 0.75 and angle of attack of 4°. Stagger angle, 0°; aspect ratio, 2.34.

Figure 23 shows another view of a part of the passage vortex taken with the camera pointed almost directly up-

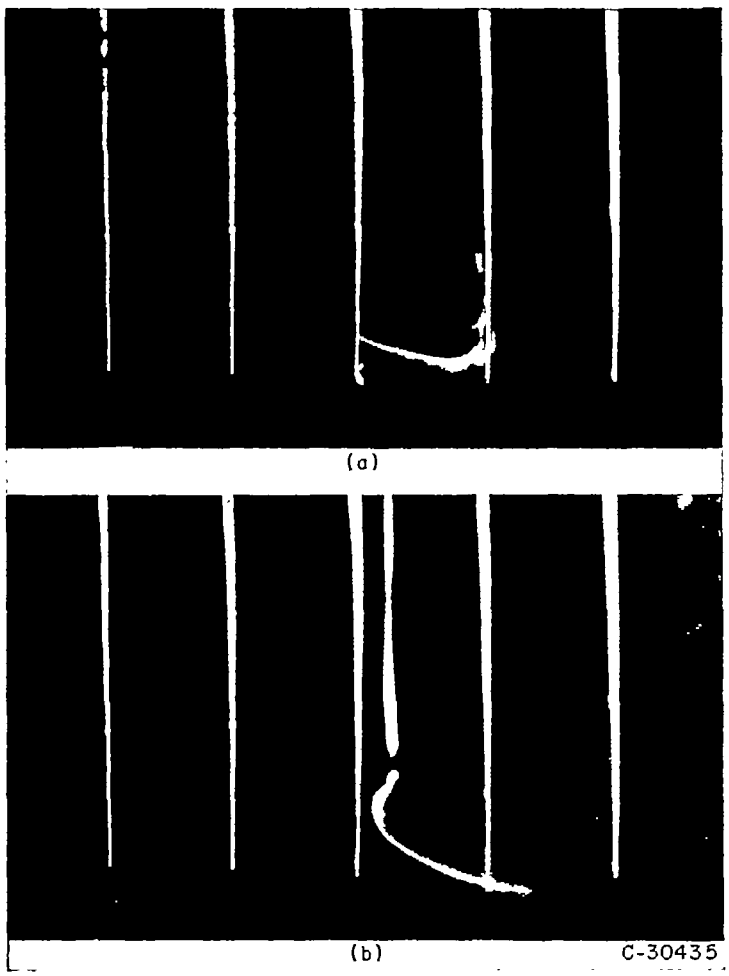


(a) Probe away from wall at nose of blade.
(b) Probe away from wall in mainstream.

FIGURE 20.—Streamline pattern in cascade with solidity of 2.0 and angle of attack of 20°. Stagger angle, 0°; aspect ratio, 2.34.

stream into the vortex. Careful examination of this figure discloses that the portion of the passage vortex shown here does not actually touch the suction surface. The outer portion of the passage vortex, which does contact the suction surface, was obtained by admitting smoke away from the wall on the pressure surface of the passage. This is in accordance with the pattern of passage vortex formation described earlier; that is, the boundary-layer roll-up is such that the outer layers of the passage vortex are derived from inlet boundary-layer flow near or on the pressure-surface side of the passage; the central portions of the passage vortex are derived from the inlet boundary layer nearer the suction side of the passage.

Another part of the passage vortex in the 45° rectangular bend is presented in figure 24. Here the vortex is clearly shifting in a direction away from the wall and also away from the suction surface.

The formation of a passage vortex in the wall boundary layer of the 60° rectangular bend is shown in figure 25. The turning sections of these passages are circular arcs, all having equal radii of curvature. The introduction of a large quantity of smoke made it possible to observe the continued twisting of the vortex downstream of the blade row (fig. 26).

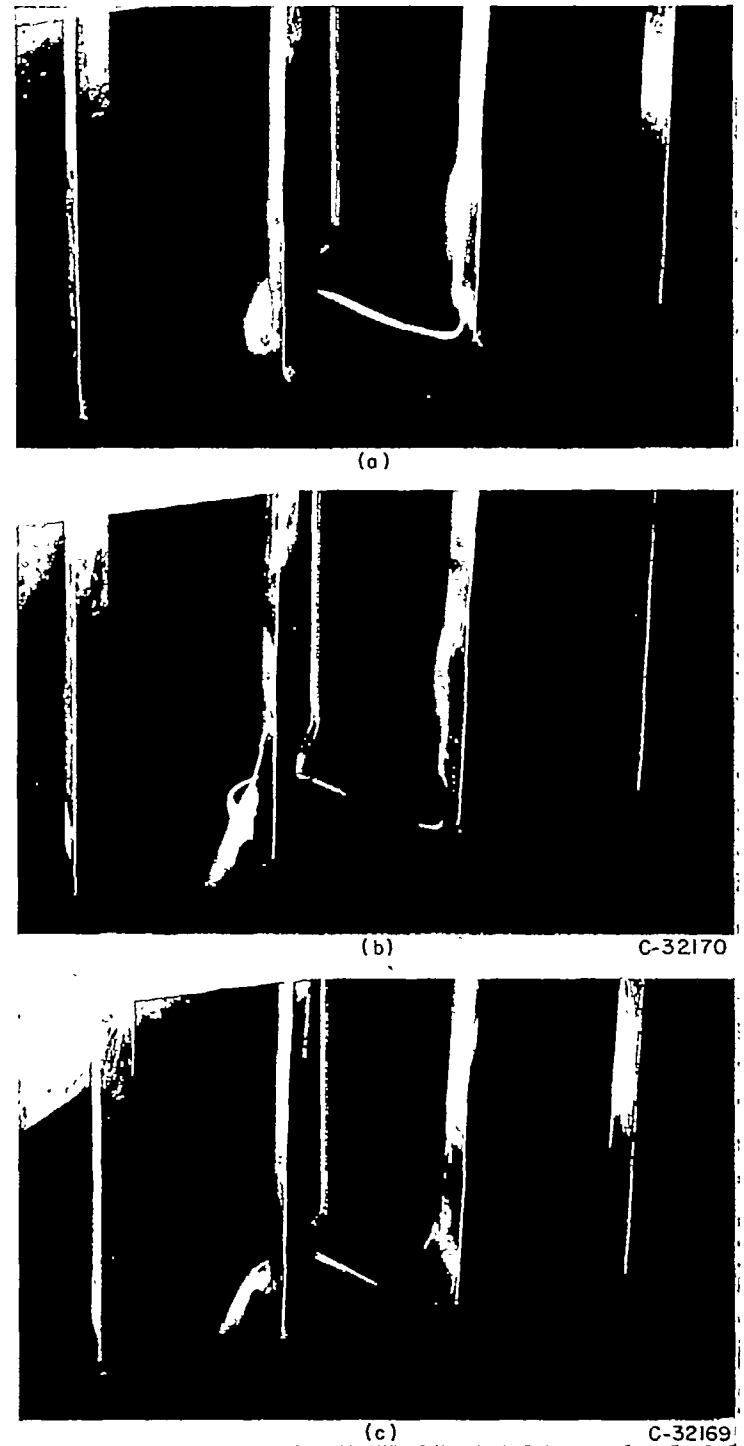


(a) Fillet on blade pressure surface.
(b) Fillet on blade suction surface.
(c) Fillets on both blade surfaces.

FIGURE 21.—Streamline pattern in cascade with blade fillets. Stagger angle, 0°; solidity, 1.5; angle of attack, 11°; aspect ratio, 2.34.

An overhead view of the deflection of a boundary-layer streamline across the passage is presented in figure 27 (a). When viewed in this direction, perpendicular to the surface in which the streamlines are flowing, the streamlines appear quite faint; and so it is considerably more difficult to obtain good, high-contrast pictures from above than from downstream.

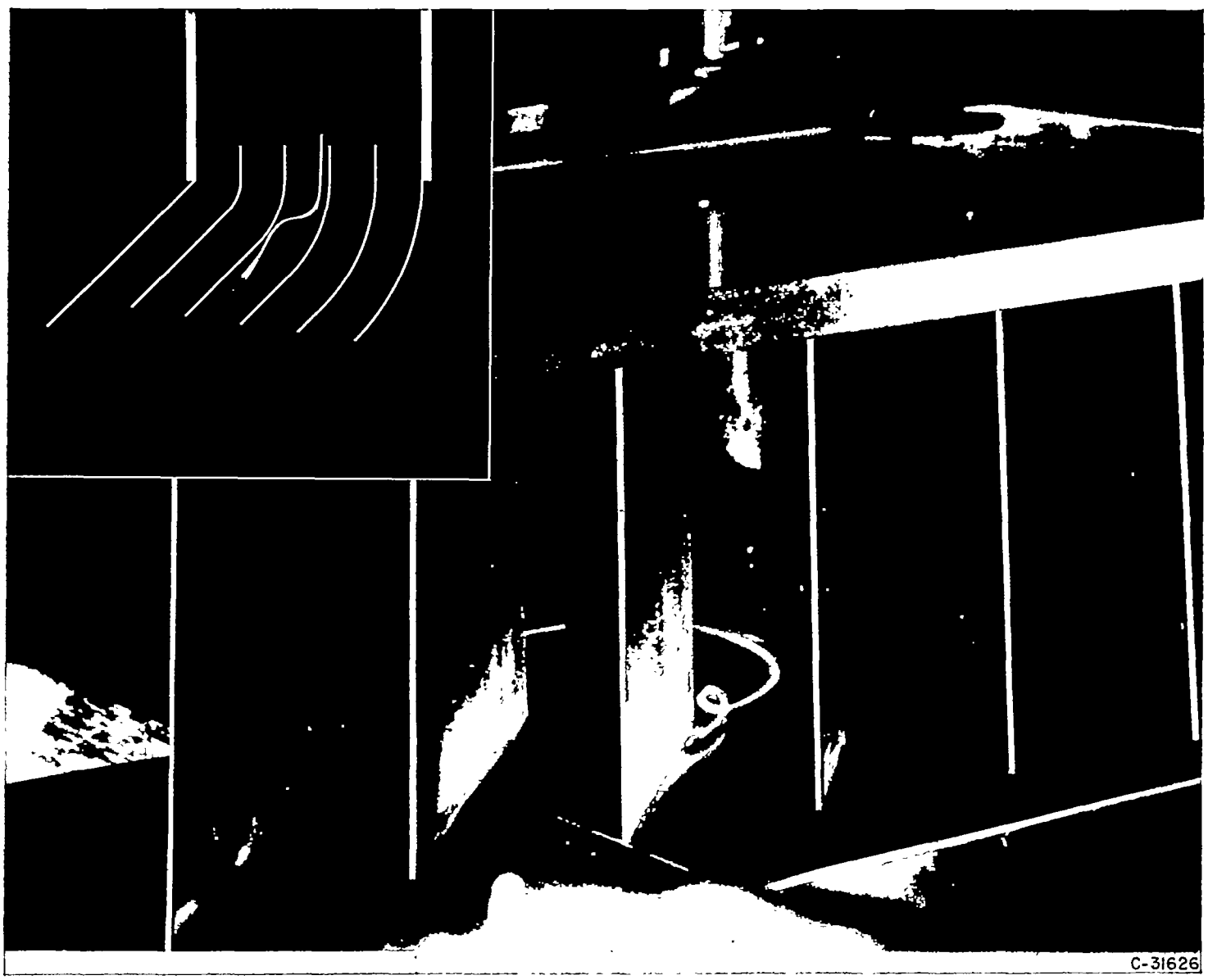


FIGURE 22.—Roll-up of wall inlet boundary layer to form passage vortex in 45° rectangular bend. Smoke introduced on wall near blade pressure surface.

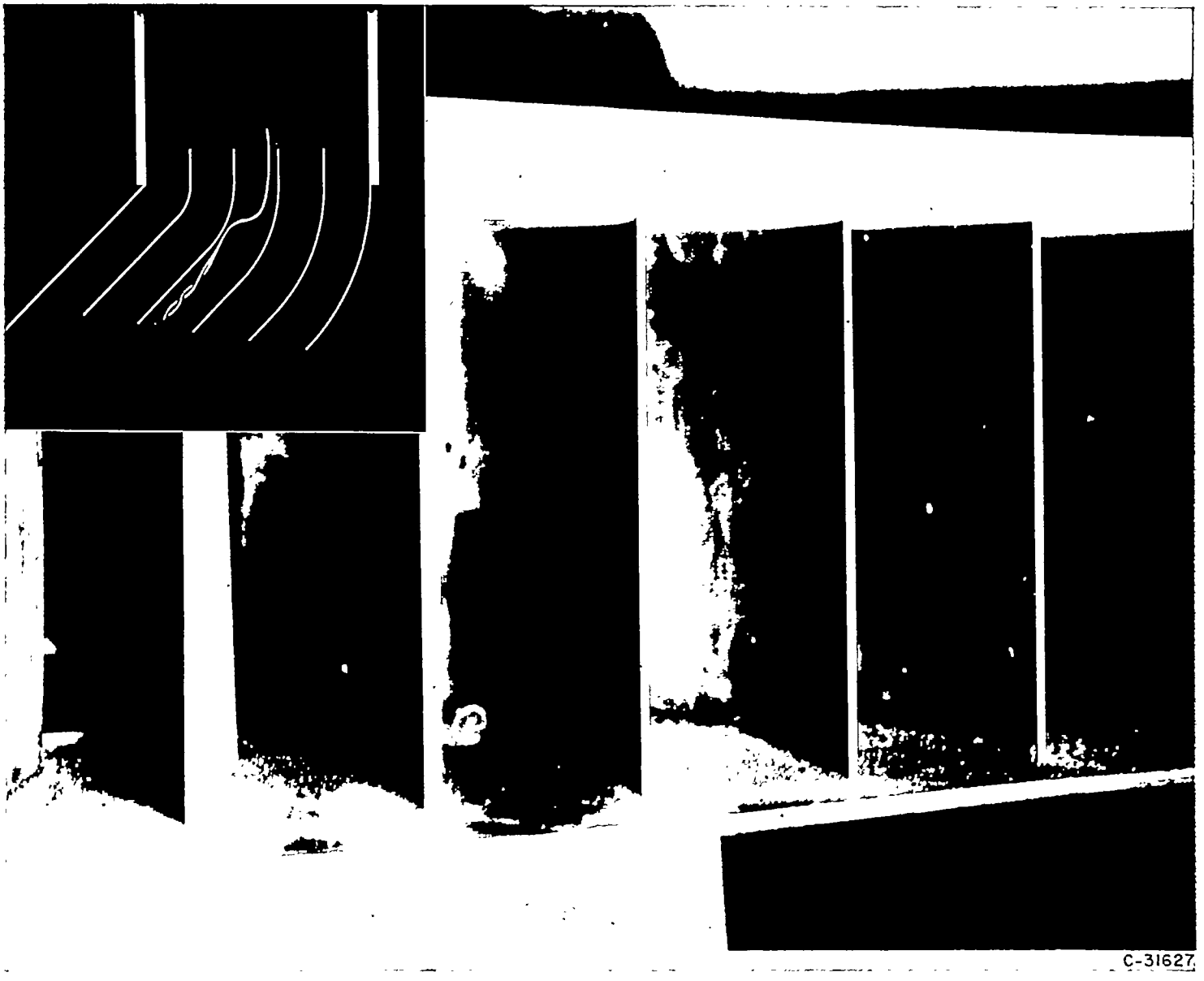


FIGURE 23.—Passage vortex in 45° rectangular bend. Smoke introduced on wall near blade pressure surface.

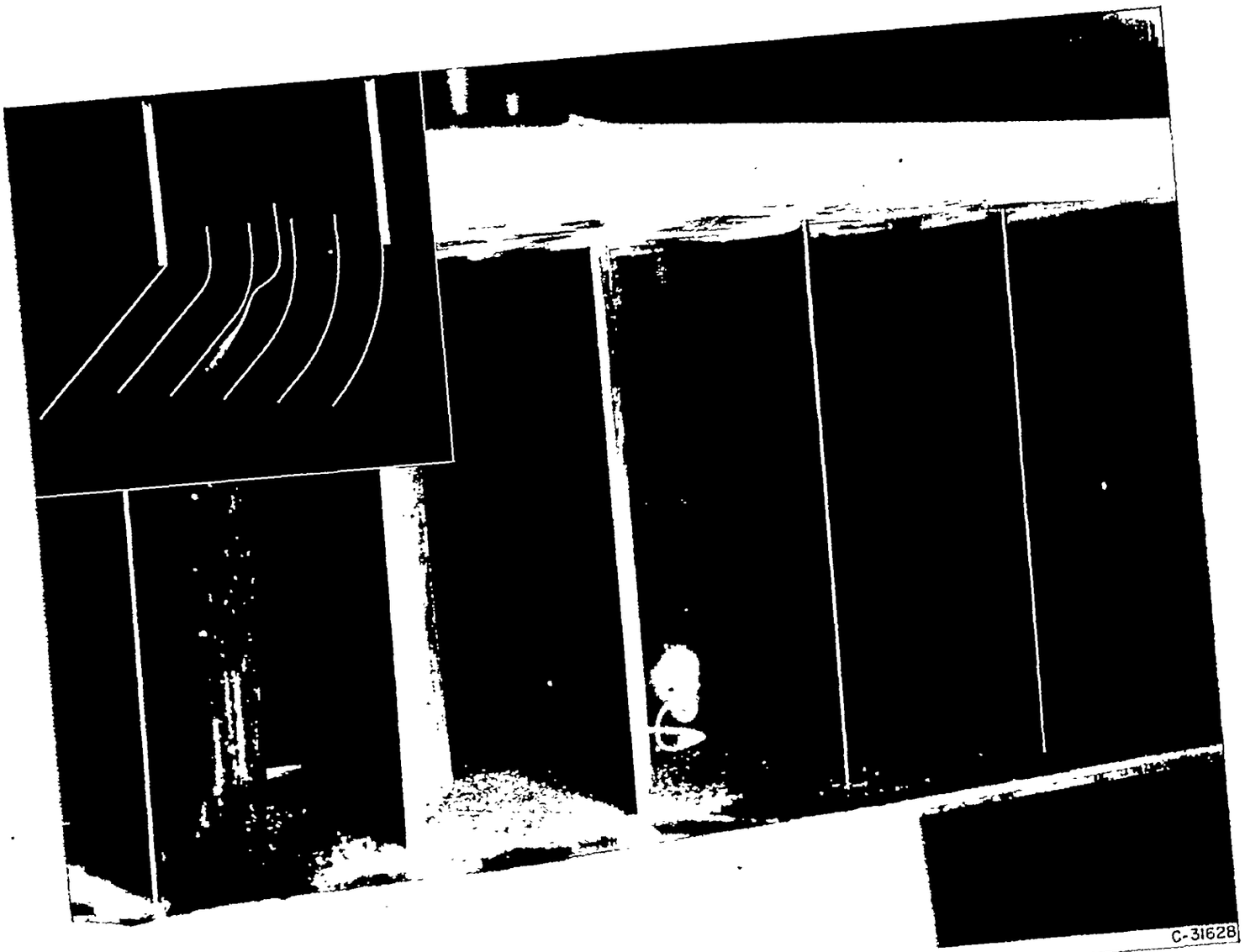


FIGURE 24.—Shift of secondary-flow passage vortex away from wall of 45° rectangular bend. Smoke introduced on wall near midchannel position.

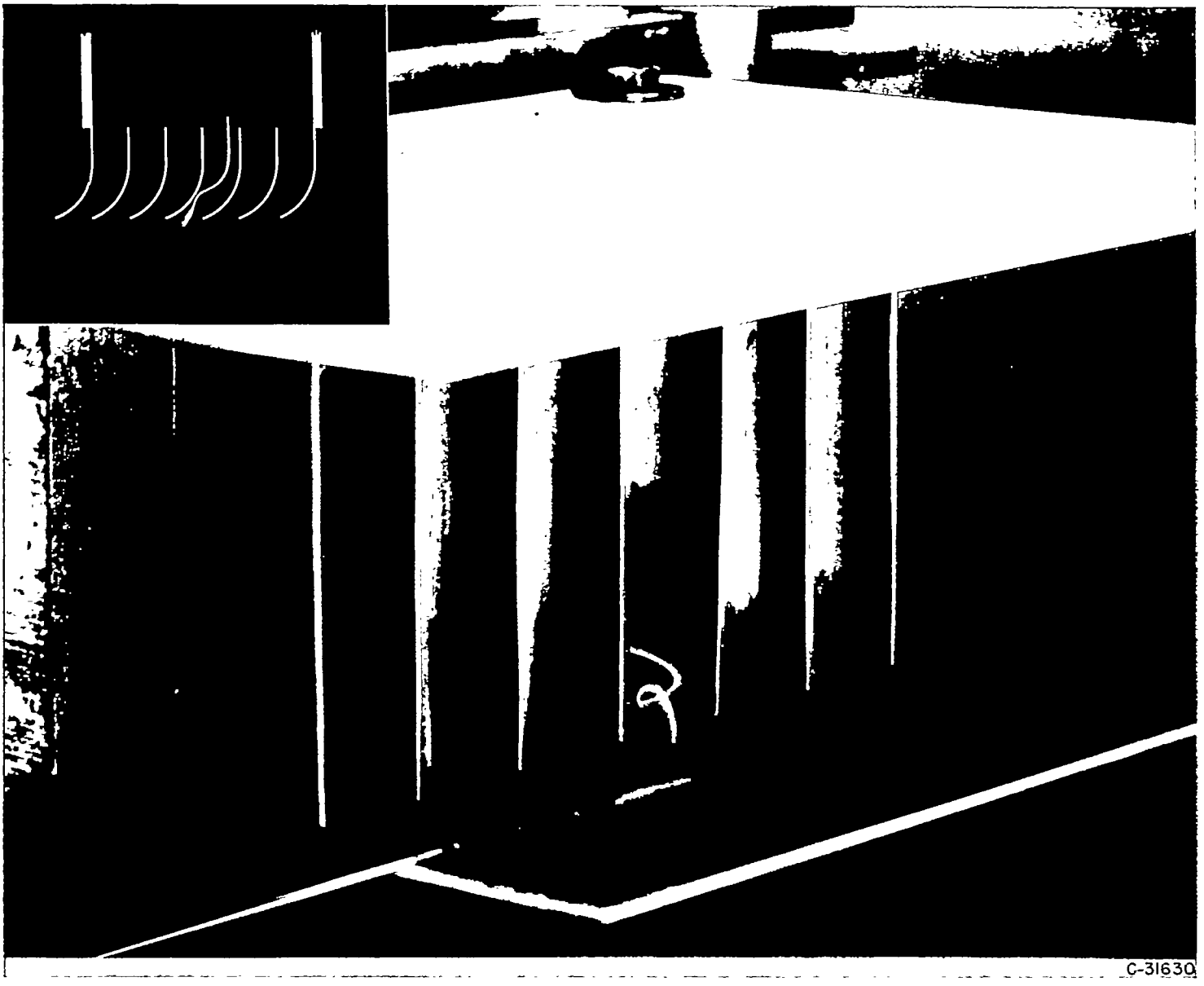


FIGURE 25.—Roll-up of wall inlet boundary layer to form passage vortex in 60° rectangular bend. Smoke introduced on wall near blade pressure surface.

FIGURE 26.—Continued twisting of passage vortex downstream of blade row.

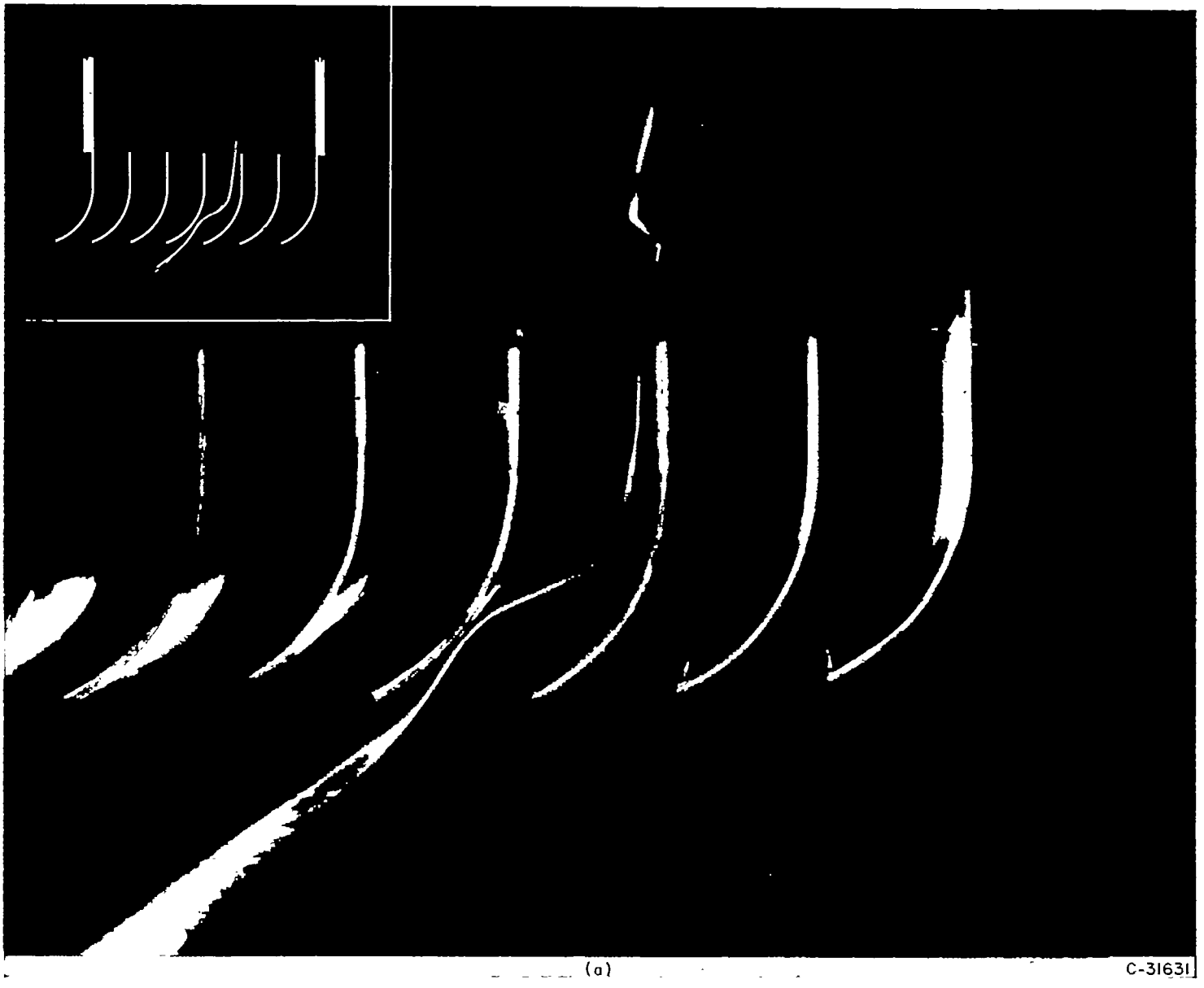


(a) Probe on wall in passage at inlet to 60° rectangular bend.

FIGURE 27.—Secondary-flow deflection across channel in 60° rectangular bend.

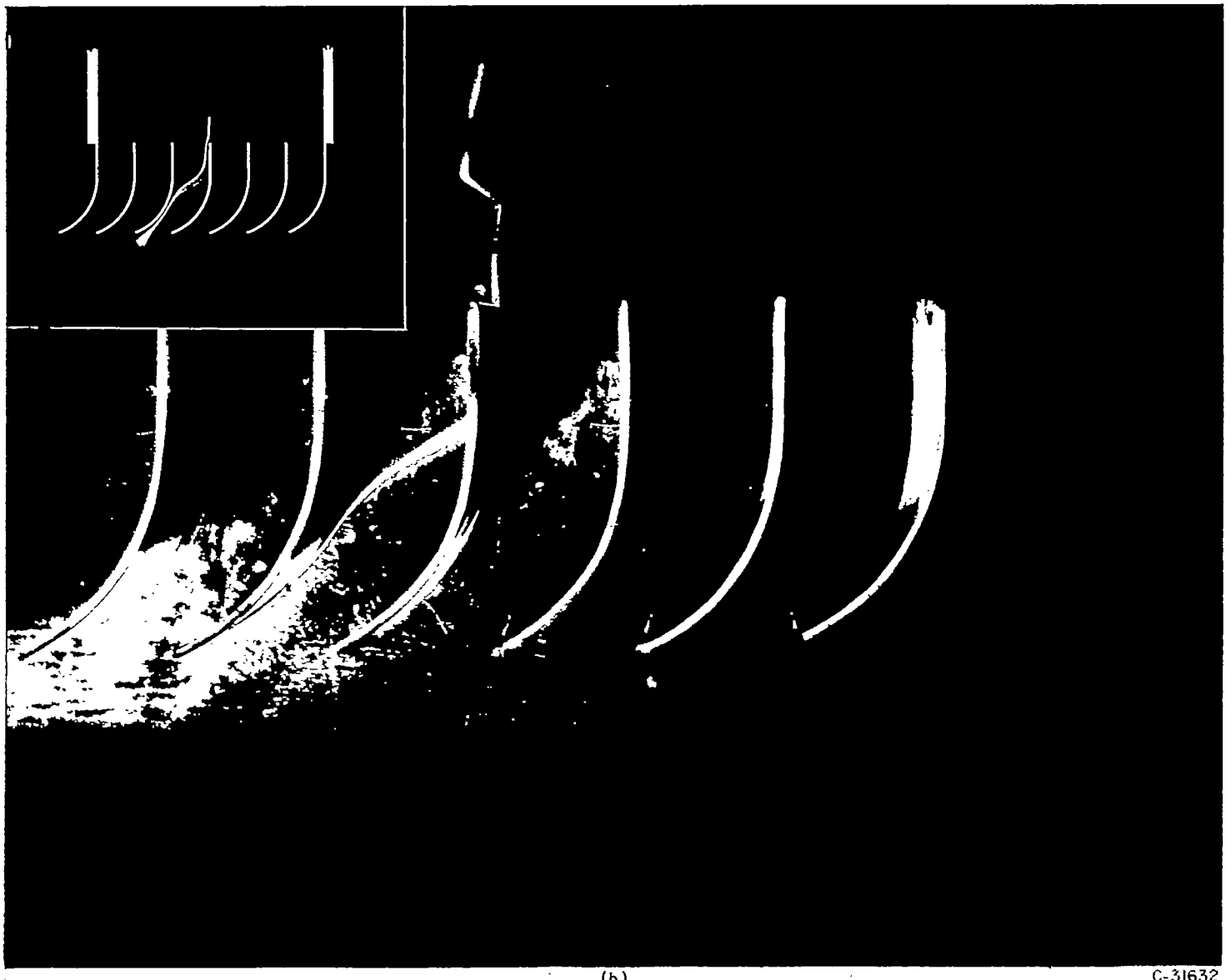


(b) Probe on pressure surface ¼ inch from wall in 60° rectangular bend.

FIGURE 27.—Concluded. Secondary-flow deflection across channel in 60° rectangular bend.

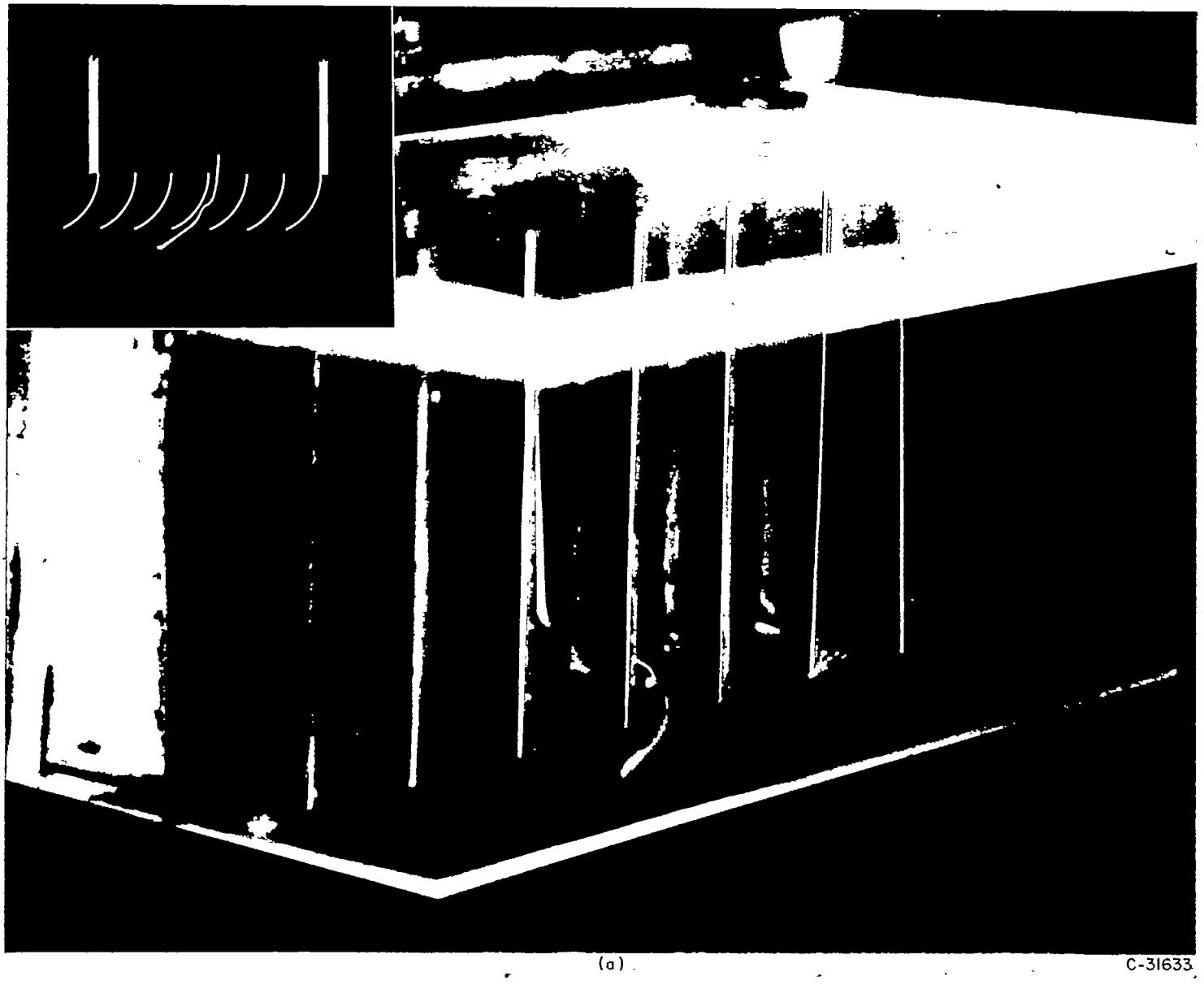


(a) Roll-up of wall boundary layer to form passage vortex. Smoke introduced on wall near suction surface.

FIGURE 28.—Formation of secondary-flow passage vortex in 60° cascade of blades.

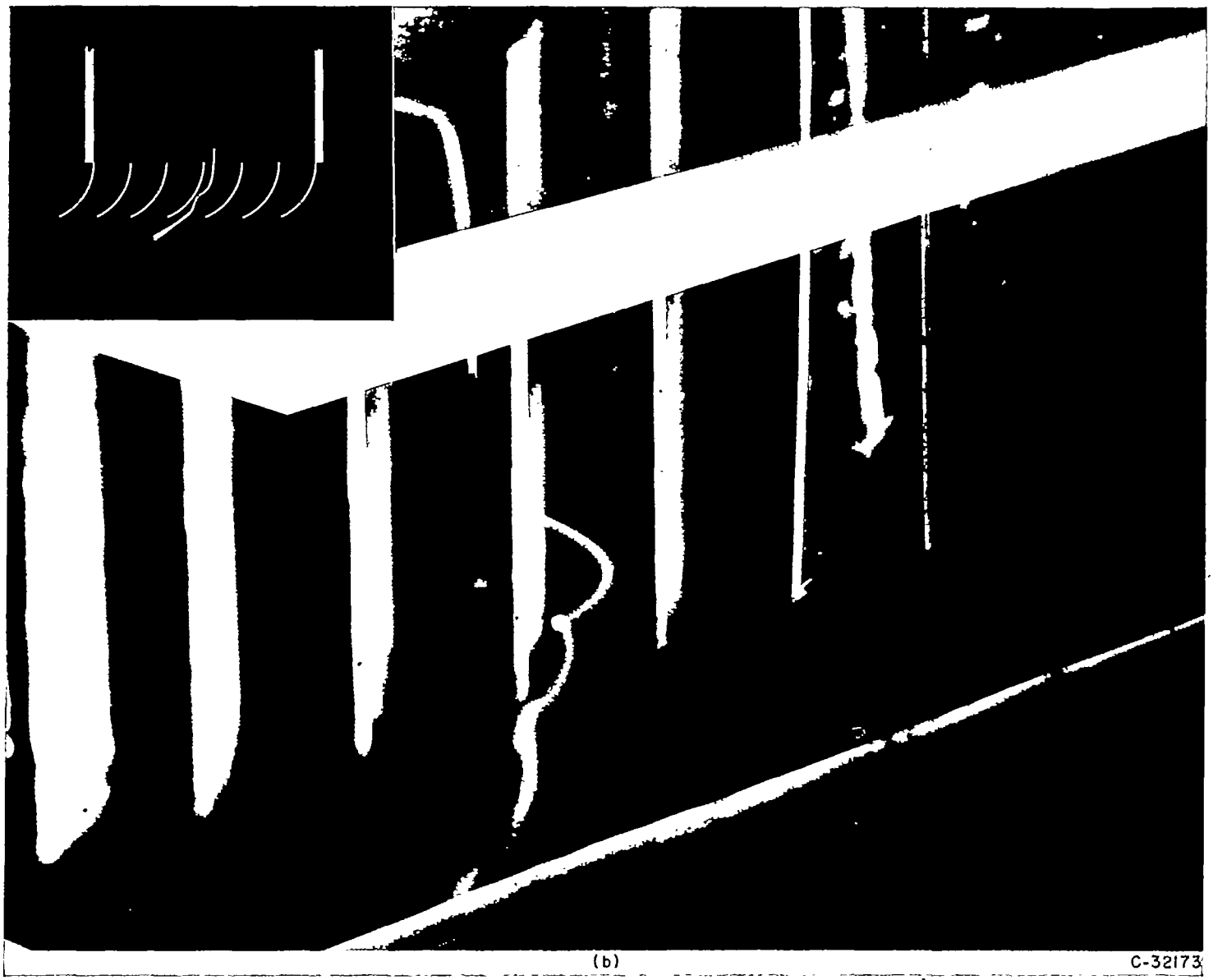


(b) Roll-up of wall boundary layer to form passage vortex. Smoke introduced off wall near suction surface showing continued twisting of vortex downstream of cascade.

FIGURE 28.—Continued. Formation of secondary-flow passage vortex in 60° cascade of blades.

(c) Deflection of flow off blade pressure surface across passage into passage vortex.

FIGURE 28.—Concluded. Formation of secondary-flow passage vortex in 60° cascade of blades.

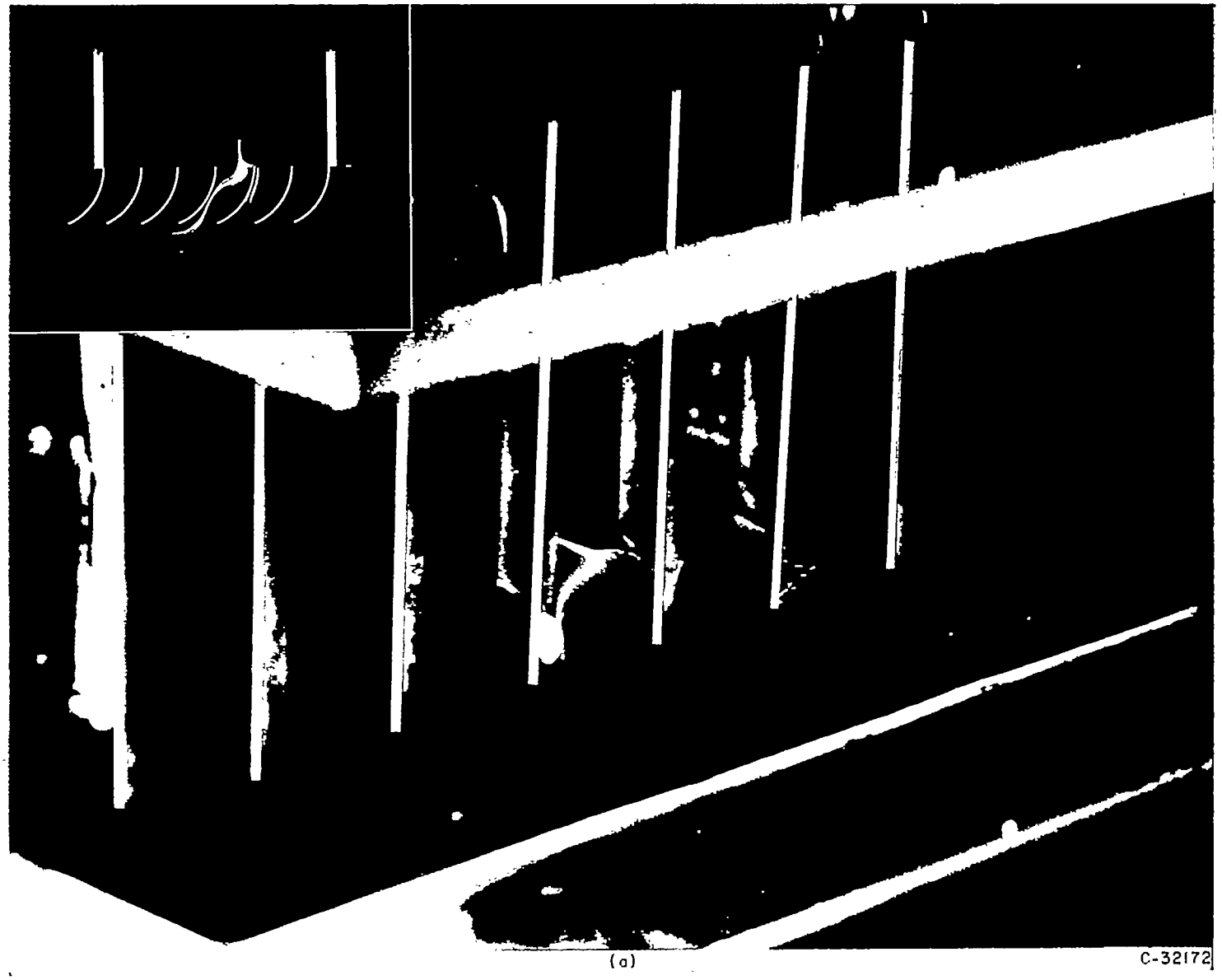


(a) Downstream view.

FIGURE 29.—Nose effects in boundary layer of 60° cascade of blades. Smoke introduced on wall near midchannel position.

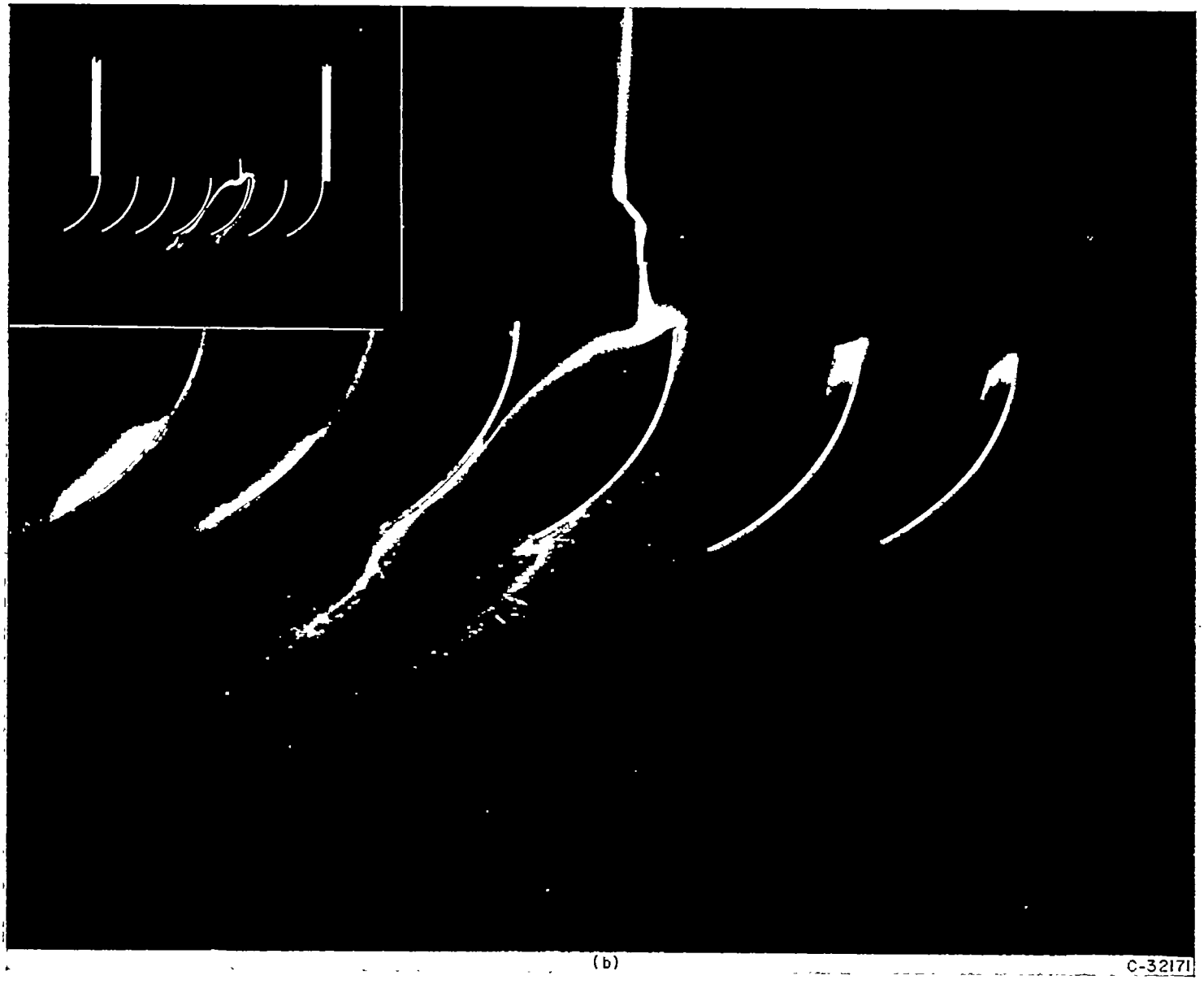


(b) Overhead view.

FIGURE 29.—Concluded. Nose effects in boundary layer of 60° cascade of blades. Smoke introduced on wall near midchannel position.

This streamline (fig. 27 (a)) does not actually contact the suction surface of the passage; that is, it is not in the outermost layer of the vortex. For figure 27 (b), the smoke was admitted on the pressure surface of the bend about ¼ inch away from the end wall. In this case, the streamline pictured is one that actually does reach the suction surface across the passage.

**Comparison of secondary flow in bends and cascades.**—In this section, the secondary-flow patterns obtained with the rectangular bends having a turning angle of 60° are compared with those obtained with a two-dimensional cascade of sheet-metal blades having a turning angle of 60°. The total turning, the rate of turning, and the blade spacing are the same for both configurations. With the exception of the leading-edge region, the main-flow streamline patterns were likewise essentially the same.

Figures 28 (a) and (b) show the way two of the streamlines in the end-wall boundary layer of the 60° cascade roll up in the passage vortex. Some of the fluid in the passage vortex of this configuration comes from the pressure surface of the blade at a distance from the wall (fig. 28 (c)).

For figure 29 (a), the smoke was admitted at the inlet to the blade row and at the wall, but closer to the pressure surface than in figures 28 (a) and (b). It appears from figure 29 (a) that, in this 60°-turning cascade of sheet-metal blades (with the tangent to the blades at the inlet being in the axial direction), a well-defined stagnation region exists near the blade leading edge on the pressure side. The smoke trace in the photograph approaches this region, divides in two, and flows around it. One part of the smoke follows a cross-channel flow pattern; the other part flows around the blade leading edge and downstream along the blade suction surface in the adjoining passage. An overhead view of this phenomenon appears in figure 29 (b). This difference in behavior of the boundary layers of the cascade and the bends can be explained qualitatively as follows. The main streamline pattern for the given cascade should have the form depicted in figure 30 (a); that is, a stagnation point should exist on the pressure surface of the blade slightly downstream of the leading edge. The high pressures that must exist in this region force some of the smoke (fig. 29 (b)) on one side of the stagnation streamline to flow upstream and around the nose of the blade. On the other side of the stagnation streamline, smoke flows across the channel. The adverse pressure gradients in the vicinity of the wall in the region immediately upstream of the stagnation point give rise to a relatively large separated-flow area. In the elbow configuration previously discussed, such a stagnation region on the pressure surface does not exist. The main streamline pattern should have the form shown in figure 30 (b), because the straight entrance section affords a gradual loading of the turning surfaces. Thus, despite the fact that the mean streamlines through the passages are relatively the same for the 60° bends and for the corresponding cascade, the boundary-layer flows are noticeably different.

In figure 31 (a), the probe admitting the smoke has been shifted toward the suction side of the passage, just enough

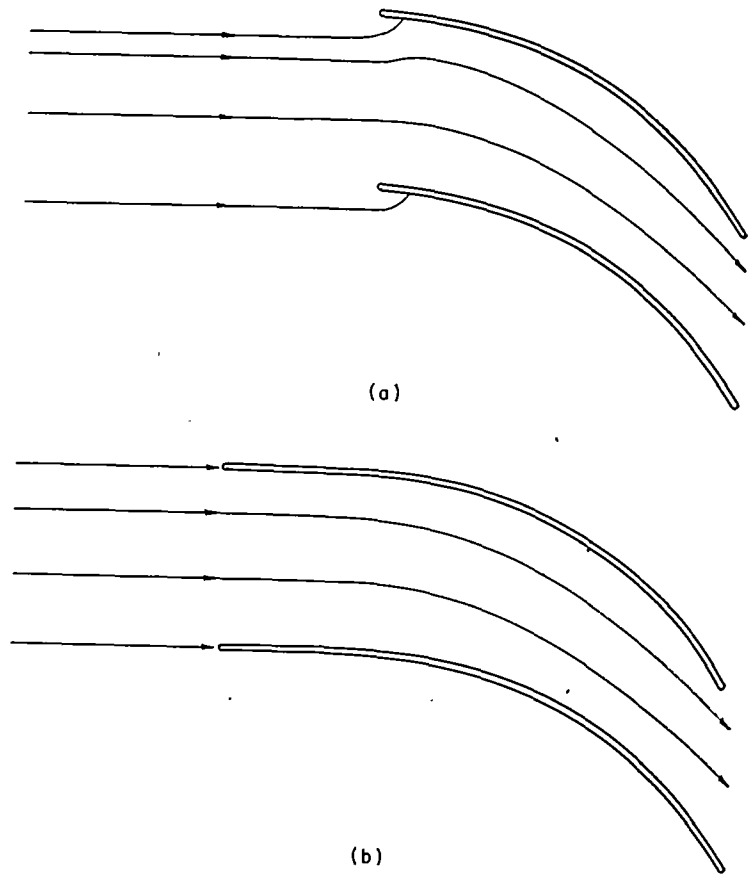


(a) Streamline pattern in 60° cascade.
(b) Streamline pattern in 60° bend.

FIGURE 30.—Comparison of streamline patterns in 60° cascade and 60° bend.

for the smoke trace to clear the stagnation region. The path of the smoke trace, compared with that in figure 27 (a) for the 60° bend, is somewhat distorted. In figure 31 (b), the probe has been moved even closer to the suction side, yet the flattened trajectory still is evidence of the effects of the separated-flow region.

**Remarks on flows in bends and cascades.**—For purposes of photography, the tests of the secondary flows in the high-turning bends and cascades were much more satisfactory than the tests on the basic two-dimensional cascade. As a result of the high turning involved, the passage vortex roll-up was very well defined. Each smoke trace maintained its identity long enough to enable good photographic evidence of a true vortex formation in the passage.

The accumulation of low-momentum fluid near the suction surface was here seen to be a passage vortex. After its initial formation, the flow in this vortex on its way downstream shifted spanwise out from the end wall.

Comparisons of the boundary-layer flows in bends and cascades disclosed possible large discrepancies between them. The study of secondary flows in rectangular bends may then facilitate theoretical analyses of flow-deflection paths, but the results may not be applicable directly to cascade boundary-layer flows.

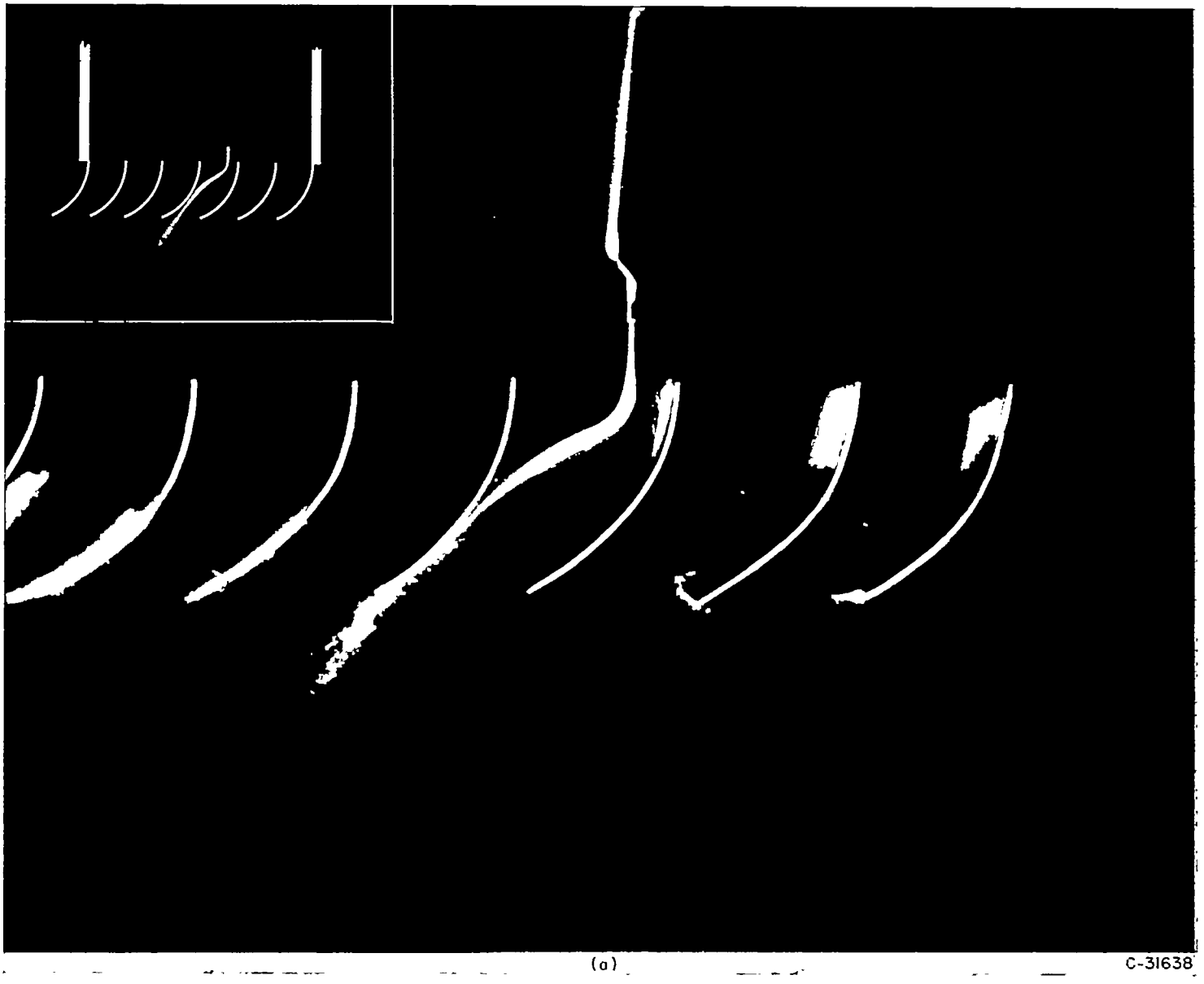


(a) Smoke trace just outside nose stagnation region.

FIGURE 31.—Secondary-flow streamlines in boundary layer of 60° cascade showing effects of stagnation region near nose.

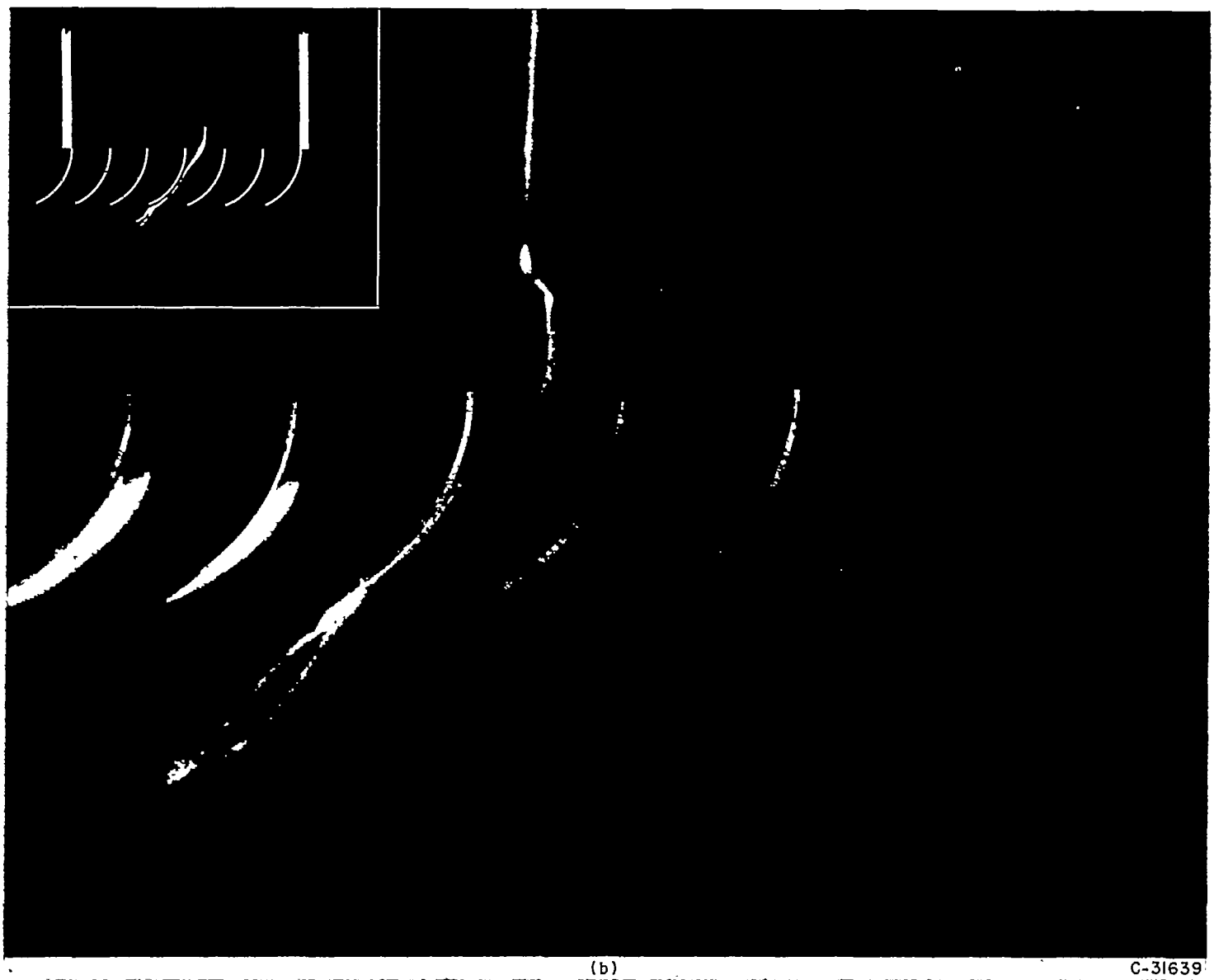


(b) Smoke trace near suction surface at inlet.

FIGURE 31.—Concluded. Secondary-flow streamlines in boundary layer of 60° cascade showing effects of stagnation region near nose.

SECONDARY FLOWS IN THREE-DIMENSIONAL CASCADES

The flow-visualization technique was applied to an annular-turbine-nozzle cascade designed for high subsonic and for supersonic Mach numbers in order to extend the scope of this investigation into typical turbomachine flow conditions with radial pressure gradients and with the complicating addition of shock phenomena. The information concerning cross-channel deflections and passage vortex formation obtained in the basic two-dimensional cascade, together with the results obtained with hydrogen sulfide and paint flow traces, provided a clear understanding of secondary flows in three-dimensional cascades (ref. 5). In reference 5, careful surveys of total pressure and flow angle made at the discharge of the turbine-nozzle blades revealed the presence of a substantial loss core near the inner shroud. The loss core near the outer shroud was very much smaller at the lower pressure ratio investigated in reference 5 and decreased almost to the vanishing point at the higher pressure ratio. (Figs. 8 (e) and (f) of ref. 5, which present some results of the surveys, are reproduced for convenience herein as fig. 32.) These results indicate the presence of sizable inward radial flows in the cascade. Accordingly, the hydrogen sulfide and the paint flow-trace methods were applied to the cascade.

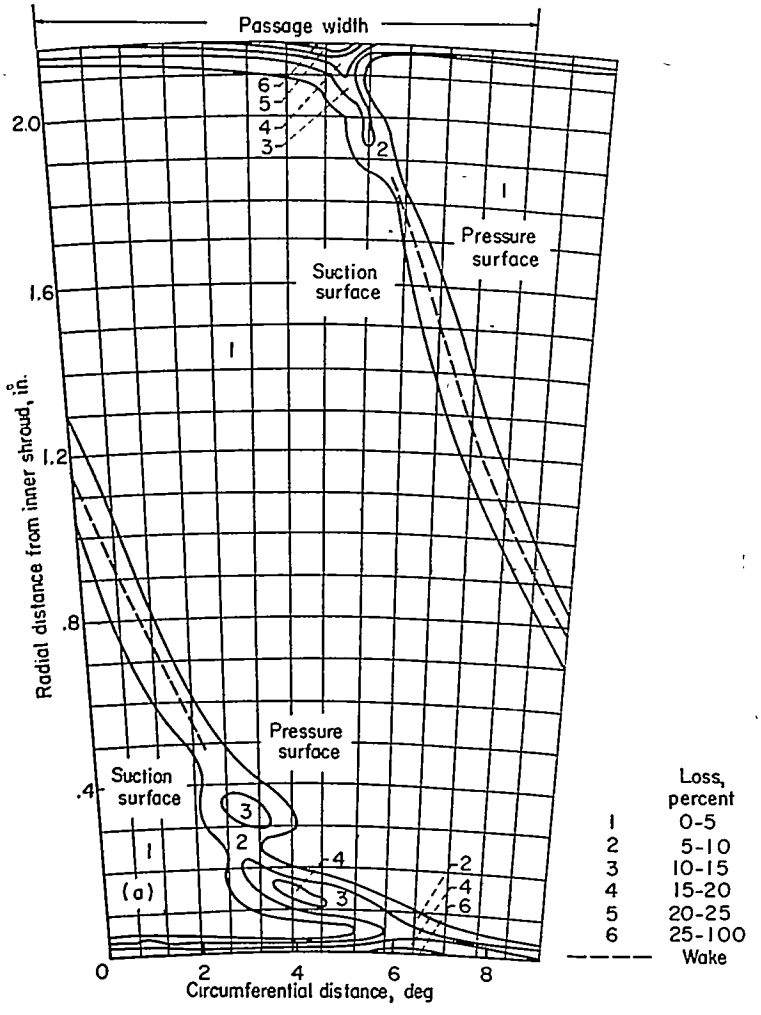


(a) Hub discharge Mach number, 0.94.

FIGURE 32.—Contours of loss across one blade passage of annular-nozzle cascade.

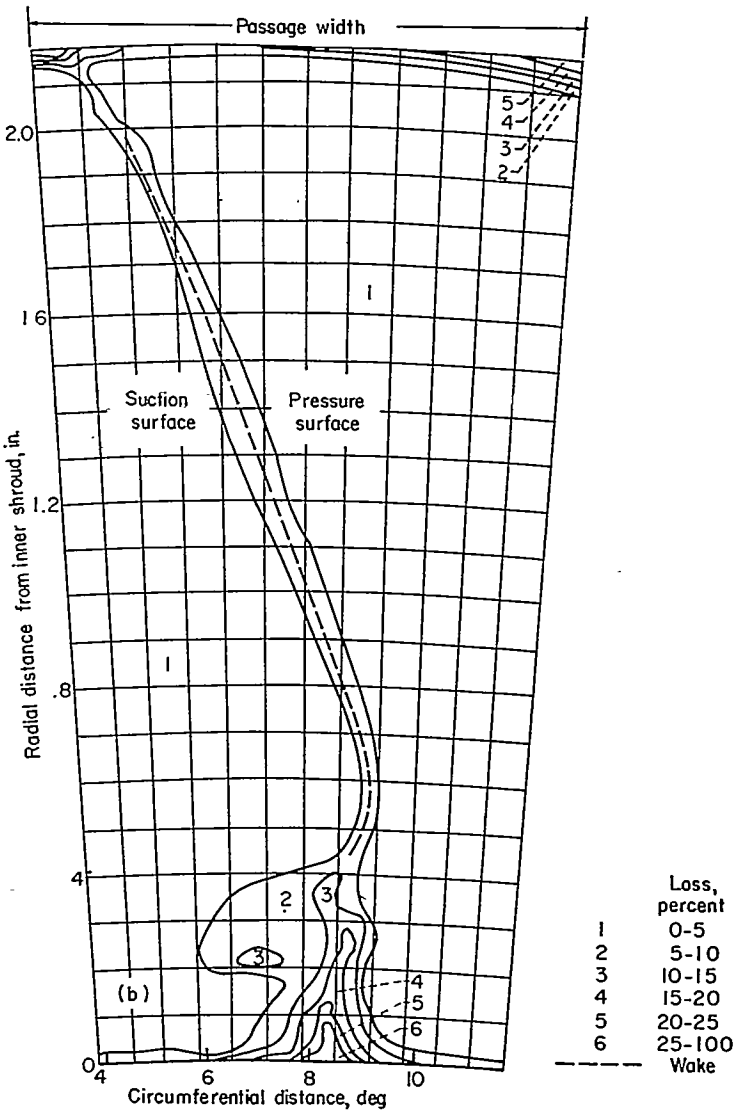


(b) Hub discharge Mach number, 1.46.

FIGURE 32.—Concluded. Contours of loss across one blade passage of annular-nozzle cascade.

Figures 11 and 12 show the results of the hydrogen sulfide tests and demonstrate the typical cross-channel deflection pattern. Paint-trace evidence of radial flows in the blade wakes and on the blade suction surfaces is presented in figures 16, 18 (c), and 19 of reference 5. In particular, figure 16 of reference 5, reproduced herein as figure 33, is a striking indication of radial flows along the blade suction surface in a region of thickened boundary layer produced by the intersection of a flow discontinuity (at the supersonic Mach number) with the suction surface.

Reference 5 attempts to evaluate these radial flows and concludes: "The inner-wall loss core associated with a blade of a turbine nozzle cascade is largely the accumulation of low-momentum fluids originating elsewhere in the cascade. This accumulation is effected by the secondary-flow mechanism, which acts to transport the low-momentum fluids across the channels on the walls and radially in the blade wakes and boundary layers. At one flow condition investigated, the radial transport of low-momentum fluid . . . accounted for approximately 65 percent of the inner-wall loss core."

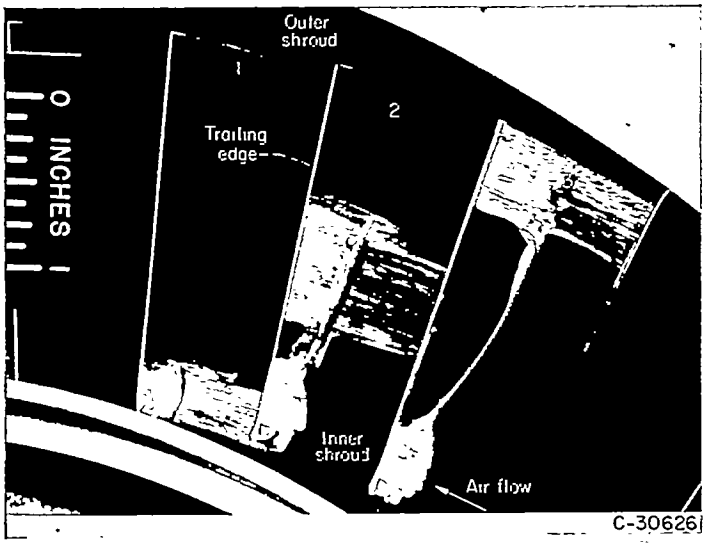


FIGURE 33.—Enlarged view of inward radial flow of low-momentum fluid showing paint traces of secondary flow along blade suction surface at nozzle discharge of annular-nozzle cascade.

Figure 34 (fig. 21 of ref. 5) presents an over-all sketch of the secondary-flow components in the annular-turbine-nozzle cascade. Similar tests on another annular-nozzle configuration (ref. 5) disclosed the same pattern of secondary flows but with better evidence of radial flows in the blade wakes at the lower pressure ratios.

### TIP-CLEARANCE EFFECTS IN TWO-DIMENSIONAL CASCADE WITH LOW-TURNING BLADES

In order to simulate more closely the conditions in a turbomachine, tip clearances of 0.060 and 0.014 inch were provided in the two-dimensional cascade. The effects of this tip clearance were studied by means of the smoke visualization method. One of the end walls of the cascade was then replaced by an endless moving belt whose direction and speed could be varied, in order to study the tip-clearance effects with relative motion between blades and wall.

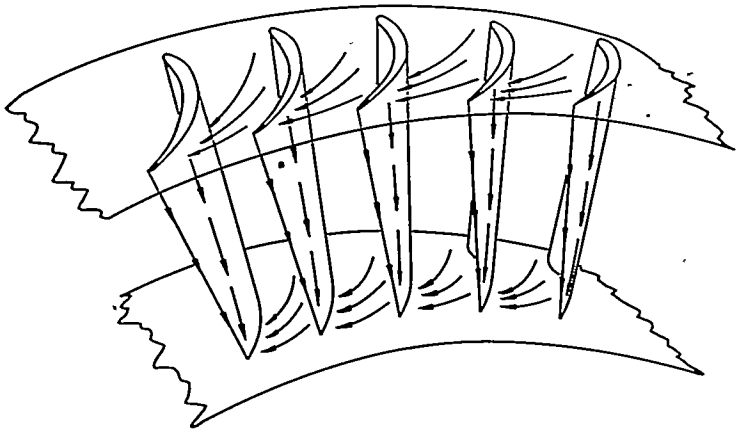

FIGURE 34.—Secondary-flow components in annular-nozzle cascade as indicated by paint and hydrogen sulfide traces.

**Tip clearance.**—The possibility that blade tip-clearance flow might oppose the formation of the passage vortices and thus reduce these flow disturbances was investigated. The flow patterns at clearances of 0.014 and 0.060 inch (0.4 and 1.7 percent span, respectively) are shown in figures 35 and 36, respectively. The point of principal interest arising from this study was the fact that with tip clearance the passage vortex heretofore observed was displaced but was neither eliminated nor apparently reduced in magnitude.

The deflection of the flow along the pressure surface (fig. 35 (a)) is greater than for blades without tip clearance, because a large part of the flow under the blade tip comes from flow off the blade pressure surface. For this particular probe location, the flow was observed to cross under the blade tip at the midchord position. This blade boundary-layer flow, which crosses under the blade, forms a vortex lying against the suction surface. This tip-clearance vortex rotates in a direction opposite to that of the secondary-flow

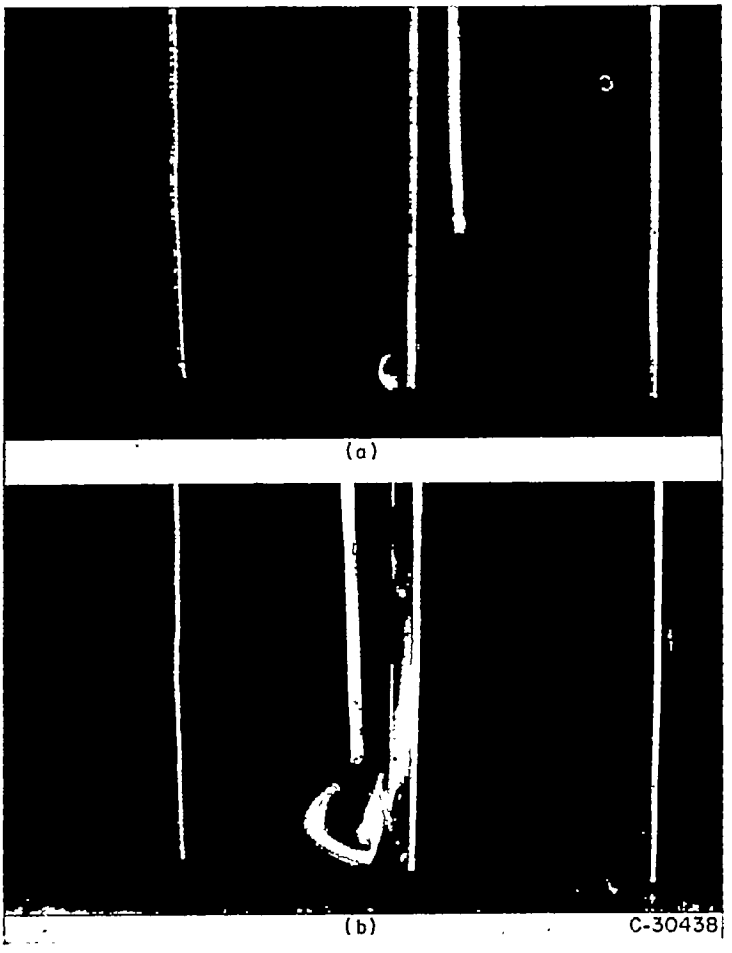


(a) Probe away from wall on pressure side of blade.
(b) Probe on wall in midchannel.

FIGURE 35.—Streamline pattern in cascade with 0.014-inch blade tip clearance. Stagger angle, 0°; solidity, 1.5; angle of attack, 11°; aspect ratio, 2.34.

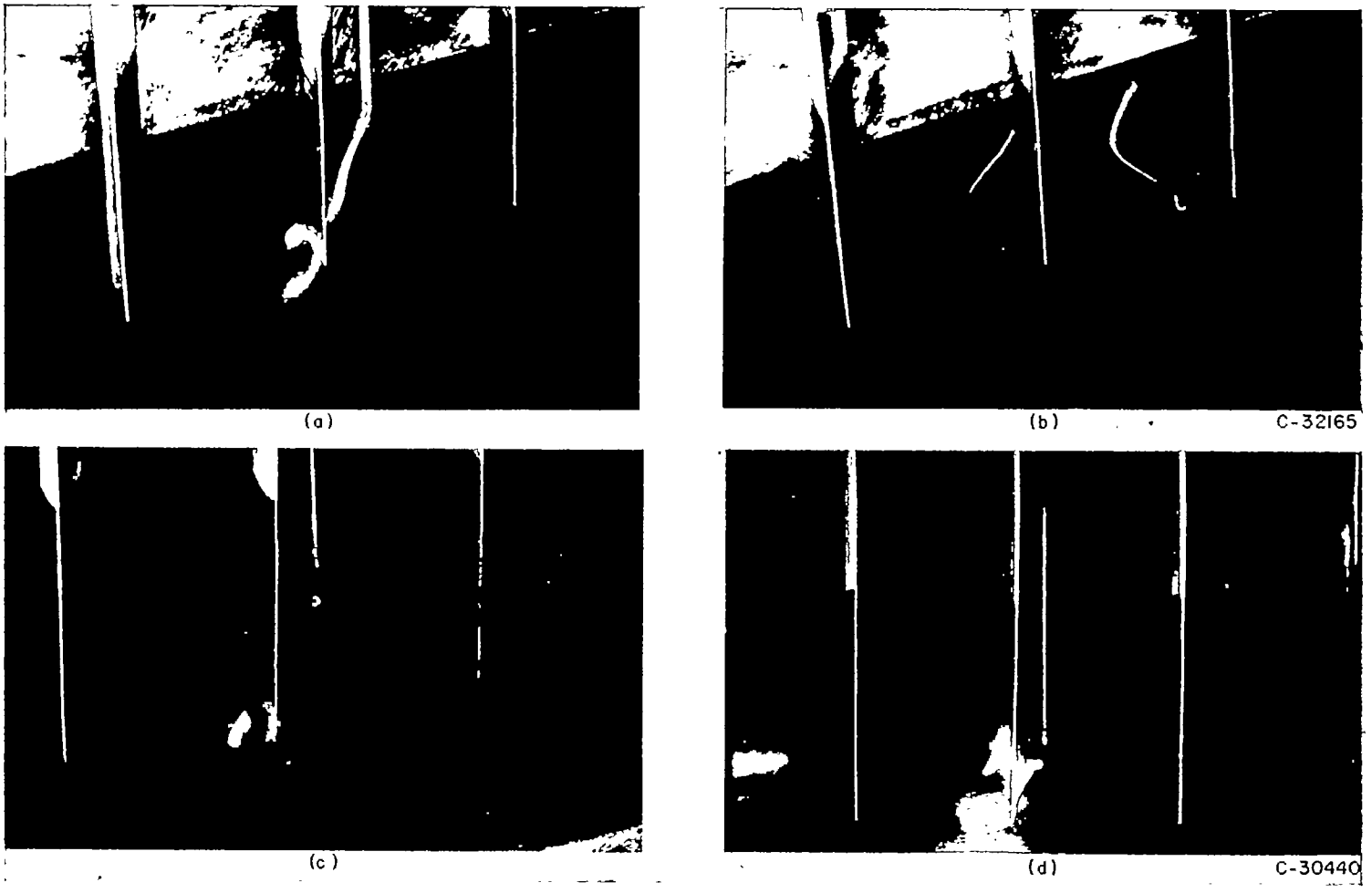


(a) Probe on wall near nose of blade; stagger angle, 45°.

(b) Static taps at inlet near nose of blade and in mid-channel positions; stagger angle, 45°.

(c) Static tap near nose of blade and probe on wall near nose of blade; stagger angle, 45°.

(d) Probe away from wall on nose of blade; stagger angle 0°.

FIGURE 36.—Streamline patterns for cascade with 0.060-inch blade tip clearnace. Solidity, 1.5; angle of attack, 11°; aspect ratio, 2.34.

vortex and preempts the region where the secondary-flow vortex would form if no tip clearance were present. Nevertheless, figure 35 (b) shows that the usual passage vortex still exists and is merely displaced by the tip-clearance vortex. Essentially the same phenomenon for 0.060-inch blade tip clearance is illustrated in figures 36 (a) to (c). The tip-clearance vortex in figure 36 (a) was traced out by smoke admitted through a probe. Figure 36 (b) is a side view of the displaced passage vortex and was obtained when the smoke was admitted through wall static taps upstream of the blades. Figure 36 (c) depicts the pattern obtained from smoke admitted through the probe to show the tip-clearance vortex, while smoke admitted simultaneously through a wall static tap shows the usual secondary-flow vortex. The manner in which the tip-clearance vortex flows contiguous to the secondary-flow vortex can be seen in the figure.

A particularly striking picture of the tip-clearance vortex forming in a cascade with 0.060-inch blade clearance is shown in figure 36 (d).

**Relative motion between blades and wall.**—The investigation of the flow behavior when relative motion existed between the cascade blades and the cascade end wall disclosed some unexpected results. In particular, it had been assumed a priori that the moving wall would tend to increase the flow of the wall boundary layer as well as of the blade boundary layer off the leading surface and to pull them under the blade tips in the direction of the wall motion. However, figure 37 indicates that this assumption is invalid. Comparison of the smoke deflection in figure 37 (a), where the wall is stationary, with figures 37 (b) and (c), where the motion of the wall is such as to make the pressure surface the leading surface, shows that flow on the blade is actually deflected away from the wall. Similarly, figure 38, where the suction surface is leading, shows increased deflection of the flow away from the wall with increasing wall speed; figures 38 (a), (b), and (c) illustrate the patterns for the stationary wall, for the wall moving at moderate speed, and for the wall moving at high speed, respectively.

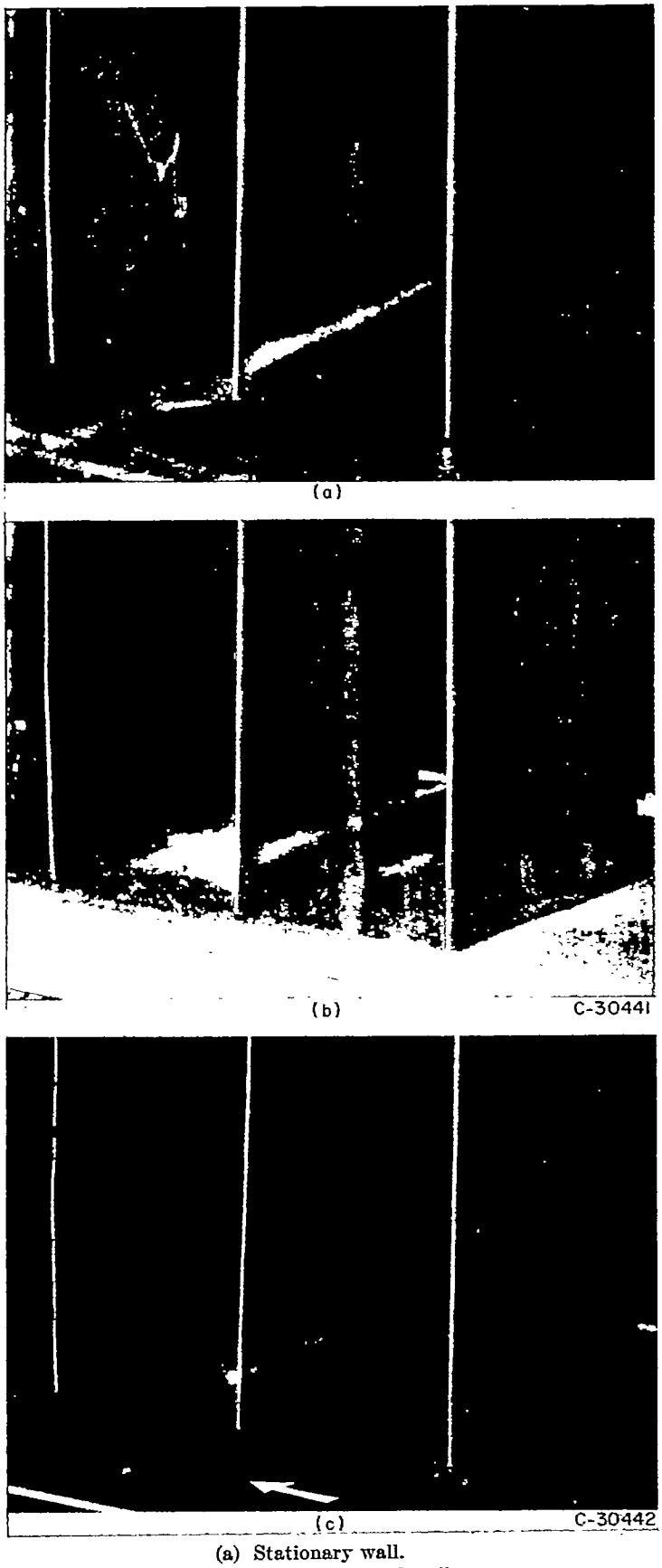


(a) Stationary wall.
(b) Moderate-speed wall.
(c) High-speed wall.

FIGURE 37.—Streamline deflections on blade pressure surface with probe on nose of blade. Pressure surface leading; blade tip clearance, 0.014 inch; stagger angle, 0°; solidity, 1.5; angle of attack, 11°; aspect ratio, 2.34.

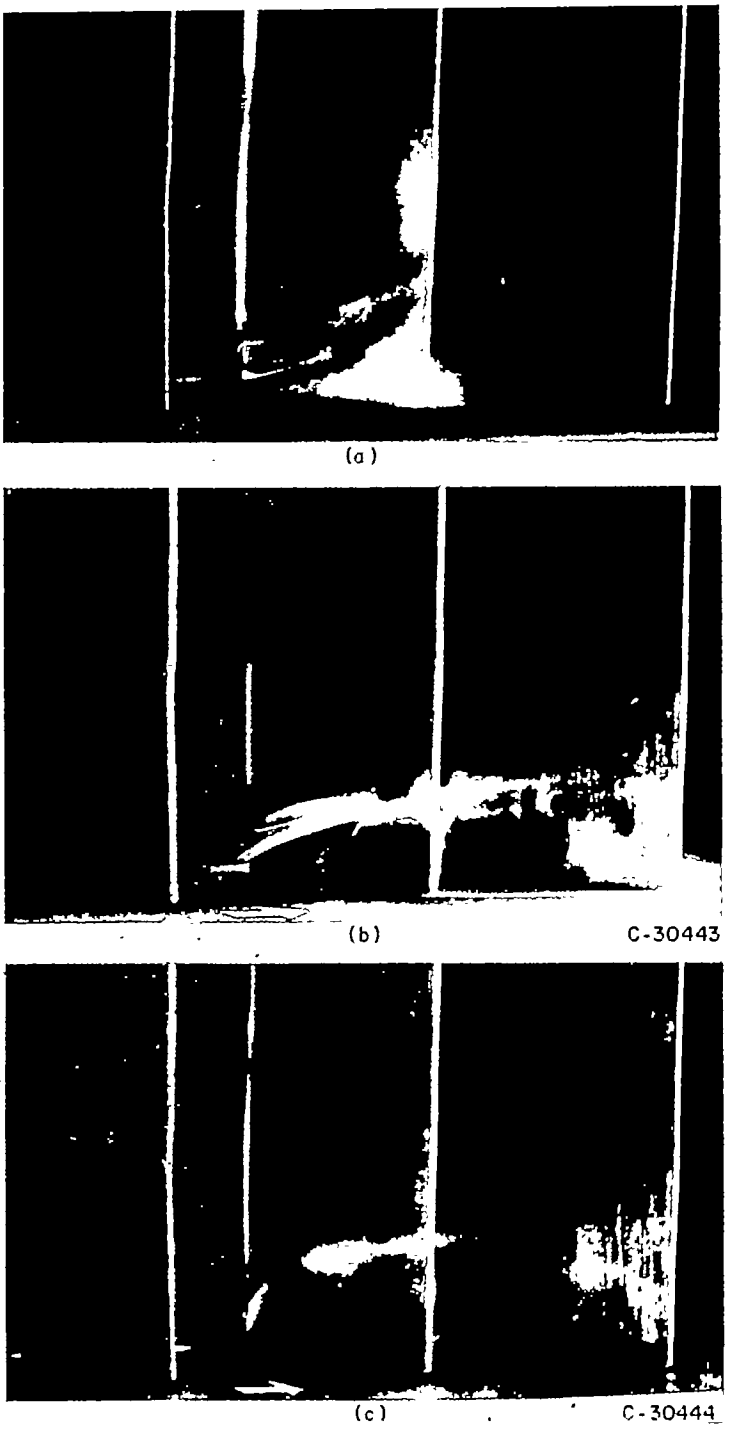


(a) Stationary wall.
(b) Moderate-speed wall.
(c) High-speed wall.

FIGURE 38.—Streamline deflections on blade suction surface with probe on nose of blade. Suction surface leading; blade tip clearance, 0.014 inch; stagger angle, 0°; solidity, 1.5; angle of attack, 11°; aspect ratio, 2.34.

The explanation of the observed phenomenon is that the blades have a scraping action on the flow near the moving wall. The blade leading surface scrapes up fluid entrained on the moving wall and thus imparts a rolling motion to the air in the vicinity of the leading surface. Figure 39 shows this roll-up when the pressure surface is leading; figure 40 portrays the same type of roll-up when the suction surface is leading. One consequence of this scraping effect is the virtual elimination of the tip-clearance vortex associated with a stationary wall for this configuration (figs. 35 and 36).

The patterns on the pressure surface of a blade when the suction surface is leading are shown in figure 41. Comparison of the flow deflection in figure 41 (a) (wall stationary) with figures 41 (b) and (c) (wall moving) shows that wall motion increases the flow deflection on the pressure surface toward the wall. Smoke injected near the moving wall actually flowed down the blade onto the wall and was carried across to the suction surface of the adjacent blade.

Similarly, figure 42 shows that the moving wall, with the pressure surface leading, deflects the flow on the suction surface toward the wall. In this case, it was also observed that

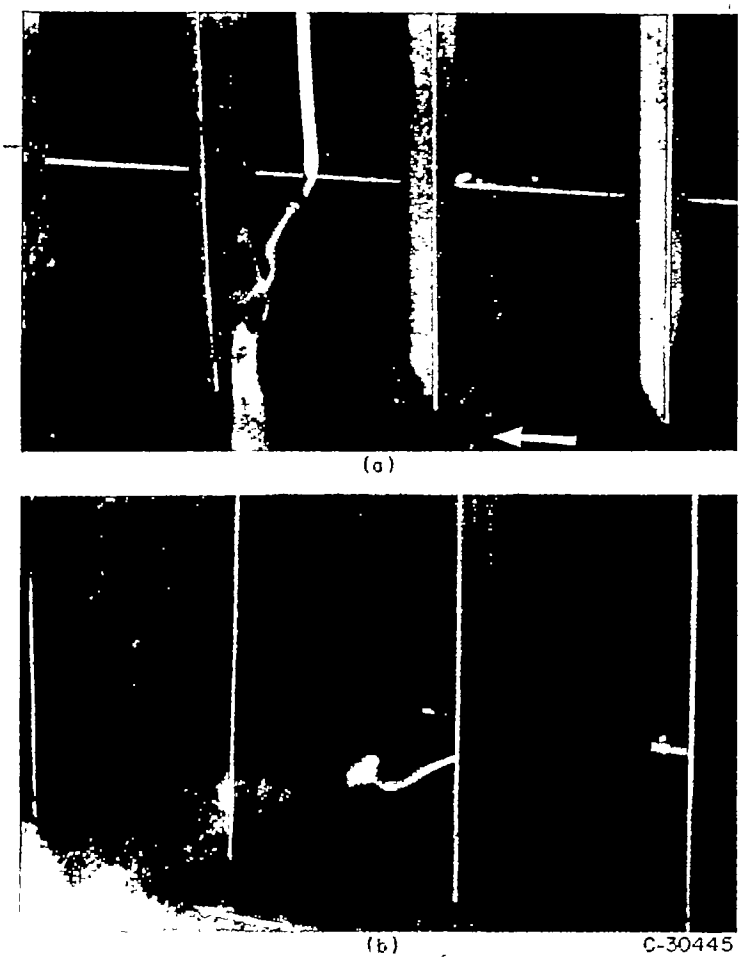


(a) Downstream view.
(b) Side view.

FIGURE 39.—Streamline patterns showing scraping effect of blade with probe near pressure surface. Pressure surface leading; moderate-speed wall; blade tip clearance, 0.014 inch; stagger angle, 0°; solidity, 1.5; angle of attack, 11°; aspect ratio, 2.34.

FIGURE 40.—Streamline patterns showing scraping effect of blade; suction surface leading.

smoke flowed down the blade suction surface onto the wall and was carried over to the pressure surface of the adjacent blade. A photograph of this effect was unobtainable because of the severe diffusion that existed when smoke was so introduced. Furthermore, this action of the moving wall with the pressure surface leading removed the stagnant-air region previously existing on the blade suction surface near the trailing edge so that the flow now remains attached to the entire blade suction surface.

**Remarks on tip-clearance effects.**—Instead of reducing secondary-flow effects, tip clearance in the basic two-dimensional cascade merely displaced the secondary-flow vortex and provided another vortex rotating in the opposite direction. The two vortices rotated side by side without much mixing and thus constituted a considerably larger flow disturbance than did the secondary flows alone.

When the wall moved past the blade tips, the net effect was that flow near the wall was scraped off and rolled up by the blade leading surfaces, while the low-momentum fluid on the blade trailing surfaces was pulled off the blades.

When the pressure surface was leading, this behavior served in this configuration (1) to improve flow characteristics on the blade suction surface even at some spanwise distance from the tip by reducing the blade boundary layer that exists when the wall is stationary (this boundary-layer reduction is desirable, because it reduces the tendency toward separation on the blade suction surface); (2) to replace the secondary-flow vortex and tip-clearance vortex on the suction surface by a different roll-up near the blade leading surface; and (3) to improve generally the tip flow on the pressure surface and the blade tip loading in the sense that the tip flow is prevented from deflecting under the blade, which would reduce the pressure difference across the blade tip. The patterns of the flow obtained with the pressure surface leading simulate to a degree the absolute fluid motion in an axial-flow-compressor stator or the relative motion in the compressor rotor.

When the suction surface was leading, for the configuration tested, this behavior served (1) to aggravate the effects at the suction surface by piling up low-energy fluid there that increased the secondary-flow effects while adding a new roll-up near the leading surface (this pile-up of low-energy fluid is undesirable, because it increases the tendency toward separation on the blade suction surface), and (2) to aggravate the tip effects at the pressure surface by increasing the deflection of the flow and thereby impairing the blade loading at the tip. In this case, where the suction surface is leading, the flow patterns simulate to a degree the relative motion of the fluid at the blade tips of a turbine rotor.

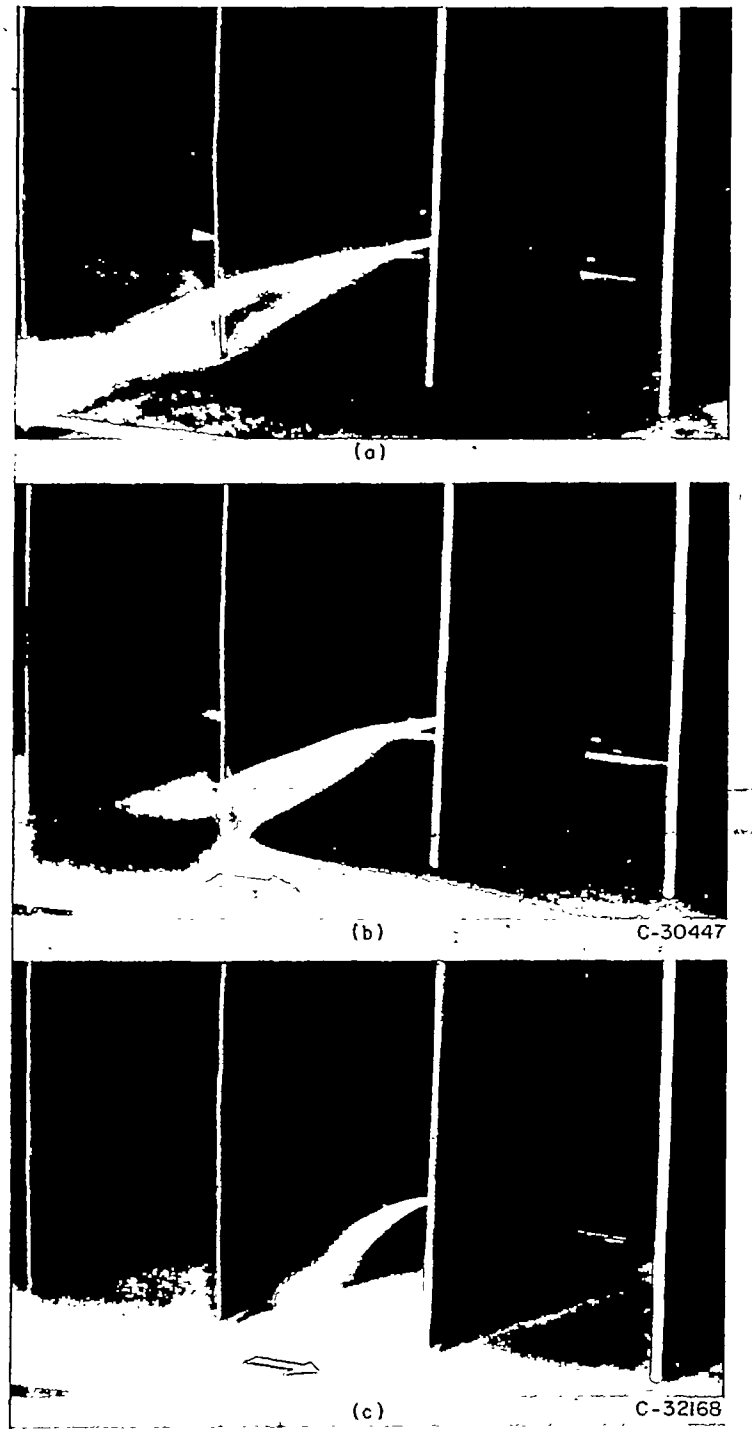


(a) Stationary wall.
(b) Low-speed wall.
(c) High-speed wall.

FIGURE 41.—Streamline deflections on blade pressure surface with probe on nose of blade. Suction surface leading; blade tip clearance, 0.014 inch; stagger angle, 0°; solidity, 1.5; angle of attack, 11°; aspect ratio, 2.34.

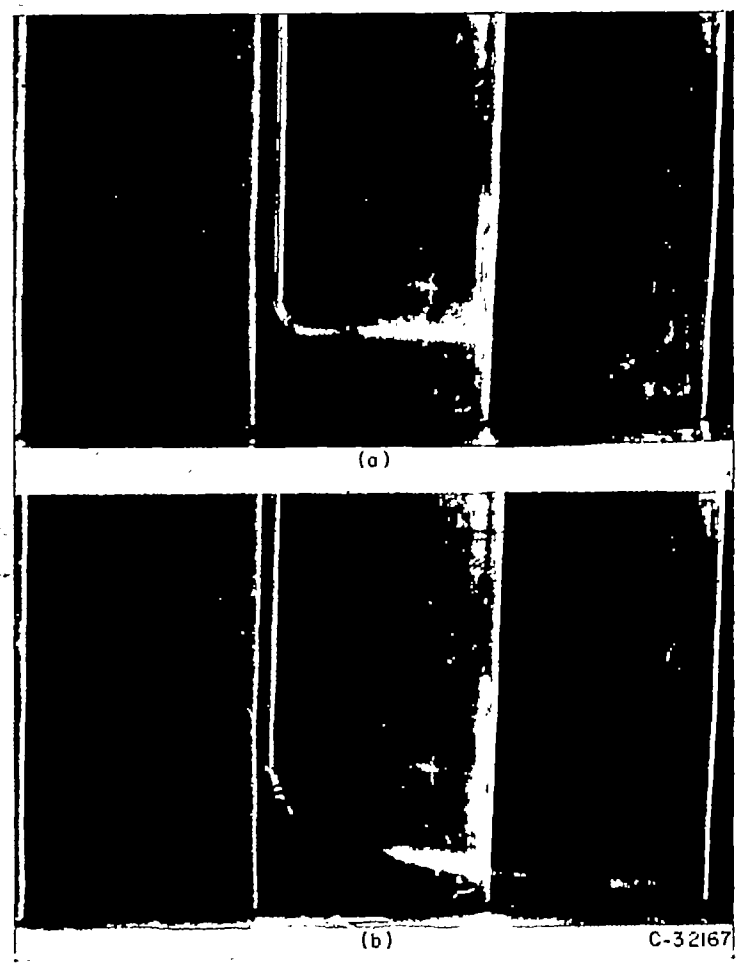


(a) Stationary wall.
(b) Moderate-speed wall.

FIGURE 42.—Streamline deflection on blade suction surface with probe on nose of blade. Pressure surface leading; blade tip clearance, 0.014 inch; stagger angle, 0°; solidity, 1.5; angle of attack, 11°; aspect ratio, 2.34.

The foregoing observations offer a possible explanation for the larger tip losses encountered in turbines as compared with compressors. They also indicate that, whereas shrouding appears to be undesirable in compressors, it may be beneficial for turbine configurations similar to the one studied herein with low turning and low blade tip stagger.

### TIP-CLEARANCE EFFECTS WITH HIGH-TURNING BLADES

**Preliminary considerations.**—As noted in the previous section, the blade tip-clearance flows and the scraping effects produced by relative motion between blades and wall may lead to boundary-layer separation and reduced tip loading in a turbine rotor. This condition would result in the extraction of less work from the gas at the tip section. Total-temperature measurements behind turbine rotors generally indicate that there is a deterioration of blade performance near the tip.

However, in several recent experimental investigations of high-speed turbines at the NACA Lewis laboratory, this quite typical decline in turbine blade performance at the tip section was notably absent. The turbine blading configurations involved were fairly typical of high-speed turbine rotors, that is, large-turning (high circulation), high-tip-stagger blades. Consideration of these results along with those of the previous section suggested the possibility that, under certain conditions, a balance might be established between passage vortex and scraping effects on the one hand and tip-clearance effects on the other that would enhance good blade tip loading.

It was reasoned that the scraping effect, which in the configuration of the previous section was so large that it masked completely the passage and tip-clearance vortex effects, would be reduced considerably when the blade tip orientation was more tangential in direction. The chord line of the tip sections of high-tip-stagger blades is pointed more nearly in the direction of relative blade-wall motion than in the case examined in the previous section. Physically, the blades might be considered to have a slicing action on the wall boundary layer rather than the kind of scraping action seen before. It was reasoned further that the tip-clearance vortex would become larger with higher turning (circulation) in the blades as a result of the increased gradient of pressure through the clearance space from the pressure surface to the suction surface of the blade. It has already been established that the passage vortex becomes larger with increasing turning. As has been previously noted, some of the flow forming the passage vortex comes off the pressure surface of the blade. This effect might be somewhat reduced by the tip-clearance action, which diverts into the tip-clearance vortex some of the blade boundary-layer flow that would, otherwise (with zero clearance), deflect off the blade pressure surface, onto the wall, and across into the passage vortex.

**Tests with moving wall and high-turning blades.**—Smoke studies were conducted in the two-dimensional cascade, with the moving wall, to investigate the possibilities discussed in previous sections. The 45°-stagger-angle configuration was used to permit large turning. Figure 43 presents photographs of the results of an investigation of blades with approximately 125° turning. In this configuration, the leading edge of the blades have zero angle of incidence with the main flow, and the trailing edges of the blades point approximately 10° from the direction of the wall motion. A schematic sketch of the apparatus appears in figure 43 (a).

Because of the high turning of the cascade blades, the camera had to be directed broadside at the smoke and could not be aimed along smoke paths. This necessitated the use of large quantities of smoke to obtain any photographs at all; those which were obtained are pictures of projected smoke patterns only.

In figure 43 (b), the smoke was introduced with the probe at the leading edge of the middle blade of the cascade on the pressure surface (the photographs show suction surfaces only) and spanwise about one-third of the way up the blade. The wall is stationary. Some of the smoke was deflected down the pressure surface and through the tip-clearance space and formed a very large tip-clearance flow region on the suction side of this middle blade. This tip-clearance flow can be seen near the wall against the suction surface of the middle blade in figure 43 (b). The excess smoke that did not follow this pattern can be seen passing downstream to the right in the photograph. No suitable photographs could be obtained of the passage vortex roll-up. This vortex roll-up, which was observed during the tests to occur in the upstream third of the passage and to roll around the large region occupied by the tip-clearance flow, made a sharp surface of demarcation defining this region.

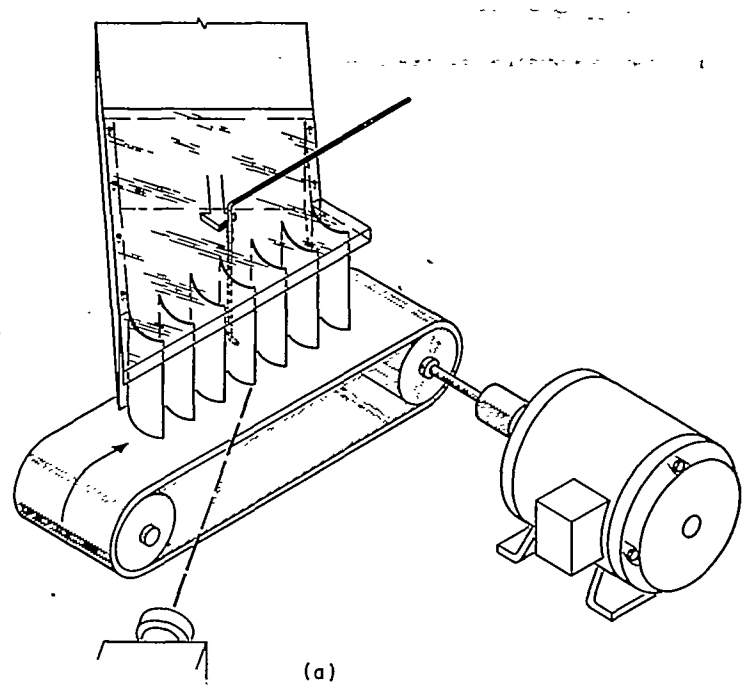


(a) Schematic diagram of apparatus.

FIGURE 43.—Tip-clearance effects with relative motion between wall and high-turning blades. Smoke introduced on pressure surface of middle blade.

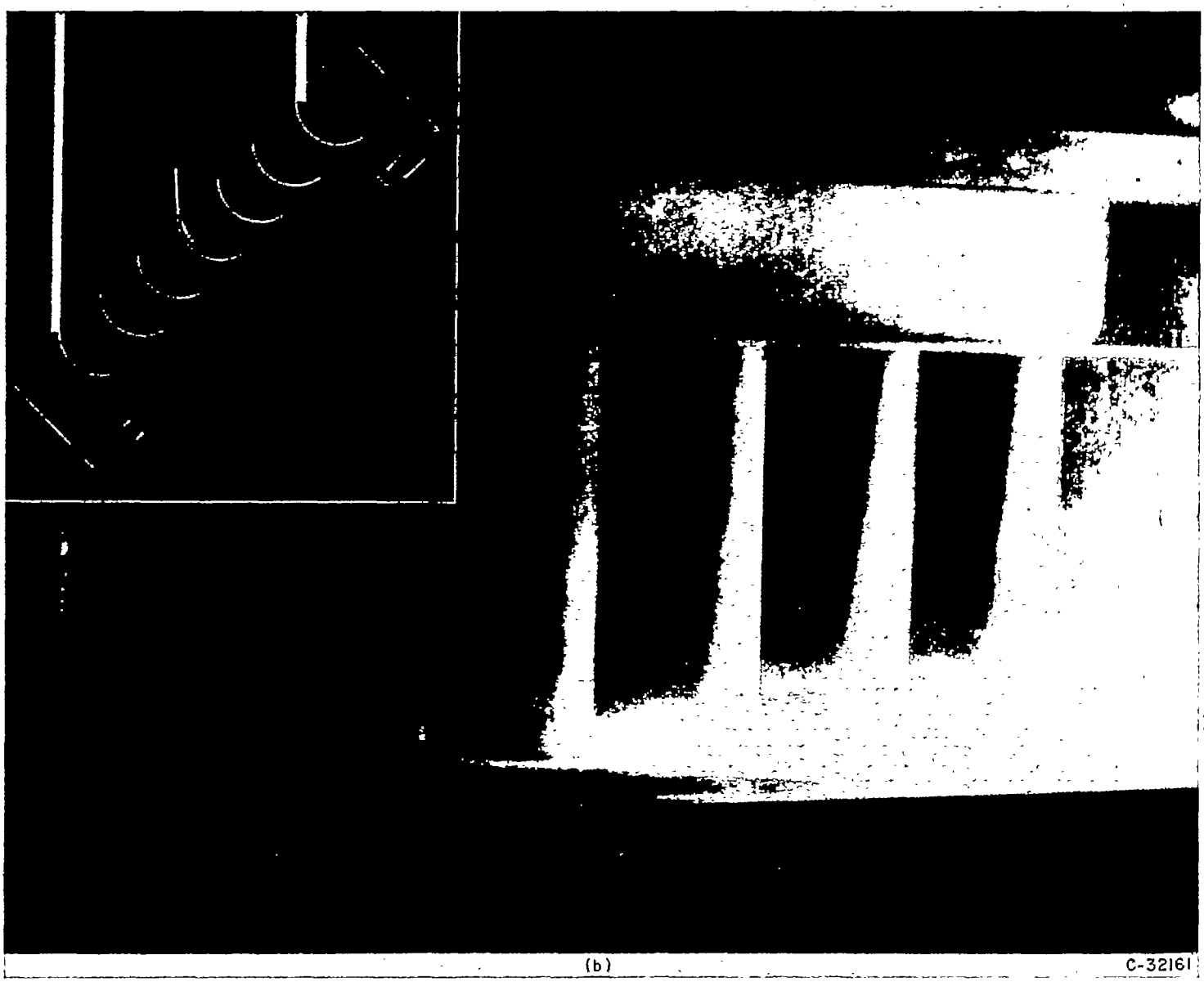


(b) Stationary wall.

FIGURE 43.—Continued. Tip-clearance effects with relative motion between wall and high-turning blades. Smoke introduced on pressure surface of middle blade.

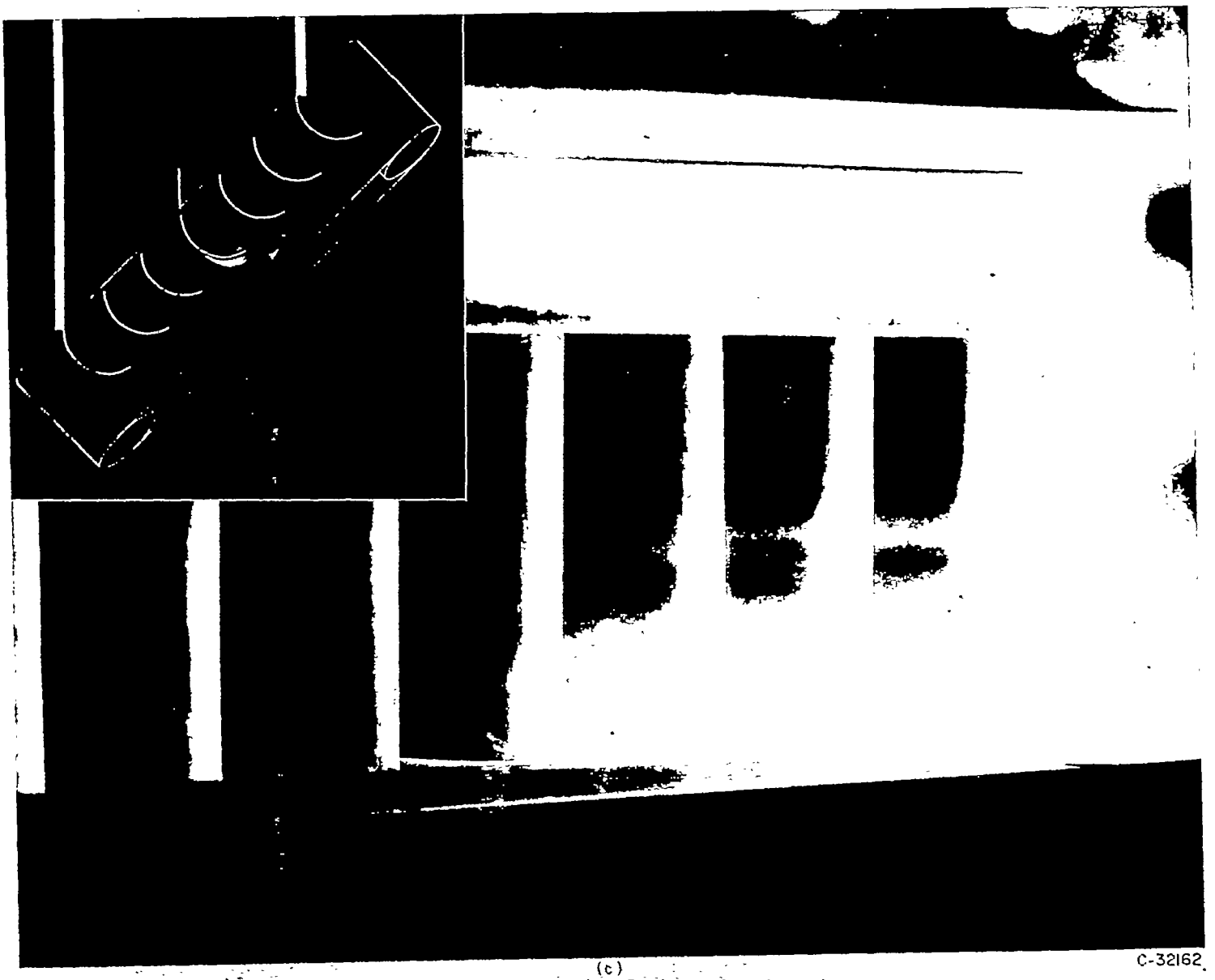


(c) Moderate-speed wall.

FIGURE 43.—Continued. Tip-clearance effects with relative motion between wall and high-turning blades. Smoke introduced on pressure surface of middle blade.

308555—56——14

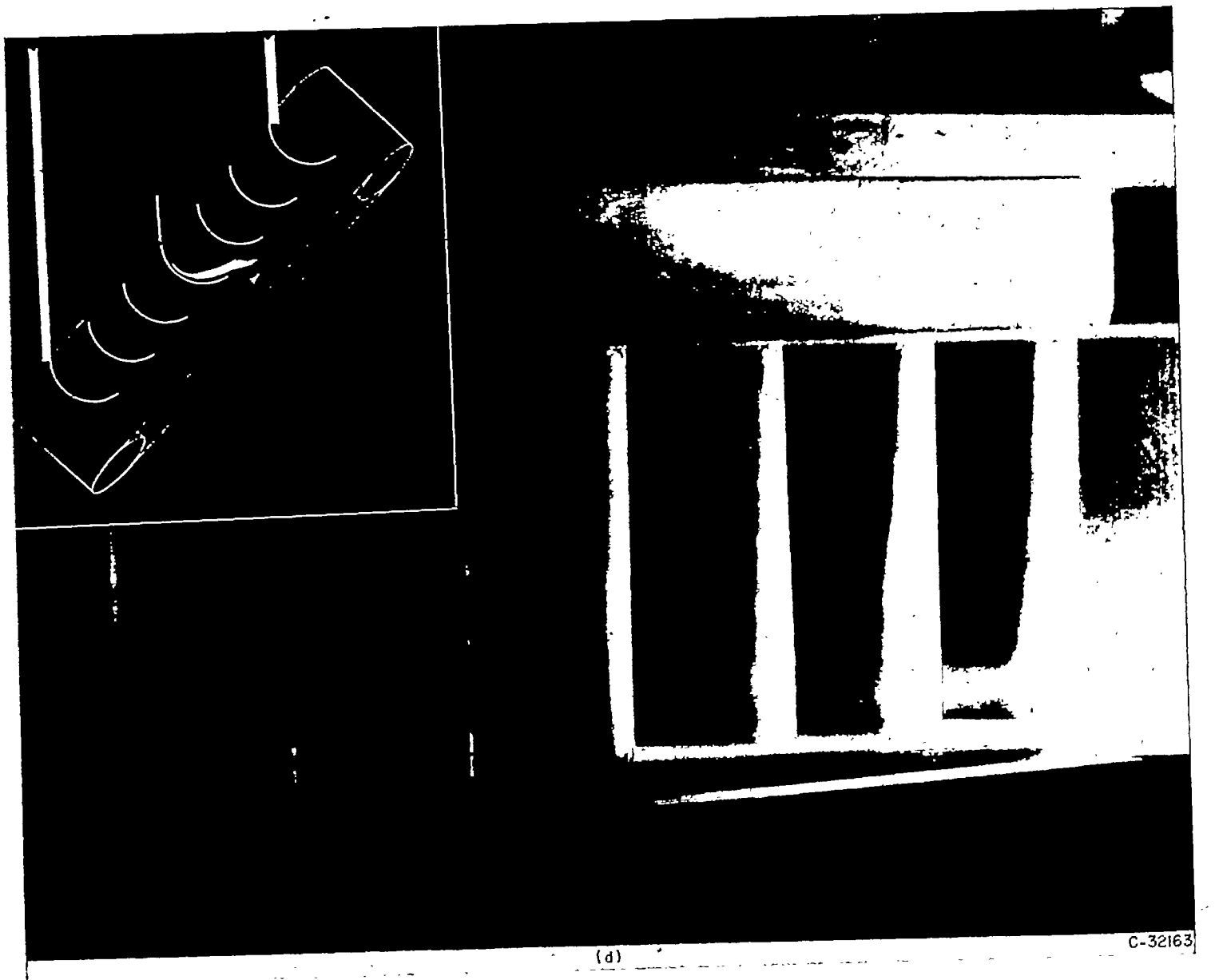


(d) High-speed wall.

FIGURE 43.—Concluded. Tip-clearance effects with relative motion between wall and high-turning blades. Smoke introduced on pressure surface of middle blade.

With the wall moving at moderate speed (fig. 43 (c)), the tip-clearance flow, seen against the suction surface, decreased considerably. The region occupied by this flow was correspondingly reduced, with the result that smoke introduced in the boundary layer at the passage inlet could now approach closer to the suction surface than with the wall stationary.

With the wall at a higher speed (fig. 43 (d)), no tip-clearance flow to the suction surface was observed. Smoke introduced in the inlet boundary layer for the most part flowed quite smoothly downstream. This indicates that such a balance was established between the passage vortex and the scraping effects on the one hand, with the powerful forces tending to create tip-clearance flow on the other hand, as to produce relatively undisturbed flow throughout the passage. As a matter of fact, the flow through the passage under these conditions was smoother than in earlier configurations where less turning and smaller tip-clearance forces were involved.

**Tests in low-speed turbine rotor.**—The photographs presented in figure 44 illustrate more clearly the variation in relative magnitude of the tip-clearance and scraping effects with variation in relative blade-to-wall speed. These photographs were obtained by Hubert W. Allen and Milton G. Kofskey of the NACA Lewis laboratory from their application of the smoke flow-visualization technique to the tip-clearance region of a low-speed turbine designed specifically for that purpose. The photographs in figure 44 were taken with the camera downstream looking toward the discharge section of the turbine rotor, which is rotating in a counterclockwise direction. In figure 44 (a), at low rotor speed, the tip-clearance flow dominates the flow picture. The smoke that is introduced through a static tap in the outer shroud at the rotor blade midchord position, axially, is seen in this figure to overtake the blade and to roll up near the suction surface of the blade in the vortex roll-up direction typical of a tip-clearance vortex. At a somewhat higher rotor speed (fig. 44 (b)), the increased scraping effect has reduced the region occupied by the tip-clearance flow. The tip-clearance vortex can be seen in figure 44 (b) to be smaller in size and to lie closer to the rotor blade than before. At the highest rotor speed, the scraping effect has increased greatly (fig. 44 (c)) and now masks the tip-clearance flow completely, so the photograph shows the formation of a typical scraping vortex near the leading (suction) surface of the rotor blade. Somewhere between these last two speeds is a balance point for these effects, and at this balance point the flow disturbances in the tip region are reduced to a minimum.

These photographs, taken in an actual turbine configuration, confirm the possibility advanced earlier of controlling the relative magnitudes of the tip-region flow disturbances of a turbine rotor. It appears possible, therefore, to improve the flow conditions in the turbine rotor tip region by balancing against each other the secondary-flow effects that cause the flow disturbances there.

**Remarks on tip-clearance effects in turbine rotors.**—In a cursory investigation, it was found that a balance could be established between passage vortex and scraping effects on the one hand and tip-clearance effects on the other, which would result in improved flow conditions throughout the passage and its boundary-layer regions. It may be inferred, therefore, that the possibility certainly exists of designing high-speed turbine rotor configurations in such fashion as to reduce separation and to prevent reduced loading on the blades at the tip section. This possibility depends upon evaluating and regulating the relative sizes of the secondary and blade tip-clearance flow effects.

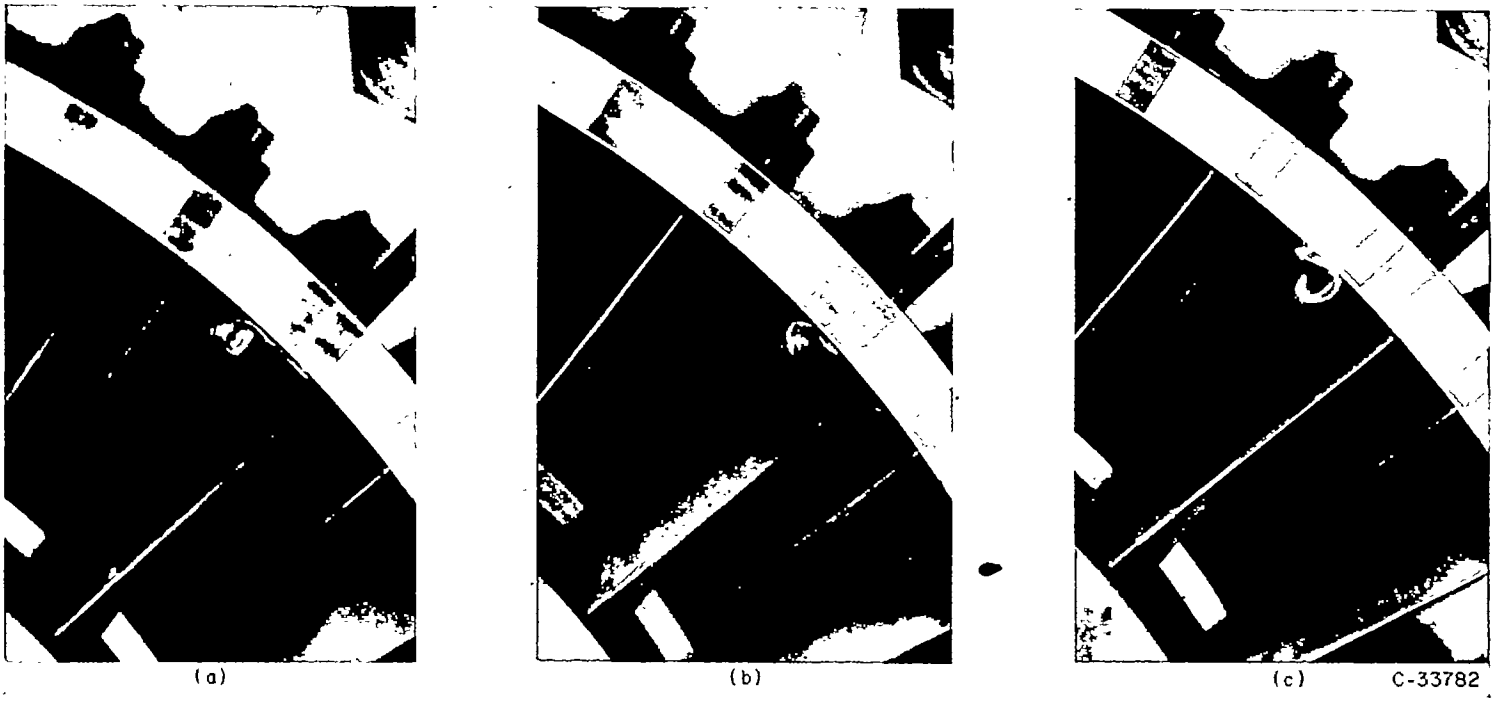


(a) Low-speed rotor. (b) Higher-speed rotor. (c) Highest-speed rotor.

FIGURE 44.—Change in relative magnitudes of tip-clearance and scraping effects in turbine rotor with varying rotor speed.

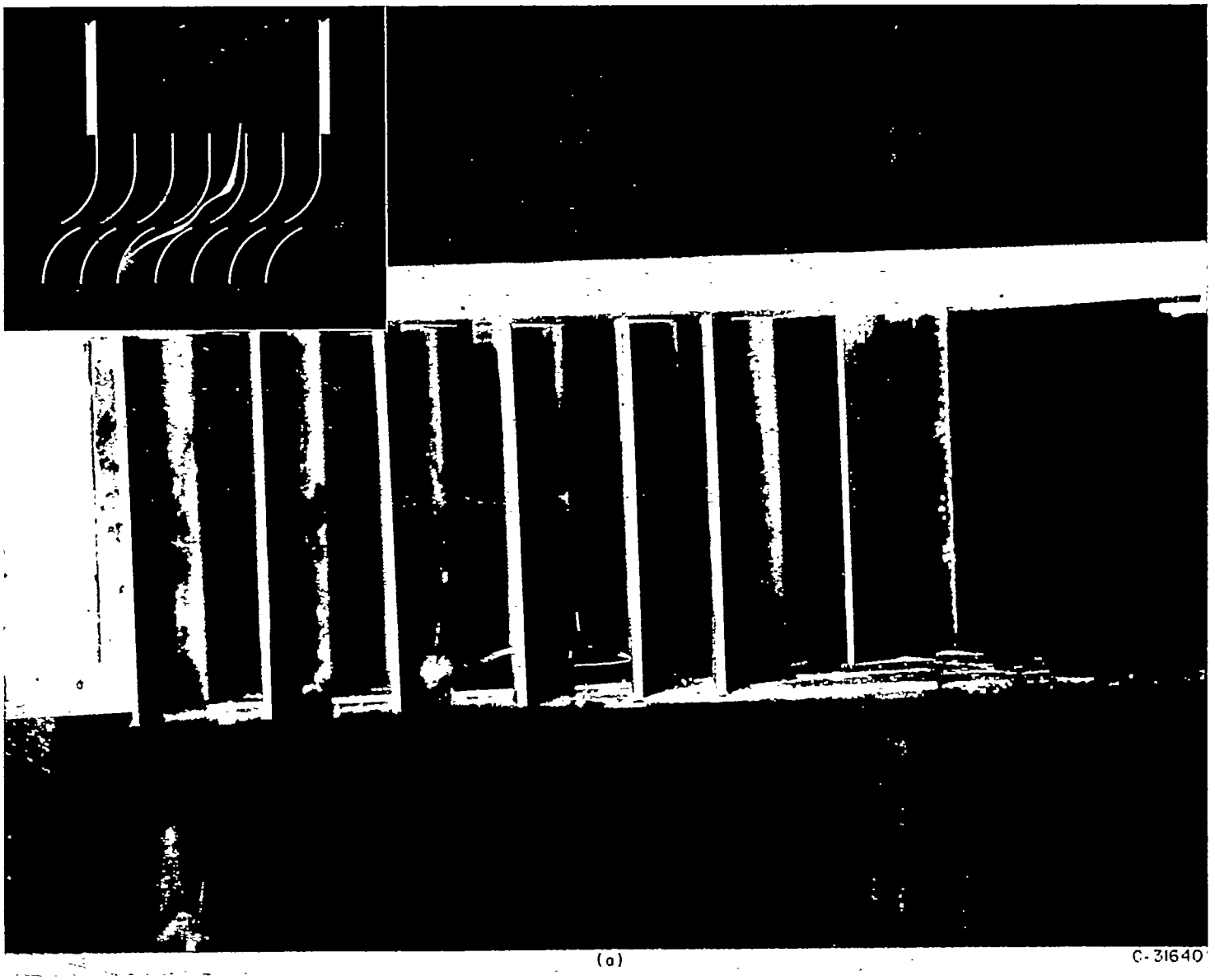


(a) Probe on wall at inlet to upstream cascade near pressure surface.

FIGURE 45.—Passage vortex generated when upstream cascade strikes pressure surface of blade in downstream cascade.

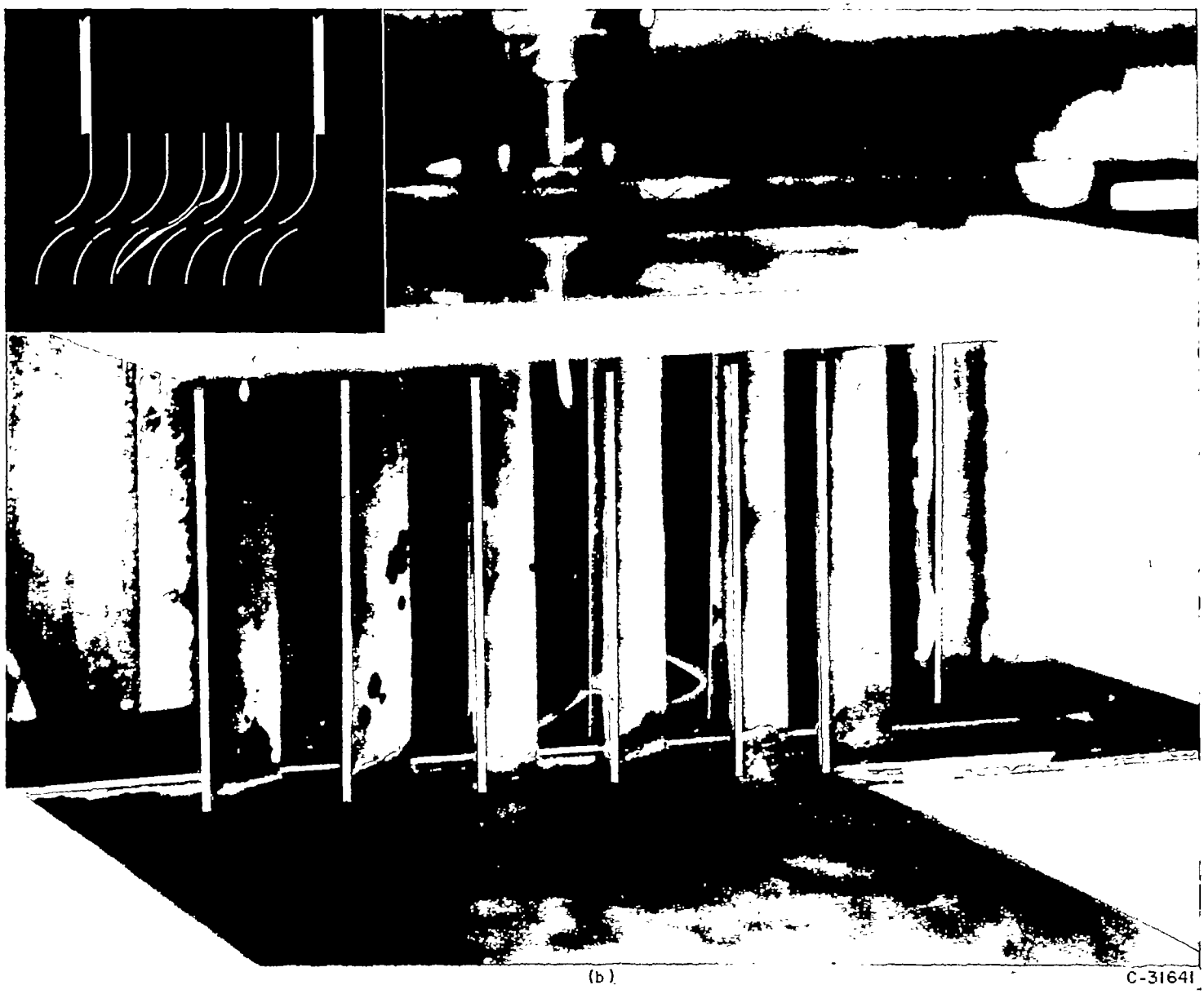


(b) Probe on wall at inlet to upstream cascade near suction surface.

FIGURE 45.—Concluded. Passage vortex generated when upstream cascade strikes pressure surface of blade in downstream cascade.

This investigation also suggests a reason for apparently conflicting experimental results concerning the effects of tip clearance on turbomachine performance. Decreasing the tip-clearance spacing in a turbine configuration for which the scraping effect is already the largest flow disturbance would be detrimental to the turbine performance. However, in a turbine configuration for which the tip-clearance flow effect is largest, decreasing the tip-clearance spacing would serve to improve the turbine performance.

In more moderate-speed turbine rotors, with typically less blade stagger at the tip than is usual with the high-speed rotors, it may not be possible to reduce the scraping effects sufficiently. For such turbines, where the centrifugal-stress problems are not too acute, shrouding of the rotors appears to be a more likely method of blade tip-loading control. Shrouding such turbine rotors might well reduce or eliminate both the scraping and tip-clearance effects and could result in better flow conditions in the turbine rotor-tip region. It should also be noted carefully here that shrouding a turbine rotor that operates near the balance point of the flow disturbances without the shroud could upset that balance. In addition, there might well be some undesirable effects produced by the action of the shrouding on the upstream boundary-layer coming into the turbine rotor. These considerations probably account for the apparently conflicting experimental results concerning turbine rotor shrouding obtained by various investigators.

### SECONDARY FLOW IN TANDEM CASCADES

**Flow patterns in tandem cascades.**—The construction of the tandem cascades was described in the EXPERIMENTAL SETUPS section of this report. Smoke traces disclosed that the mainstream followed the turnings through both cascades quite smoothly. The secondary-flow pattern in the wall boundary layer for each 60° cascade by itself was the same as shown previously (figs. 25 to 28); that is, each generated its own passage vortex, which then extended downstream.

The behavior of the vortex generated by the upstream cascade provided the chief interest in this flow-visualization study. This vortex did not turn as much as the main flow in passing through the downstream cascade. Instead, it displayed a strong tendency to continue in the same direction as when it left the upstream cascade. When the relative spacing of the cascades was such that this vortex passed through the downstream cascade without touching a blade there, it was not turned back to the axial direction. Because of the setup used, it was impossible to get overhead pictures of this phenomenon so that the discharge angle of the vortex might be ascertained. The best estimate that could be made in this series of qualitative studies is that the vortex tube does turn somewhat in passing through the second blade row but that the discharge angle of the vortex is nearer 60° from axial than axial.

The resistance to turning of the vortex tube is shown in figure 45. In figure 45 (a), the smoke was introduced at the inlet to the upstream cascade and at the wall. The smoke trace is seen to cross the passage in this cascade. The deflection of the streamline away from the wall also is apparent from its spanwise position in the photograph as it enters the second or downstream cascade. Then (see fig. 45 (a)), the vortex tube, instead of turning with the main flow, proceeds in its path until it collides with the pressure surface of a blade in the second cascade. An observer could see the flow in the vortex tube strike the pressure surface and deflect downstream. At the low airspeeds of these tests, flow separation was observed on the pressure surface of the blade in the region of the impact.

Figure 45 (b) shows the same phenomenon when the smoke is introduced at a different position in the inlet boundary layer of the first cascade.

**Remarks on secondary flows in tandem cascades.**—This tandem-cascade investigation demonstrates the resistance to turning of the secondary-flow vortices as they extend downstream. The preliminary results of these tests indicate one way in which the secondary flows, with little actual energy involvement per se, may give rise to considerable losses as a result of their behavior in subsequent stages of turbomachines. This behavior pattern of the vortex tubes suggests the need for further investigations into the nature of the

vortices, the way they penetrate the main flow field, and what becomes of the main flow in the vicinity of the origin of the rolled-up vortex and along the path the vortex traverses.

## CONCLUSIONS

1. The pattern of secondary-flow behavior in boundary layers of cascades and rectangular elbows, which occurs whenever there is turning of the mainstream, consists of a three-dimensional roll-up of end-wall boundary layer in a region near the suction surface to form a passage vortex. No trailing-edge vortex phenomenon was observed. The size and tightness of this passage vortex depends principally upon the turning of the mainstream.

2. It is characteristic of a passage vortex to shift in a direction away from the end wall and from the blade suction surface as it moves downstream and to resist subsequent turnings with the mainstream. The latter result is particularly evident in the tandem-cascade studies, where a vortex passing from one cascade through another strikes the pressure surface of a blade in the downstream cascade and causes flow disturbances. These disturbances may account for a large part of the losses attributed to secondary flows in turbomachines.

3. The existence of blade tip clearance in a cascade induces a vortex near the suction surface (formed from flow under the blade tip), which rotates in a direction opposite to the passage vortex. The tip-clearance vortex displaces the passage vortex from the region near the blade suction surface and rotates side by side with it without appreciable mixing. The magnitude of the tip-clearance vortex varies with blade loading.

4. When relative motion exists between the cascade blades and the cascade end wall, the leading surfaces of the blades with moderate blade tip stagger "scrape" up entrained fluid near the wall and impart a rolling motion to the air in this region, while, on the trailing surface, boundary-layer fluid is aspirated off the blade onto the wall. With the pressure surface leading (compressor case), the scraping effect improves blade tip-loading characteristics. With the suction surface leading (turbine case) the scraping effect is detrimental to blade tip-loading characteristics. For turbines with high blade tip stagger, it appears possible to obtain a balance between tip-clearance effects and passage vortex and blade-scraping effects. As a result, the normally large disturbed-flow area (and deterioration of turbine blade performance at the tip) near the suction surface can be reduced.

5. The passage vortex formation is the principal secondary-flow phenomenon in rectangular bends, as it is in cascades. However, as a result of the nose effect in cascades, the boundary-layer flows are noticeably different from those in bends.

LEWIS FLIGHT PROPULSION LABORATORY
NATIONAL ADVISORY COMMITTEE FOR AERONAUTICS
CLEVELAND, OHIO, *February 11, 1953*

## REFERENCES

1. Carter, A. D. S.: Three-Dimensional-Flow Theories for Axial Compressors and Turbines. War Emergency Issue No. 41, pub. by Inst. Mech. Eng. (London). (Reprinted in U. S. by A. S. M. E., Apr. 1949, pp. 255–268.)
2. Squire, H. B., and Winter, K. G.: The Secondary Flow in Cascade of Aerofoils in a Nonuniform Stream. Jour. Aero. Sci., vol. 18, no. 4, Apr. 1951, pp. 271–277.
3. Hawthorne, William R.: Secondary Circulation in Fluid Flow. Proc. Roy. Soc. (London), ser. A, vol. 206, no. A1086, May 7, 1951, pp. 374–387.
4. Eichenberger, Hans P.: Shear Flow in Bends. Tech. Rep. No. 2, Office Naval Res., Gas Turbine Lab., M. I. T., Apr. 15, 1952. (Contract N5ori07848.)
5. Rohlik, Harold E., Kofskey, Milton G., Allen, Hubert W., and Herzig, Howard Z.: Secondary Flows and Boundary-Layer Accumulations in Turbine Nozzles. NACA Rep. 1168, 1954. (Supersedes NACA TN's 2871, 2909, and 2989.)